DP-1643
Distribution Category: UC-25

HYDROGEN COMPATIBILITY HANDBOOK FOR STAINLESS STEELS

DP--1643

DE83 017051

GEORGE R. CASKEY, JR.

Approved by

R. L. Folger, Research Manager
Hydrogen and Ceramic Technology Division

Publication Date: June 1983

E. I. du Pont de Nemours & Co.
Savannah River Laboratory
Aiken, SC 29808

PREPARED FOR THE U. S. DEPARTMENT OF ENERGY UNDER CONTRACT DE-AC09-76SR00001

ABSTRACT

This handbook compiles data on the effects of hydrogen on the mechanical properties of stainless steels and discusses this data within the context of current understanding of hydrogen compatibility of metals. All of the tabulated data derives from continuing studies of hydrogen effects on materials that have been conducted at the Savannah River Laboratory over the past fifteen years. Supplementary data from other sources are included in the discussion. Austenitic, ferritic, martensitic, and precipitation hardenable stainless steels have been studied. Damage caused by helium generated from decay of tritium is a distinctive effect that occurs in addition to the hydrogen damage from tritium which is the same as for the other hydrogen isotopes protium and deuterium. The handbook defines the scope of our current knowledge of hydrogen effects in stainless steels and serves as a guide to selection of stainless steels for service in hydrogen.

CONTENTS

CONTENTS, Contd

LIST OF TABLES

LIST OF FIGURES

LIST OF FIGURES, CONTD

HANDBOOK OF DATA ON HYDROGEN COMPATIBILITY OF STAINLESS STEELS

INTRODUCTION

This handbook is based on studies of hydrogen effects in metals that have been conducted at the Savannah River Laboratory (SRL) over the past 15 years. The major part of this continuing study deals with austenitic, martensitic, and precipitation hardenable stainless steels and is the subject of this handbook. The handbook also includes data on high nickel alloys, iron-nickel, iron-chromium alloys and pure nickel. These alloys are similar to the stainless steels and their inclusion provides a more complete coverage of the iron-chromium-nickel ternary alloy system.

Stainless steels have been utilized in structures and equipment for hydrogen storage, rocket engines, and petrochemical processing. Temperatures range from cryogenic to several hundred Kelvin and effective hydrogen pressures often exceed 20 MPa. In addition, hydrogen may be encountered as a corrosion product and may contribute to degradation of equipment in such circumstances. The data presented in this handbook covers the effects of hydrogen on stainless steels at temperatures of 78 to 400 K and at pressures up to 69 MPa. Therefore, the results are applicable to only a portion of all possible industrial applications of stainless steel in hydrogen environments.

There are two principal sections to this handbook: Alloy Data Sheets which tabulate mechanical properties for each alloy and Hydrogen Damage which discusses the hydrogen compatibility of stainless steels. The mechanical property data for each alloy are tabulated separately on one or more data sheets and indexed by alloy number or trade name. The nominal compositions and mechanical properties of the alloys are included in tables immediately following the index. The discussion of hydrogen damage draws upon published information from the technical literature to supplement the SRL data.

The scope of the data accumulated on hydrogen damage varies widely among the alloys that have been studied. In all cases, tensile property measurements have been emphasized and fracture modes examined. Fracture-mechanics-type specimens have been studied in several alloys. Studies of Type 304L stainless steel have been the most extensive. They include bar, cross-rolled plate, and High Energy Rate Forged (HERF) stock. The effects of grain size, heat treating temperatures, and quench rates on susceptibility to hydrogen damage have also been examined.

Mechanical behavior, fracture modes, helium embrittlement which may arise by beta decay of tritium, and hydrogen damage mechanisms are discussed. Although a uniform and consistent data base does not exist for each of the alloys, general trends in susceptibility to hydrogen damage have been identified. Changes in mechanical behavior and fracture mode attributable to hydrogen have been correlated with alloy composition, heat treatment, stress state, and test temperature. The data base does provide sufficient information for guidance in alloy selection and development of new alloys tailored to specific service requirements.

During the past decade, several international conferences and symposia have concentrated on hydrogen effects on metals, References 1 through 11. Proceedings of these meetings provide interpretation and evaluation of hydrogen damage studies as well as mechanical and physical property data on a variety of alloys other than stainless steel. Hydrogen Damage, edited by C. D. Beachem, Reference 12, is a selection of papers from the technical literature that provides an overview and insight into hydrogen damage, as does the review paper by Hirth and Johnson, Reference 13.

Many of the publications and presentations at technical meetings by researchers at the Savannah River Laboratory deal with hydrogen effects in stainless steel. Only a few have been referenced directly in the text, the remainder are listed in references 46 through 71. These papers supplement this Handbook and provide more detailed discussion of specific topics.

SUMMARY

The susceptibility of stainless steels to hydrogen damage has been evaluated primarily under rising uniaxial load rather than under static or fatigue loading conditions. Smooth, notched, and fatigue cracked specimens have been tested and hydrogen damage assessed by measuring either fracture strain or the J-integral. As shown in Table 1, stainless steels may be ranked qualitatively according to the severity of damage measured on specimens precharged with hydrogen at hydrogen pressures up to 69 MPa prior to testing.

Ranking of alloys will not in general be the same for static or fatigue loading as for rising load conditions as seen in Table 2. Slow-crack growth under static loading has been reported for A-286, JBK-75, and Nitronic®-40 at stresses substantially below the ultimate tensile strength, but not for Type 304L stainless steel.

The J-integral analysis of tensile data has been applied to tests of smooth and C-shaped specimens. Both J at maximum load and tearing resistance (change of J with crack length) are sensitive to alloy composition, crack orientation relative to deformation texture, and test environment. The susceptibility to hydrogen damage of several alloys was evaluated by the J-integral. Results were similar to evaluation based on reduction- in-area in smooth bar tensile test but more sensitive to orientation. The J-integral is more versatile than a ductility parameter as it is applicable to specimen designs that do not have an easily measured ductility parameter.

Helium embrittlement at ambient temperature has been found in five types of austenitic stainless steel: HERF Type 340L, HERF Type 316, HERF Nitronic® 40 (21-6-9 steel), HERF A-286, and annealed JBK-75 (a modified A-286). Helium was generated within the specimens by radioactive decay of tritium which had been diffused into the alloys at 420 K from high pressure (65 MPa) gas. Fracture toughness of the alloys decreased with increasing accumulation of helium. Damage was least in HERF Type 316 and greatest in HERF Nitronic® 40 and JBK-75. Sustained load tests indicate that the stress intensity for crack initiation and propagation also decreases with increasing helium concentration. Helium damage appears to be additive to the damage caused by the hydrogen isotopes and on a per atom basis appears to be more severe than hydrogen damage.

Additional observations on hydrogen damage may be derived from the data:

TABLE 1

Ranking of Hydrogen Damage*

Minimal	Moderate	Severe .
316	304N	CG-27
310	304L	17-4
	Inconel® 718	216
309S**	Nitronic®-40	Tenelon®
Nitronic®-50	A-286	18-18 Plus®
Incoloy® 800H	JBK-75	Ni
X18-3 Mn**	AM363**	AM350
Ni-SPAN-C**	18-2 Mn**	
Carpenter 20Cb-3		

* Based on tensile ductility. Nominal compositions of these alloys are listed in Table AI.

** Ranking of these alloys is tentative.

TABLE 2

Hydrogen Damage Susceptibility

	Property or Relative Property*			
	Type 316	Type 304L	A-286 (JBK-75)	Nitronic®-40
Tensile Properties (Rising Load)				
Notch Strength (H_2/He)	-	0.74	0.86	0.72
Notch Ductility (H_2/He)	-	0.50	0.38	0.19
Disc Burst Pressure (H_2/He) (Rising Load)	1.00	0.55	0.98	-
Fatigue Life (H_2/He) (Fluctuating Load)	1.00	-	-	-
Slow Crack Growth (Sustained Load)				
Threshold Stress Intensity	No Crack Growth Detected in HERF 132 MPa $\sqrt{m}$	No Crack Growth Detected 100 MPa $\sqrt{m}$	44-116** MPa $\sqrt{m}$	100 MPa $\sqrt{m}$

* Values <1.00 show effect of hydrogen by comparison with data obtained in helium atmospheres.

** Variable depending upon heat treatment and precipitate morphology.

- In Fe-Cr-Ni base alloys environmental hydrogen compatibility at room temperature is maximized for alloys containing 15 to 30% nickel. The role of other alloy elements has not been established, but small additions of molybdenum (2 to 3%) appear beneficial.

- In Fe-Cr-Ni-Mn alloys, hydrogen compatibility improves as nickel content increases. Manganese is not a substitute for nickel for hydrogen compatibility in spite of the fact that manganese like nickel stabilizes austenite.

- There is a ductility minimum in the temperature range 200-300 K where hydrogen damage is most pronounced. This ductility minimum is observed even in alloys which show minimal hydrogen damage and no fracture mode change such as Type 310 and 316 stainless steels.

- Nitrogen contents greater than about 0.3 wt % appear to aggravate hydrogen damage in Fe-Cr-Ni-Mn alloys.

- Impurities normally present in commercial austenitic stainless steels (silicon, manganese, sulfur, and phosphorus) do not appear to influence susceptibility to hydrogen damage relative to pure alloys. Segregation of these elements is potentially harmful, however.

- Increased strength with no loss or a small improvement in hydrogen compatibility is achieved by high energy rate forging (HERF) of austenitic stainless steels.

- The presence of hydrogen often evokes brittle fracture modes under loading and temperature conditions where ductile failure by microvoid coalescence ordinarily occurs. However, fractography by itself is not adequate to diagnose hydrogen assisted fracture in stainless steels because each brittle fracture mode has been observed under other conditions.

HYDROGEN DAMAGE

Hydrogen damage occurs to all structural alloys, including stainless steels.[12-13] The widespread occurrence of hydrogen damage is directly connected to the easy absorption of hydrogen into metals and the high mobility of hydrogen in metals. Hydrogen interacts with lattice defects, impurities, and internal boundaries leading to a nonuniform distribution even for the equilibrium state. Consequently, hydrogen is segregated along boundaries and in regions of high stress or strain, thus localizing hydrogen damage in regions which are often favorable sites for microcrack initiation. Hydrogen segregation is more pronounced in ferritic than in austenitic steels because of the larger elastic strain of the hydrogen atom in the lattice of the ferritic steels.[11]

There is no one physical process that is responsible for hydrogen embrittlement of metals.[12-13] At least three distinguishable forms of hydrogen degradation are recognized: hydride embrittlement, hydrogen attack, and hydrogen-assisted fracture (HAF). The first two processes are understood reasonably well, whereas the last process has not yet been rationalized satisfactorily. Hydride embrittlement occurs in metals such as niobium, titanium, and zirconium, which form distinctive hydride phases which are thermodynamically stable under ordinary ambient conditions. These hydrides have a larger specific volume than the base metal from which they form and appear to be inherently brittle. The hydrides form structures with low crystal symmetry. Brittleness arises because of the limited number of slip systems available in these crystal structures.

Hydrogen attack applies to formation of a gaseous product by reaction of dissolved hydrogen with constituents such as oxygen and carbon or with oxides and carbides present in the alloy. At elevated temperature, steam or methane forms and generates microcracks containing the reaction gas under pressure. This form of hydrogen damage has been found in copper (steam embrittlement) and carbon steels (methane formation). The addition of nitrogen to stainless steels strengthens the austenite and creates a situation where reaction between hydrogen and nitrogen could produce ammonia and cause damage in the same way as oxygen or carbon. This form of hydrogen attack has not been reported, however.

Hydrogen-assisted fracture occurs in many metals, including the stainless steels. This form of hydrogen damage is characterized by the occurrence of a ductility minimum, an inverse strain rate sensitivity, and crack propagation under static load at a stress intensity less than the fracture toughness of the alloy. The nature and degree of the damage vary widely, however, depending on alloy composition, temperature, loading mode (static, cyclic, increasing), stress state, and the environment. Only a few valid generalizations can be made for hydrogen-assisted fracture of stainless steels because the above influencing factors have not been systematically investigated.

There is experimental evidence that internal boundaries may be needed for significant hydrogen damage to occur. Investigations of pure iron have demonstrated that the strength and fracture mode of single crystals are unaffected by hydrogen either precharged to the metal cathodically or charged during straining.[14] Likewise, fracture of single crystals of pure nickel is unaffected by hydrogen.[15] It is to be noted, however, that serrated yielding was observed during tensile straining of nickel at temperatures of 150 to 270 K, providing evidence of hydrogen binding to dislocations. In contrast, polycrystalline specimens of iron and nickel are known to be severely embrittled by hydrogen. No hydrogen damage studies have been attempted with single crystals of any stainless steel. However, crystals free of internal boundaries may not be attainable because of the ease of formation of annealing twins in these steels. As noted later in this report, hydrogen-assisted fracture of stainless steel frequently propagates along twin or grain boundaries. Furthermore, ductile fracture processes can be altered by hydrogen accumulation at inclusion-matrix interfaces by diffusion or a dislocation transport mechanism.[16] Hydrogen may alter either nucleation or growth of microvoids, depending upon the nature of the inclusion-matrix or precipitate-matrix interfaces.[17] Consequently, dimple size on fracture surfaces may be either decreased or increased by the presence of hydrogen.

MECHANICAL BEHAVIOR

Hydrogen has a pronounced effect on crack initiation and growth but only a small effect on deformation behavior. Therefore, mechanical properties that are sensitive to crack behavior are suited to hydrogen damage studies. The most severe tests involve high stress or large plastic strain. Fatigue and creep rupture are two such tests. However, tensile tests of smooth and notched round specimens have been the principal methods for evaluating the susceptibility of stainless steels to hydrogen damage because of low cost and simple test procedure. Change in reduction-in-area has been the most commonly used index of hydrogen damage. Generally, if there is a loss in reduction-in-area, other mechanical properties are affected also; however, the converse is not true. Consequently, the tensile test is of limited applicability as a screening test for susceptibility to hydrogen damage. Recently, J-integral techniques have been applied to analysis of tensile data of fatigue precracked specimens, either single-edge notched (SENT) or C-shaped. Impact specimens and internally pressurized tensile tubes have been tested in limited numbers.

Specimens have been tested following exposure to high-pressure (about 1 MPa to 69 MPa) hydrogen (internal hydrogen damage) or in the presence of high-pressure (69 MPa) hydrogen gas (external hydrogen damage). Tests with an external hydrogen source were conducted at room temperature only. In contrast, mechanical testing of hydrogen-charged specimens has been done at 4.2 and 78 K and at temperatures between 200 and 400 K.

Mechanical property data for the stainless steels that have been studied at SRL are collected in the Alloy Data Sheets. The tables are organized by alloy and by type of test for each alloy.

Material and Processing Variables Affecting Hydrogen Damage

There are distinct differences in the degree of hydrogen damage among the stainless steels. Alloy composition provides a simple scheme for classifying steels according to severity of hydrogen damage. Such a criterion does not, however, provide any insight into the reasons for the observed differences in response to hydrogen. Properties such as phase stability, stacking fault energy, or dislocation slip mode are related to composition and are directly related to the processes of crack initiation and propagation. Microstructure as established by heat treatment and mechanical processing modifies hydrogen damage for any given composition of steel. Thermal and mechanical treatments influence severity of hydrogen damage in a steel through changes in grain size, alloy and impurity segregation, precipitate size distribution and coherence, and dislocation substructures. Severity of hydrogen damage may be altered in practice by alloy composition, heat treatment, and mechanical processing. Examples of these effects are cited below.

Composition

Stainless steels considered in this report fall into two broad composition classes: iron-chromium-nickel and iron-chromium-nickel-manganese. The latter class of alloys all contain nitrogen which is added to strengthen the austenite.

Environmental embrittlement of iron-chromium-nickel alloys correlates with nickel content, as seen in Figure 1. These results were obtained from tensile tests in a 69 MPa hydrogen environment at room temperature. This correlation appears valid for both high purity and commercial grades of steel. Consequently, elements

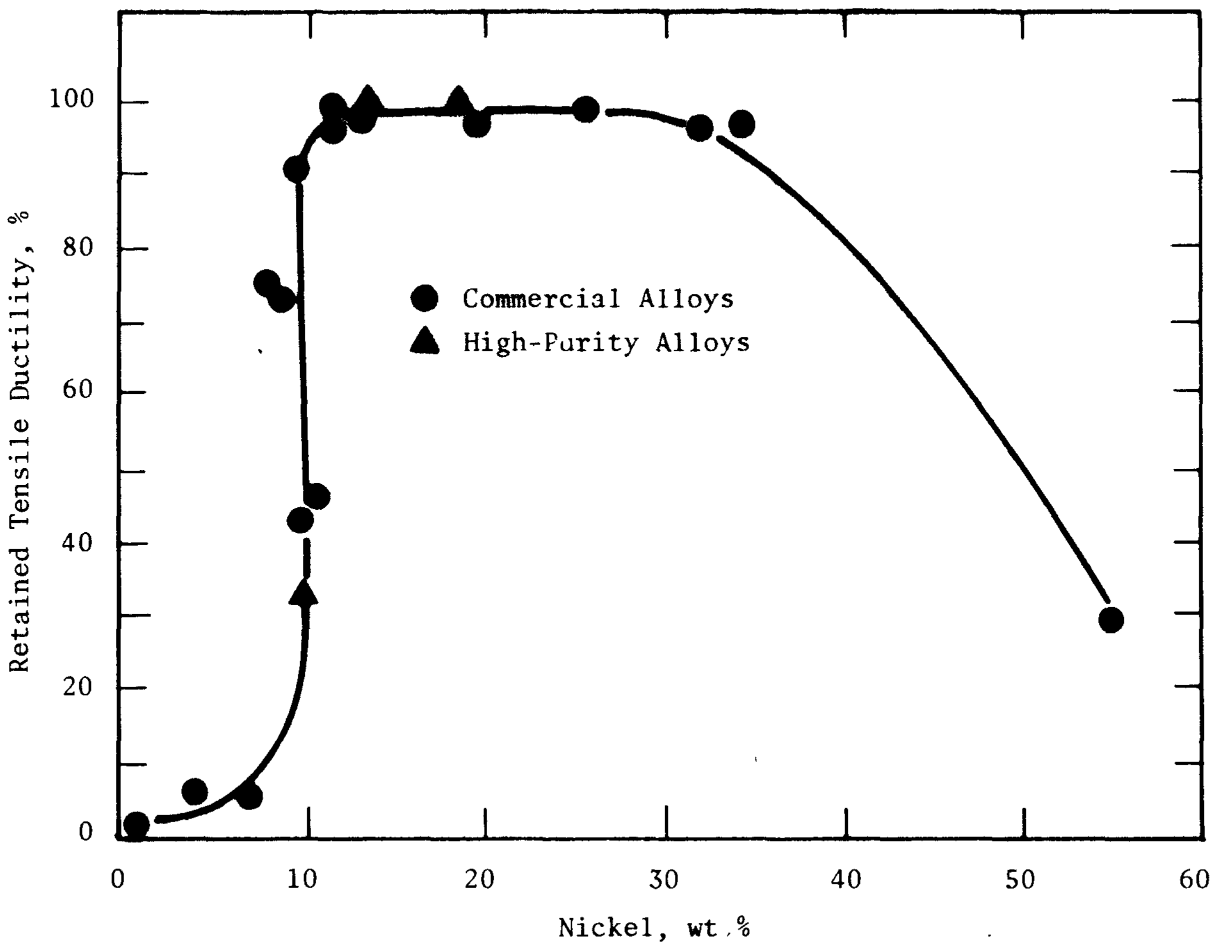

FIGURE 1. Environmental Hydrogen Damage in Fe-Cr-Ni Alloys at Room Temperature and 69 MPa Hydrogen

present as minor alloy constituents such as manganese, silicon, phosphorus, and sulfur are not primary sources of hydrogen damage. As will be shown later, however, segregation of some minor alloying elements can alter the extent of hydrogen damage.

The composition range from 8 to 14% nickel, where the marked improvement in resistance to hydrogen damage occurs, corresponds to increased austenite stability and decreased formation of martensite during plastic deformation. According to the equilibrium diagram calculated by Breedis and Kaufman for pure iron-chromium-nickel alloys, austenite is the stable phase above 19% nickel for a 20% chromium alloy at 300 K.[18] The high-purity alloys tested at SRL indicate that as little as 14% nickel will stabilize austenite with respect to transformation to α'-martensite at room temperature. Furthermore, austenite stability with respect to transformation to the epsilon phase increases as the nickel content is increased from 10 to 20%. Figure 2 shows the composition dependence of stacking fault energy, which is a measure of austenite stability with respect to the epsilon phase.[19] Both α'-martensite and epsilon phase are detrimental, as resistance to hydrogen damage is rapidly improved over the range of nickel concentrations (10 to 20%) corresponding to increased austenite stability. However, as discussed later, the relation between martensite and hydrogen damage is neither simple nor clearly demonstrated.

Hydrogen damage in the Fe-Cr-Ni-Mn alloys as measured by ductility in high-pressure hydrogen does not correlate uniquely with nickel or with equivalent nickel [Ni + 30 (C + N) + 0.5 Mn]. For several compositions, Figure 3, a range of results may be obtained. This range of behavior is probably caused by variations in nitrogen content as documented for Nitronic® 40 (21-6-9 stainless steel).[20] The higher nitrogen contents not only strengthen the alloy but also reduce the stacking fault energy, thereby promoting coplanar dislocation arrays and formation of epsilon phase.[21]

The influence of other major elements such as chromium, manganese, and molybdenum on susceptibility to hydrogen damage is not well documented. Most commercial stainless steels contain 15 to 25% chromium with 18-20% being the most common concentration. Variations in hydrogen damage among the stainless steels cannot be linked directly to chromium because the other alloying elements change simultaneously. Chromium stabilizes ferrite, which is more susceptible to hydrogen damage than austenite, therefore, a high chromium content is expected to be detrimental.

Molybdenum appears to alleviate hydrogen damage when present in small amounts, 2-3%, as indicated by comparison of Type 316 with Type 304 stainless steel. However, Type 316 stainless steel also has a nickel content about 2% higher than Type 304 stainless steel. The higher nickel cannot account completely for the reduced

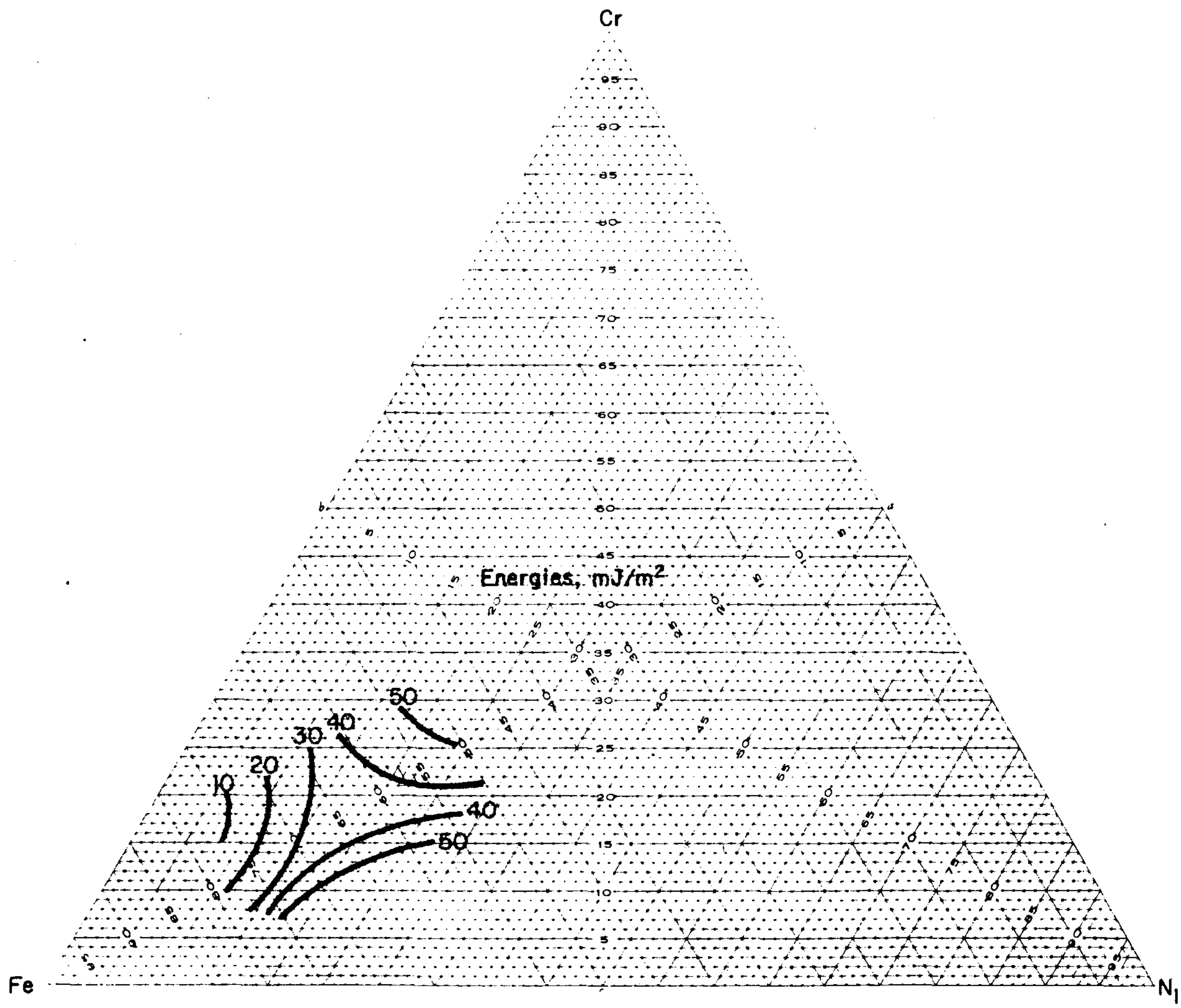

FIGURE 2. Stacking Fault Energies in Fe-Cr-Ni Alloys at Room Temperature (Ref. 19)

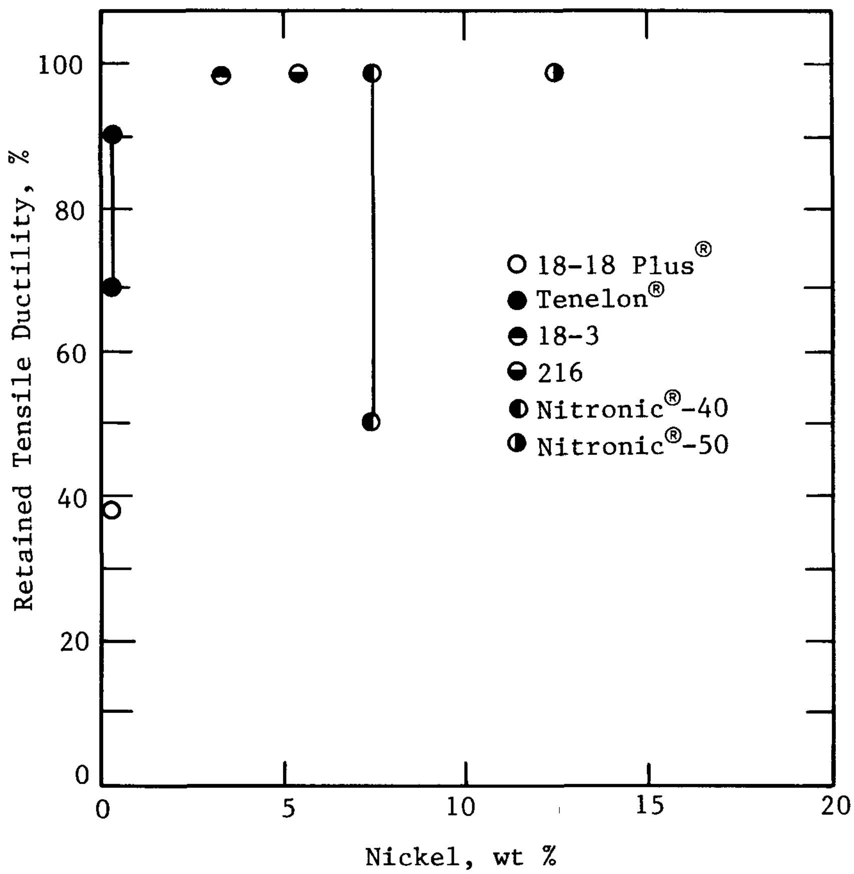

FIGURE 3. Environmental Hydrogen Damage in Fe-Cr-Ni-Mn Alloys at Room Temperature and 69 MPa Hydrogen

hydrogen damage because an alloy with 14% nickel with no molybdenum shows greater hydrogen damage than Type 316 stainless steel. Large concentrations of molybdenum (>5%) are expected to aggravate hydrogen damage because molybdenum stabilizes ferrite.

Manganese stabilizes austenite and should improve hydrogen performance of stainless steels. However, alloys with high manganese contents and little or no nickel such as Tenelon® (U. S. Steel Corp.) and 18-18 Plus® (Carpenter Technology) behave very poorly in hydrogen, Figure 3, indicating that austenite stability in itself is not sufficient to minimize hydrogen damage.

Heat Treatment

Heat treating has been shown to affect susceptibility to hydrogen damage in several ways: change of grain size, segregation or redistribution of impurities and alloying elements, and precipitation of new phases. The general patterns of variation in hydrogen damage with composition can be modified, therefore, by heat treatment.

The only study of the effect of grain size on hydrogen damage has been made with Type 304L stainless steel. As seen in Figure 4, flow stress was increased by finer grain size and the effect was greater in specimens that were saturated with hydrogen. Grain size effect on the yield strength of specimens tested in high-pressure hydrogen, was the same as for tests in helium, Figure 5. Presumably, comparable results would be obtained with the other alloys.

The grain size dependence of the flow stress (σ_f) follows the Hall-Petch relation, $\sigma_f = \sigma_o + k_f d^{-1/2}$, where σ_o and k_f are functions of strain and d is grain size. Analysis of the data demonstrates that hydrogen strengthening is associated with the back stress of dislocation pileups against internal boundaries and the increased resistance to dislocation intersection where hydrogen is present.[22] Hydrogen causes only a small increase in lattice friction stress in keeping with the relatively small lattice distortion caused by an interstitial hydrogen atom in the face centered cubic lattice.[11]

Sensitization of austenitic stainless steels occurs during heating to temperatures in the range 720 K to 1150 K, or upon cooling slowly through this range. Chromium-rich carbides of the general form $M_{23}C_6$, where M is chromium or iron, precipitate along the grain boundaries and deplete the boundary region of chromium. In nitrogen strengthened steels, the carbides may contain nitrogen also.

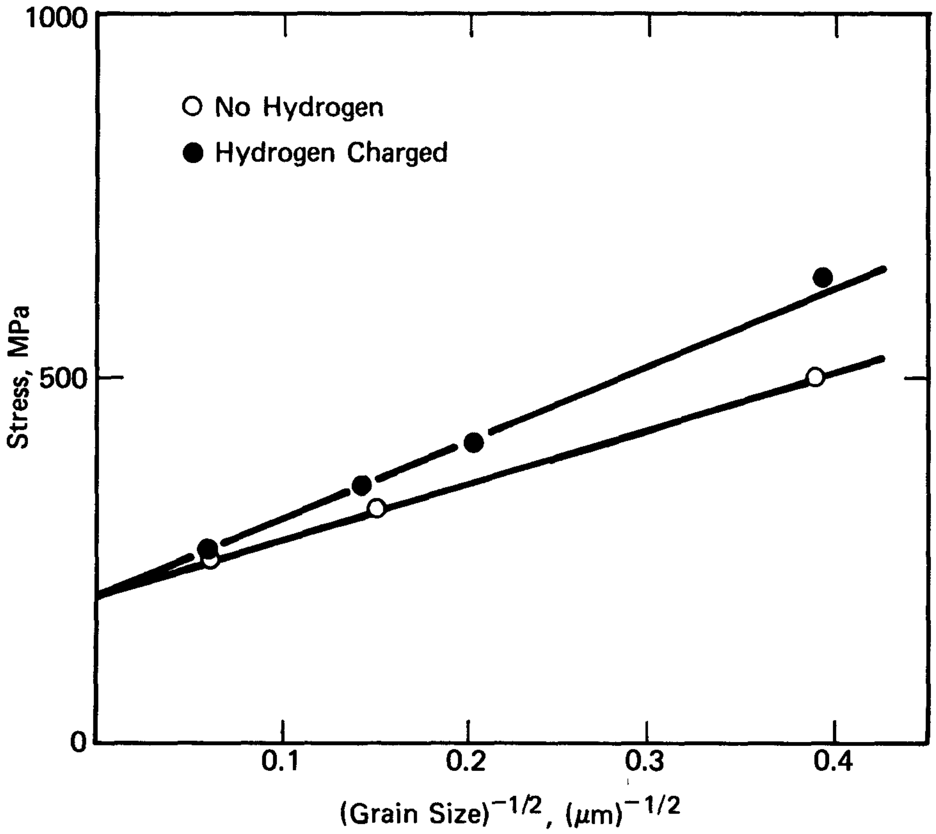

FIGURE 4. Hall-Petch Plot for Tensile-Text Specimens of Type 304L Stainless Steel at a Plastic Strain ε = 0.05

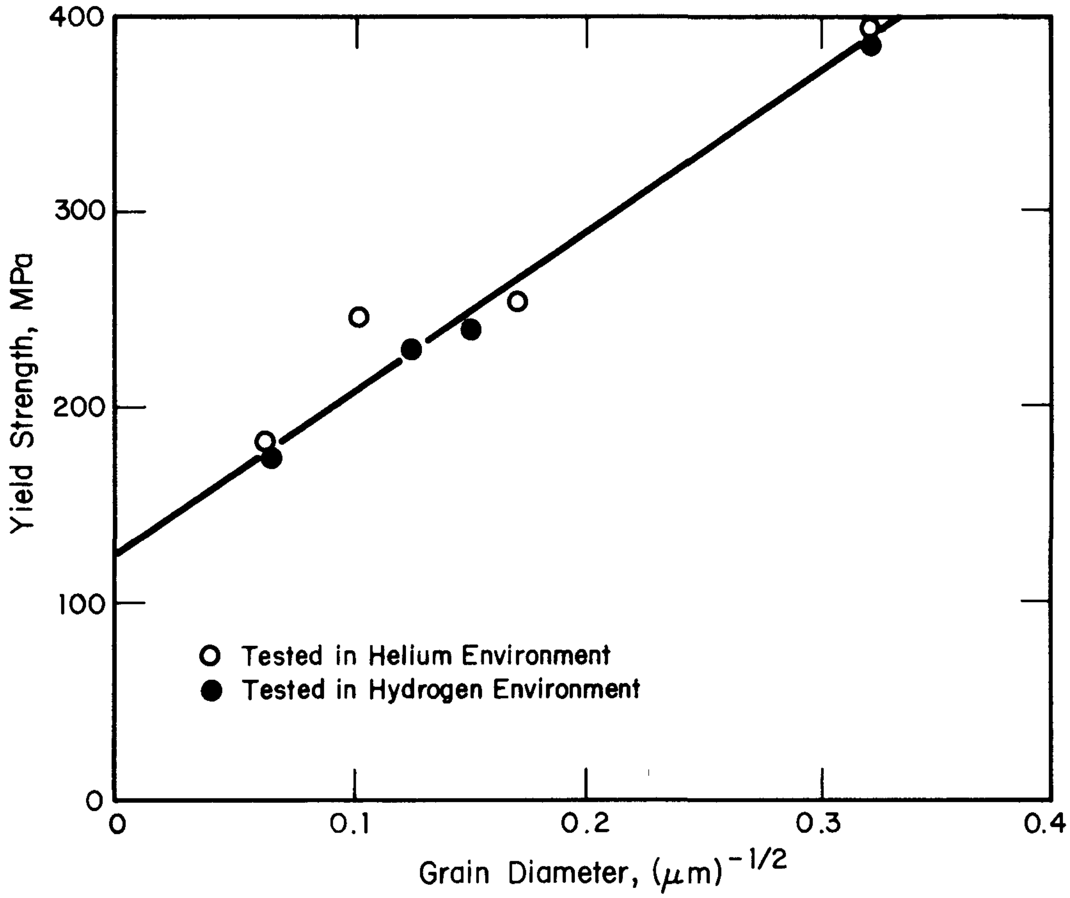

FIGURE 5. Hall-Petch Plot of Yield Strength for Type 304L Stainless Steel Tested in in High-Pressure Helium or Hydrogen Environments

The effects of sensitization anneals at about 920 K on hydrogen damage have been reported for Type 304,[23] 304L, 309S,[24] and Nitronic® 40 stainless steels. These investigations of hydrogen-assisted fracture of sensitized austenitic stainless steel do not present a consistent or uniform set of mechanical property data. Consequently, comparison of relative strength or ductility changes due to sensitization are limited. In those cases where data were collected, sensitization appears to lower the tensile strength of the alloys both for tests in air and in hydrogen. The ductility of sensitized specimens in hydrogen was less than that of the solution-annealed specimens except for Type 309S steel, where no ductility change or intergranular fracture was observed. The anomalous behavior of sensitized Type 309S steel is not attributable to composition effects such as carbon/chromium ratio or carbon + nitrogen/chromium ratio. Carbide precipitation was observed in all four alloys.

Hydrogen compatibility of precipitation hardenable alloys is sensitive to aging temperature and time. The fracture toughness of single-edge notched specimens of 17-4PH stainless steel varied substantially with aging. The most severe degradation occurred for the peak aged specimens. In the case of A-286, aging times of 4, 8, and 16 hours at 993 K resulted in small changes in fracture toughness and improved hydrogen compatibility for the shorter aging times.

Mechanical Processing

Parts for hydrogen service may be made from annealed or cold-worked bar and cross-rolled plate, or HERF stock. Further cold-working may occur during fabrication. The various working processes introduce characteristic microstructural features, affect the mechanical properties, and may change susceptibility to hydrogen damage of the stainless steel.

Suceptibility to hydrogen damage observed in tensile tubes machined from cross-rolled plate was unchanged by prior cold-work of up to 25%, Figures 6 and 7. Specimens were filled with hydrogen at 69 MPa pressure and stored 30 days at 430 K before tensile testing at room temperature. The bore of the specimen contained high-pressure hydrogen during testing.

In the case of thin sheet (0.1 mm thick), a progressive decrease in tensile ductility was found as prestrain was increased from 0 to about 12%, Figure 7.

In contrast, properties of annealed and 10% cold-worked sheet of Type 309S stainless steel were comparable. After three and a half months' exposure to hydrogen at 47.5 MPa at 345 K, tensile

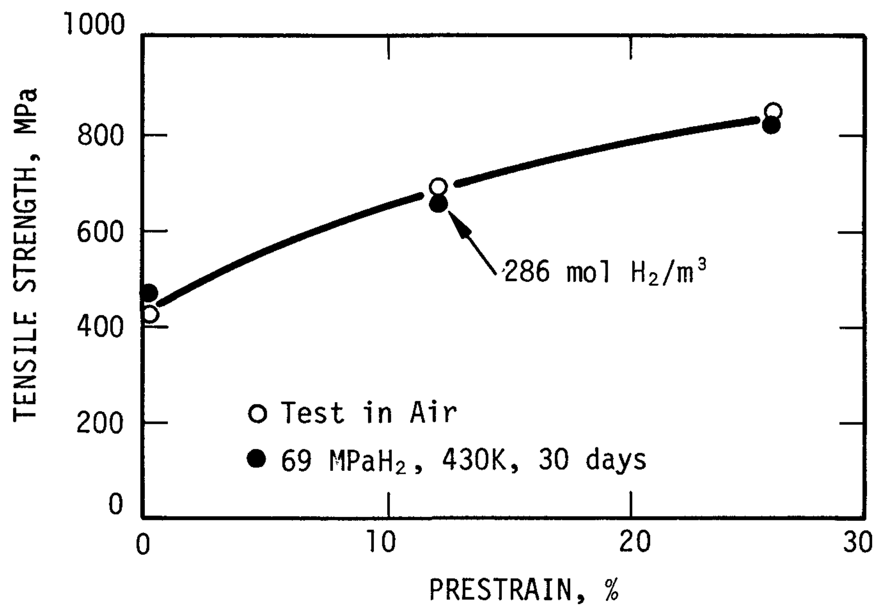

FIGURE 6. Effect of Prestrain on Tensile Strength of Type 304L Stainless Steel Tubes in Air or Hydrogen

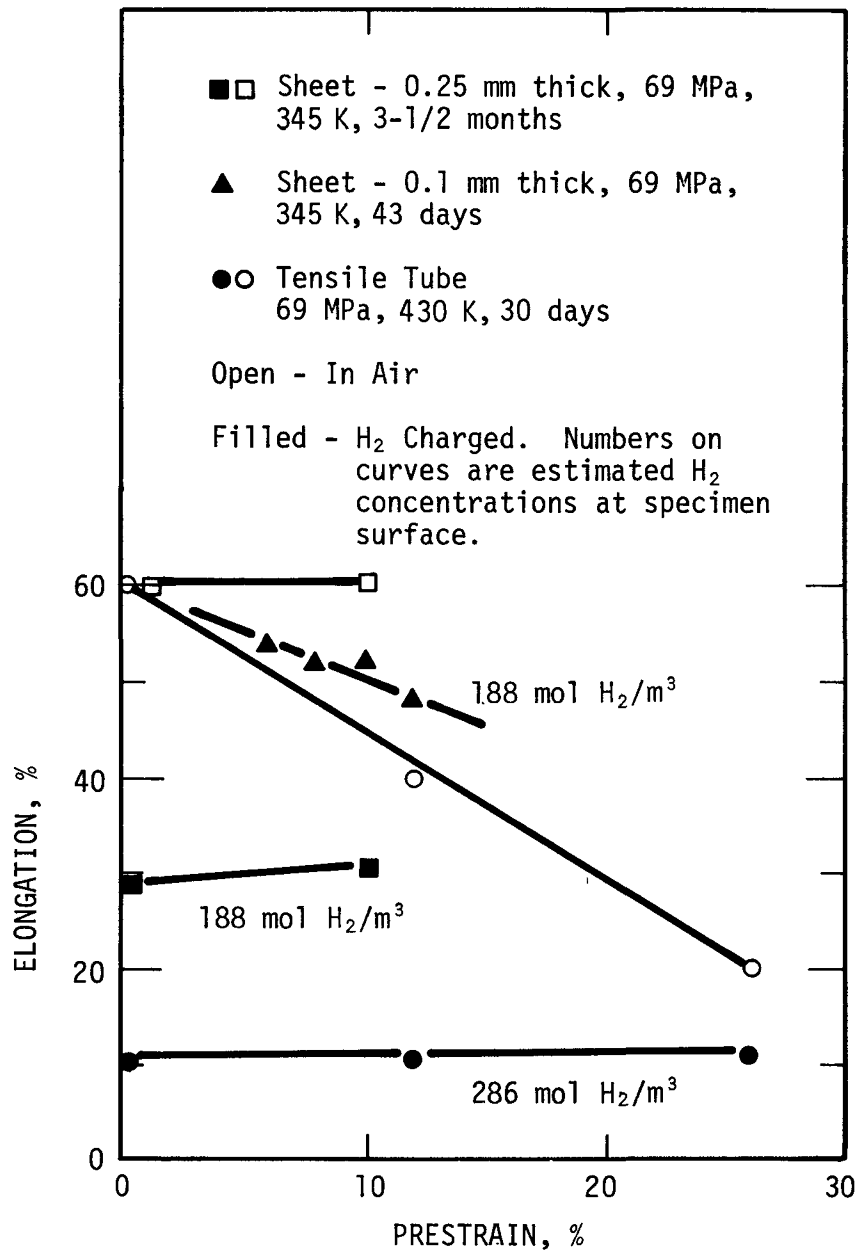

FIGURE 7. Effect of Prestrain on Elongation of Type 304L Stainless Steel in Air or Hydrogen

strength was 625 MPa for both alloys, and total elongations were 51 to 55% for the annealed sheet and 48 to 57% for the cold-worked sheet. Properties of annealed sheet were a 570 MPa tensile strength and 59 to 64% elongation prior to hydrogen exposure.

A British study on two stainless steel compositions showed that cold work increased susceptibility to hydrogen damage,[25] Figure 8. These steels have no counterpart among commercial stainless steels in the United Stated. The results further demonstrate that the effect of cold-working is greater in the 12Cr-12Ni alloy than in the 23Cr-21Ni alloy. Martensite is formed during cold-working of the former alloy, but not the latter alloy, and may account for their difference in behavior.

Tensile test data show that HERF alloys are more resistant to environmental hydrogen damage than either annealed or cold-worked alloys, Table 3. A similar result is observed for thermally charged specimens tested at room temperature. At lower test temperatures, the HERF specimens of Type 304L and Nitronic® 40 stainless steels are only marginally better than annealed specimens in terms of ductility. Yield and tensile strengths are higher in the HERF alloys, therefore, on the basis of retained ductility for a given strength level, the HERF alloys are superior to annealed alloys.

Specimens made of Nitronic® 40 cold worked 30% from HERF stock were slightly less ductile than specimens in the HERF condition during tests in high-pressure hydrogen, Figure 9. Tensile data also suggest a slight increase in susceptibility to hydrogen damage, Figure 10.

HERF develops a distinctive deformation pattern in stainless steels which has its origins in segregation in the ingot, and rolling of the plate before HERF. The effect of this pattern on susceptibility to hydrogen damage was evaluated by the J-integral. J_m, the critical force at maximum load (area under load deflection curve), and tearing resistance dJ/da (change in J with crack length, a, at maximum load), were evaluated for V-notch specimens of Type 304L, A-286, Nitronic® 50, and Nitronic® 40 stainless steels machined from HERF bars. Notches were oriented as shown in Figure 11 with respect to the forging pattern and fatigue precracked at a maximum stress intensity of 44 $MPa\sqrt{m}$. Specimens were tested in high-pressure helium or hydrogen and after prior exposure to deuterium at 69 MPa pressure for seven days at 520 K or three weeks at 620 K.

The deformation pattern caused by HERF processing affected J_m but not dJ/da for tests in high-pressure hydrogen or helium. The lowest values of J_m were for notches parallel to the flow lines, an effect especially pronounced in A-286 and Nitronic® 50

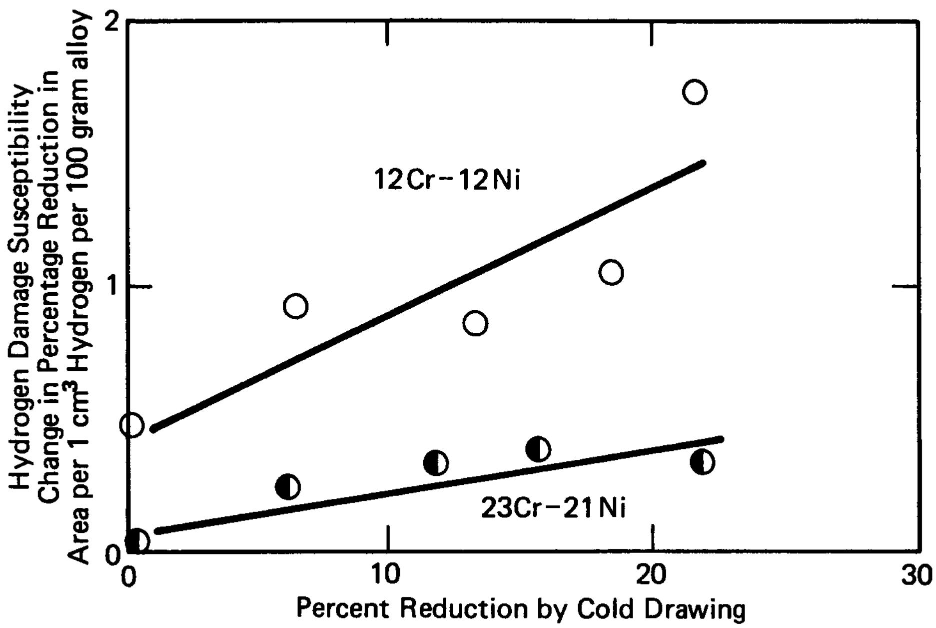

FIGURE 8. Effect of Prior Cold Work on Hydrogen Damage Susceptibility of Stainless Steels

TABLE 3

Mechanical Properties of HERF and Annealed Alloys in High-Pressure Gas

Alloy	Condition	Test* Environment	Strength, MPa** Yield	Ultimate	Ductility % Elong	Ra
304L	Annealed	He	186	565	74	81
		H_2	206	503	48	33
	HERF	He	490	660	43	77
		H_2	490	670	41	69
310	Annealed	He	179	483	67	82
		H_2	186	486	66	79
	HERF	He	470	606	21	71
		H_2	460	620	24	70
Nitronic® 40	Annealed	He	352	689	58	78
		H_2	358	696	59	77
	HERF	He	570	780	34	75
		H_2	570	790	30	73
A-286	Annealed	He	724	1117	26	47
		H_2	710	1131	34	49
	HERF	Air	875	1060	24	29
		H_2	834	1110	27	32
CG27	Annealed	He	806	1165	29	26
		H_2	855	1117	10	12
	HERF	He	1070	1385	12	12
		H_2	1034	1138	1	3

* He = 69 MPa He; H_2 = 69 MPa H_2; Air = 0.1 MPa air.

** Yield = True stress at 5% strain.
Ultimate = True stress at maximum load.

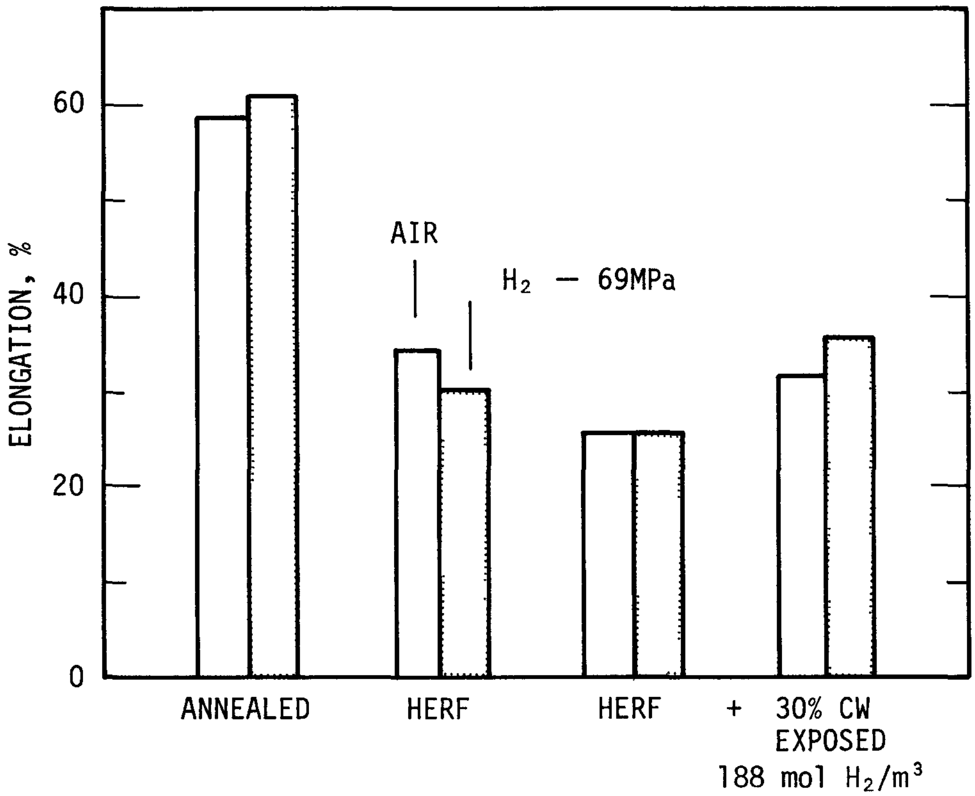

FIGURE 9. Effect of Processing on Hydrogen Damage in Nitronic® 40 Elongation

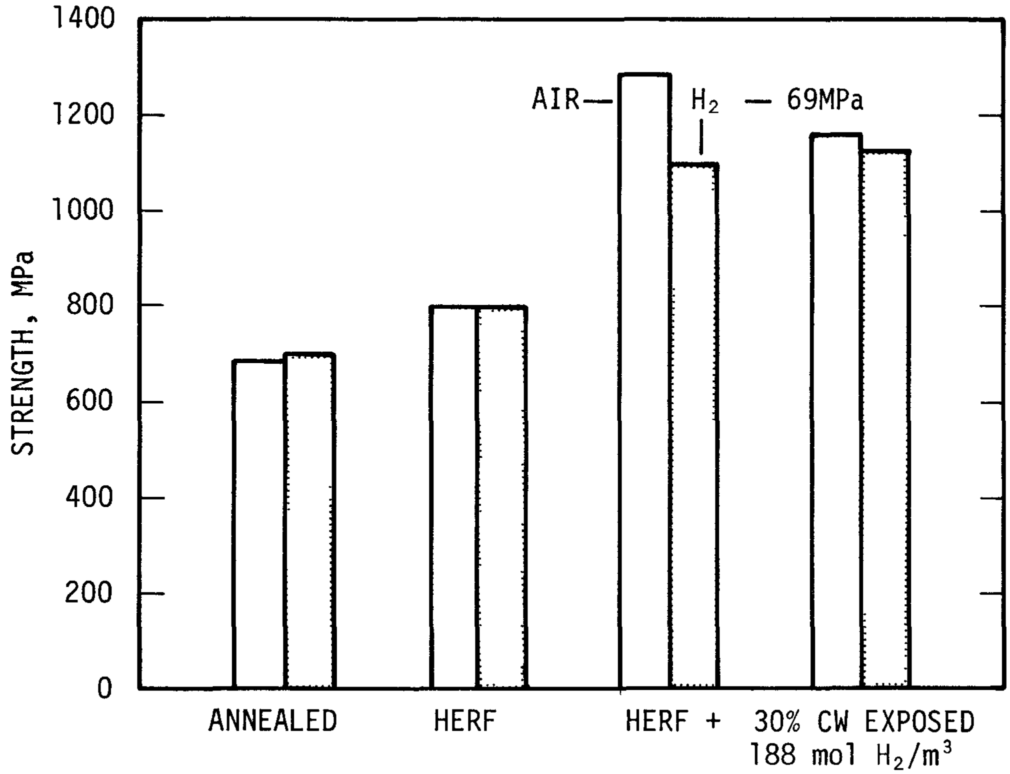

FIGURE 10. Effect of Processing on Hydrogen Damage in Nitronic® 40 Strength

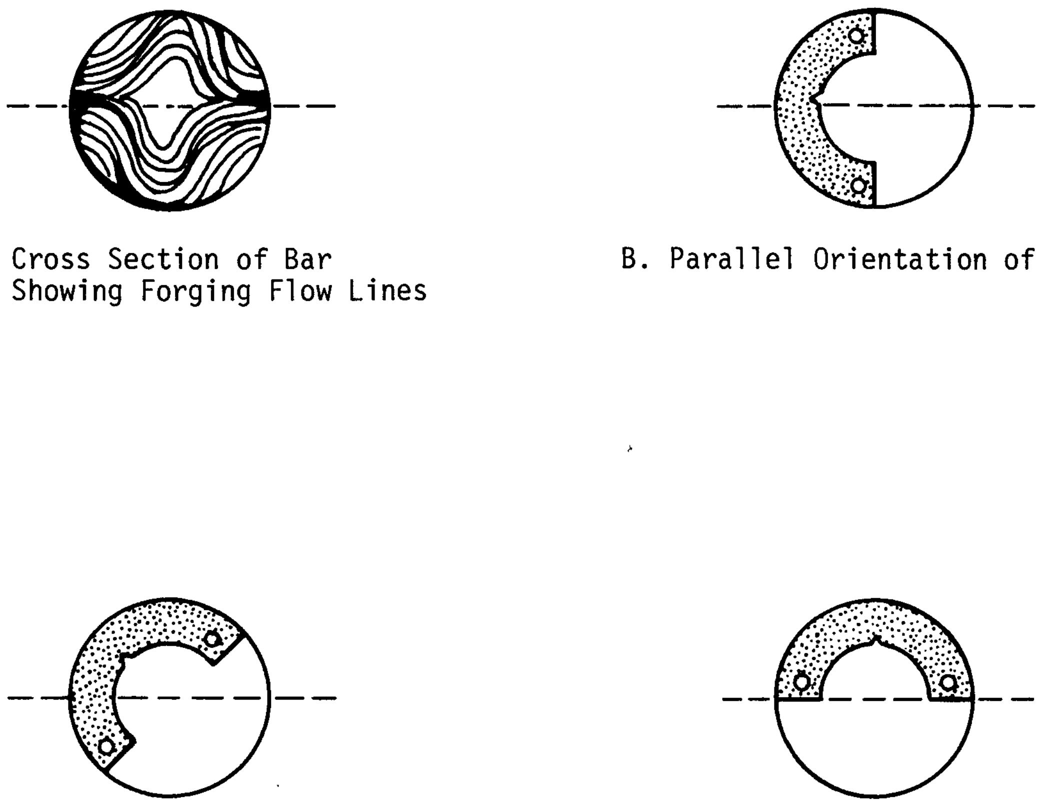

A. Cross Section of Bar Showing Forging Flow Lines

B. Parallel Orientation of Notch

C. 45° Orientation of Notch

D. 90° Orientation of Notch

FIGURE 11. Orientation of V-Notch with Respect to Forging Flow Lines in Tensile-Test Specimens Machined from Bass of HERF Stainless Steels

stainless steel. However, hydrogen damage as measured by J_m was greatest for notches 90° to the flow pattern except for Nitronic® 40, where damage was greater for 0 and 45° orientations than for the 90° orientation. dJ/da was affected relatively less by hydrogen damage than J_m.

Changes in J_m and dJ/da caused by hydrogen charging prior to testing were alloy and orientation dependent. Hydrogen exposure of A-286 stainless steel decreased J_m and dJ/da. For Type 304L stainless steel, dJ/da was unaltered and J_m was decreased for 45° and 90° orientations. For Nitronic® 40, J_m and dJ/da were increased by hydrogen exposure prior to testing, possibly because of microstructural changes that occurred during hydrogen charging.

Effect of Martensite

The above results show that the effect of cold work on hydrogen damage is variable and may be linked to martensite. A study was made of the relation between martensite and hydrogen damage. Martensite was formed in annealed specimens of Type 304L austenitic stainless steel either by thermal or mechanical treatment. Specimen surfaces were electropolished to remove the deformed outer layer that is generated during machining. This layer contains some α'-martensite in Type 304L stainless steel. The volume fracture martensite formed by the various treatments was not measured directly, but the relative quantity of martensite was indicated by the magnetic response of the specimens. The specimens were pulled to failure in a high-pressure (69 MPa) hydrogen atmosphere following thermal or mechanical treatment. Thermal treatment consisted of quenching specimens to 77 K in liquid nitrogen and holding at temperature for 10 minutes. Three mechanical treatments were used: cold reduction of 12 or 26% by cold swaging, torsional strain (70-in. lb) at room temperature or 77 K, and 10% tensile strain at room temperature or 77 K. Tensile strain at room temperature caused some transformation to ε-phase and α'-martensite formation.

Uniform elongation and plastic strain to failure for each of the treatments are reported in Table 4. Magna-gage® (American Instrument Company) readings following treatment and prior to tensile testing are given. Several important observations are apparent from inspection of the table: ductility is reduced when martensite is present prior to testing; hydrogen embrittlement does not correlate simply with volume fraction martensite, as the highest Magna-gage® readings (B) do not correspond to lowest ductility (F); the presence of an applied stress during the quench to 77 K suppresses transformation to α'-martensite (B, C, and D); the radial distribution of the martensite and possibly its orientation relative to the applied stress affect hydrogen embrittlement (B, C, F).

TABLE 4

Effect of Martensite on Subsequent Environmental Hydrogen Damage in Type 304L Stainless Steel

Treatment	Ductility Uniform Elongation	Fracture Strain	Magna-gage® Reading
A. Annealed-electropolished	79	1.31	0
B. Immersed in liquid nitrogen for 10 min	51	0.45	90 - 100
C. Applied torque and immersed in liquid nitrogen for 10 min	58	0.38	30
D. Applied tensile stress and immersed in liquid nitrogen for 10 min	60	0.42	13
E. 10% plastic strain at room temperture	75	1.11	0
F. 7.9 Nm torque at room temperature	26	0.24	30

Environmental Variables Affecting Hydrogen Damage

Degradation of mechanical properties by hydrogen depends upon several factors external to the specimen: temperature, hydrogen pressure, stress state, and strain rate. These factors control how much hydrogen enters the material and how rapidly solution and distribution of hydrogen occur within the specimen. Hydrogen redistribution to regions of high stress and the hydrogen diffusion rate relative to any imposed deformation rate directly influence severity of hydrogen damage.

Hydrogen Pressure

The severity of hydrogen damage in any alloy has been shown to relate directly to hydrogen pressure whether for hydrogen-charged specimens or for testing in a hydrogen environment. As seen in Figure 12, tensile ductility of Type 304L stainless steel falls off rapidly as hydrogen pressure is increased up to 14 MPa and then more slowly up to 69 MPa. Tensile strength of notched and fatigue cracked specimens also decreases from 780 to 660 MPa as the hydrogen pressure increases from 0.1 to 6.9 MPa. For most other alloys, testing has been at fixed hydrogen pressure of 69 MPa, and data do not exist for other pressures.

A pressure effect is seen in both tensile and threshold stress intensity data for Inconel® 718.[26] Tensile strength and reduction-in-area decrease linearly with square root of hydrogen pressure at pressure above about 10 MPa. The stress intensity at crack arrest for wedge opening loaded specimens at room temperature decreased from 90 MPa $\sqrt{m}$ to about 42 MPa $\sqrt{m}$ for hydrogen pressures of 20 MPa and higher.

Hydrogen gas pressures of 69 MPa have no significant effect on the mechanical properties of Type 310 stainless steel. However, severe hydrogen damage can be induced in Type 310 stainless steel by cathodic charging where the effective hydrogen pressure is extremely high (>>200 MPa).[27]

Test Temperature

Hydrogen damage in stainless steels has been shown to be temperature dependent for alloys where appropriate testing has been done. The most severe damage occurs at 220-280 K. As seen in Figure 13, tensile ductility in several alloys is a minimum in this temperature range. There does not appear to be any significant difference between Fe-Cr-Ni and Fe-Cr-Ni-Mn alloys in this respect, Figure 14. Furthermore, the minimum ductility ratio is observed in this same temperature range even in alloys which are affected very

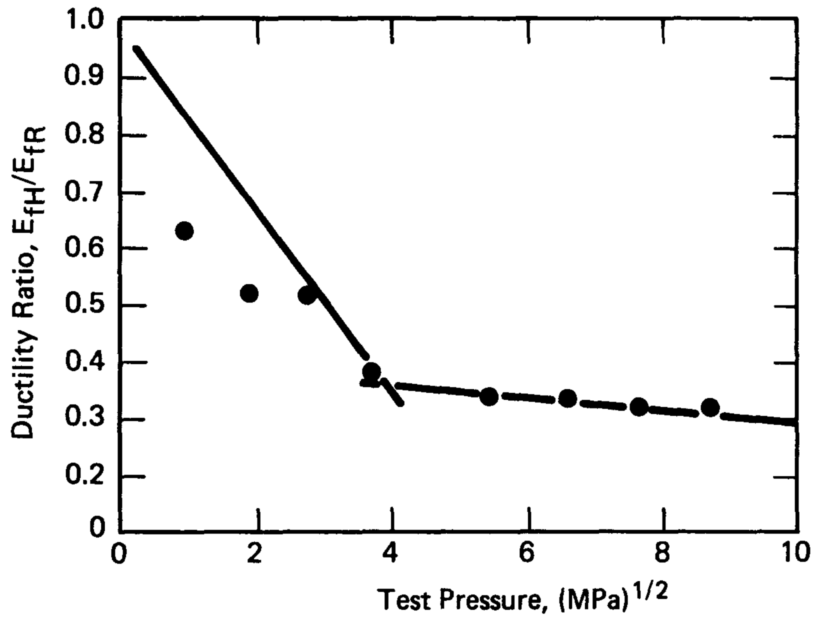

FIGURE 12. Effect of Hydrogen Pressure on Ductility of Type 304L Stainless Steel Tested to Fracture in Hydrogen at Room Temperature

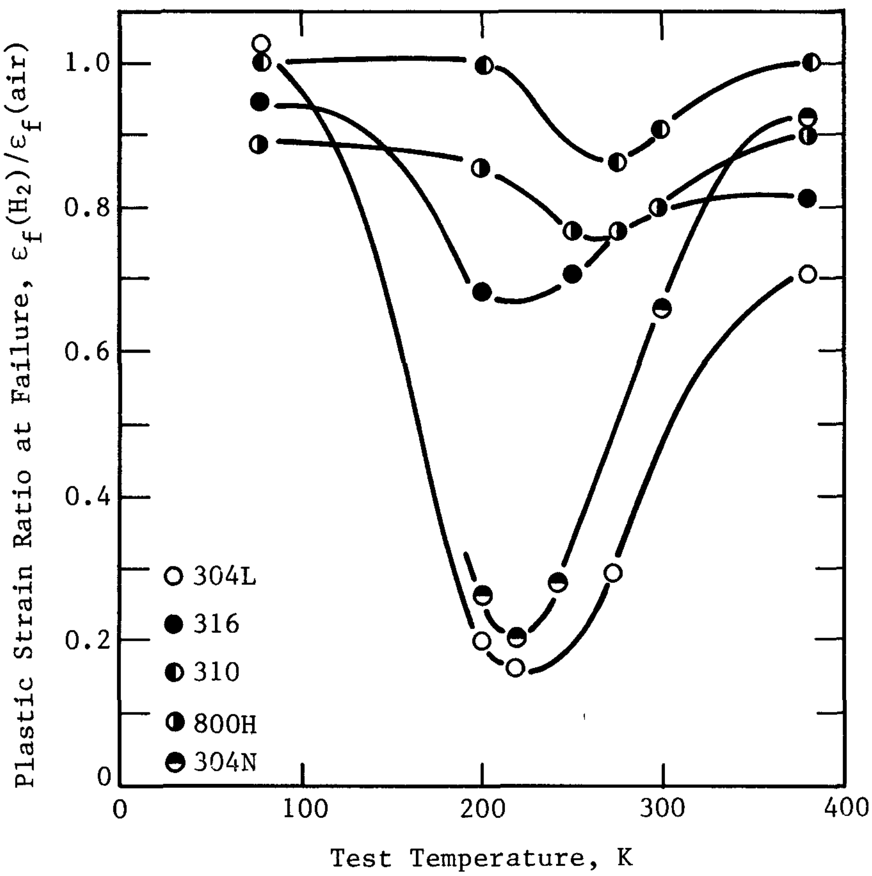

FIGURE 13. Ductility Minima in Fe-Cr-Ni Alloys Charged with Deuterium at 69 MPa and 620 K for Three Weeks

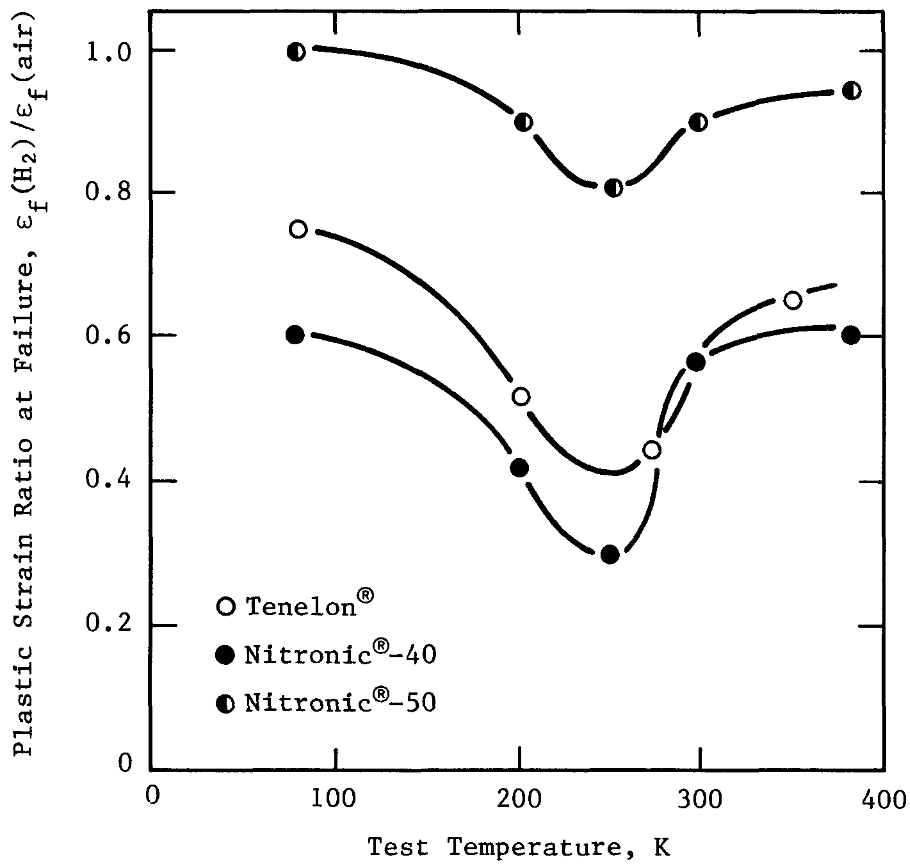

FIGURE 14. Ductility Minima in Fe-Cr-Mn-Ni Alloys Charged with Deuterium at 69 MPa and 620 K for Three Weeks

little by hydrogen, such as Nitronic® 50, Type 310, and Type 316 stainless steels. It is not known yet if the threshold stress intensity for sustained load crack growth in these stainless steels follows a similar temperature dependence. However, the data for Inconel® 718 (Huntington Alloys) lead to the inference that K_{th} and tensile ductility have a similar temperature dependence.[26]

The general trends of both test temperature and nickel content on hydrogen damage are illustrated in Figure 15 for three high-purity alloys of constant chromium content (about 18%). Isoductility lines sketched in this figure outline a region of significant hydrogen damage ($\varepsilon_p \leqslant 0.5$) at about 200-240 K that extends to 14% nickel.

Although most materials show a hydrogen-induced ductility minimum, the temperature of the minimum is not always around 220-280 K as in stainless steels. Pure nickel displays ductility minima around room temperature, at 220 K and at 150 K, but the 220 K minimum is the only one to persist over a wide range of strain rates (10^{-1} to 10^{-5} sec^{-1}).[15] Maximum hydrogen damage in Inconel® 718 is at room temperature as measured by ductility, notched tensile strength, and threshold stress intensity.[26]

Strain-induced martensite forms during low-temperature deformation of many austenitic stainless steels which are nominally stable at room temperature. For a given alloy, there is a temperature designated M_d, above which no martensite forms on deformation and below which deformation produces martensite. The amount of transformation per unit strain increases as the temperature is lowered below M_d. Table 5 lists approximate M_d temperatures for several of the austenitic steels that have been investigated. The appearance of brittle fracture and degradation of mechanical properties does not correlate with formation of strain-induced martensite. In particular, Type 316 stainless steel does not show a significant change in fracture strength or fracture mode between 250 K (no martensite) and 200 K (martensite present).

Magnetic measurements on specimens of Type 304L stainless steel strained incrementally at 200 K show that hydrogen suppresses formation of strain-induced martensite, Figure 16. However, hydrogen appears to enhance martensite formation during deformation at 250 and 298 K. Suppression of martensite formation was seen also in Tenelon® at 200 K and Nitronic® 40 at 78 K, Figure 17.

Stress State and Strain Rate

Plastic deformation and fracture characteristics are affected by stress state and strain rate. Severity of hydrogen damage,

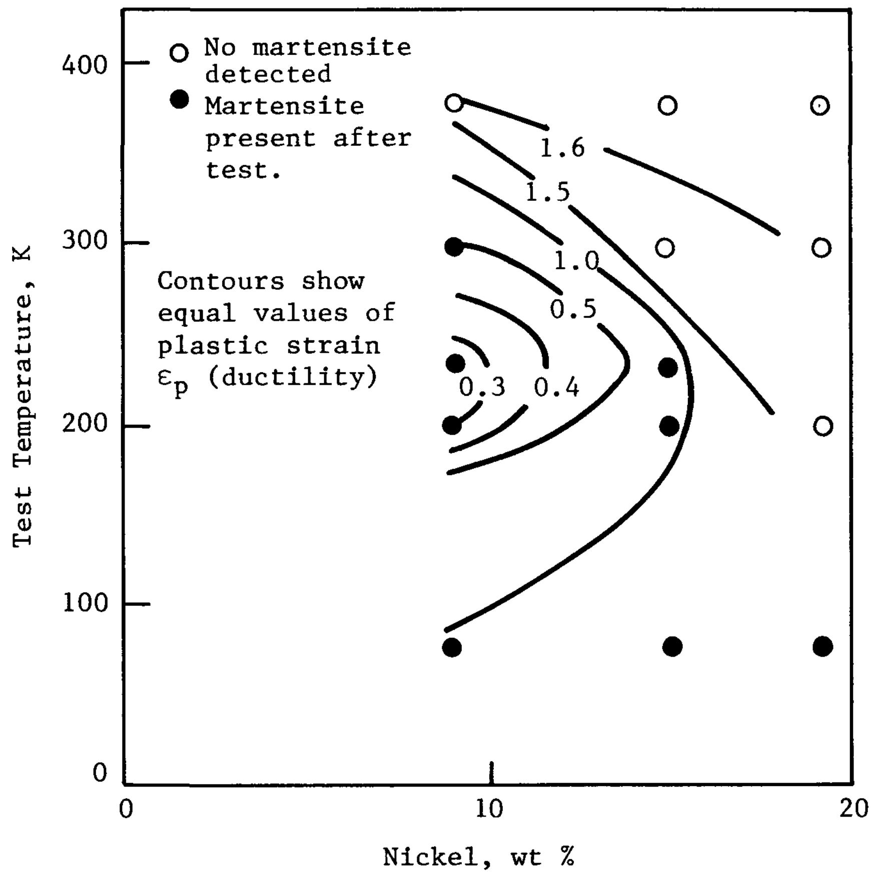

FIGURE 15. Isoductility Diagram for Hydrogen-Charged Fe-Cr-Ni Alloys

TABLE 5

Temperatures for Strain-Induced Martensite Formation

Alloy*	M_d Temp, K
304L	350
310	<4
316	220
I800H	<78
Tenelon®	200*
Nitronic® 40	~100
Nitronic® 50	~150
A	>370
B	250
C	150

* Martensite forms at temperatures near 200 K, but not at either higher or lower temperatures.

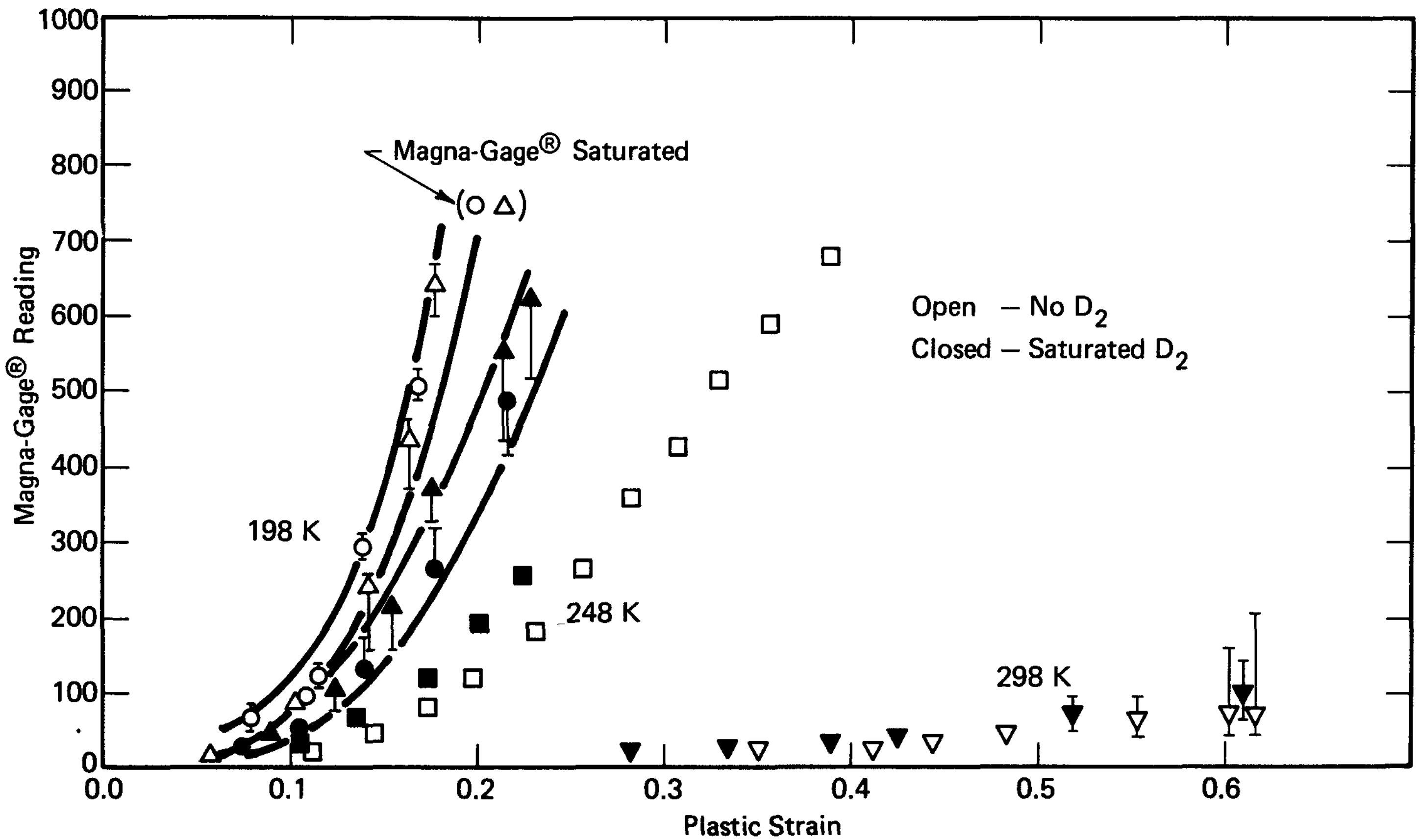

FIGURE 16. Effect of Hydrogen on Strain-Induced Martenite Formation in Type 304L Stainless Steel

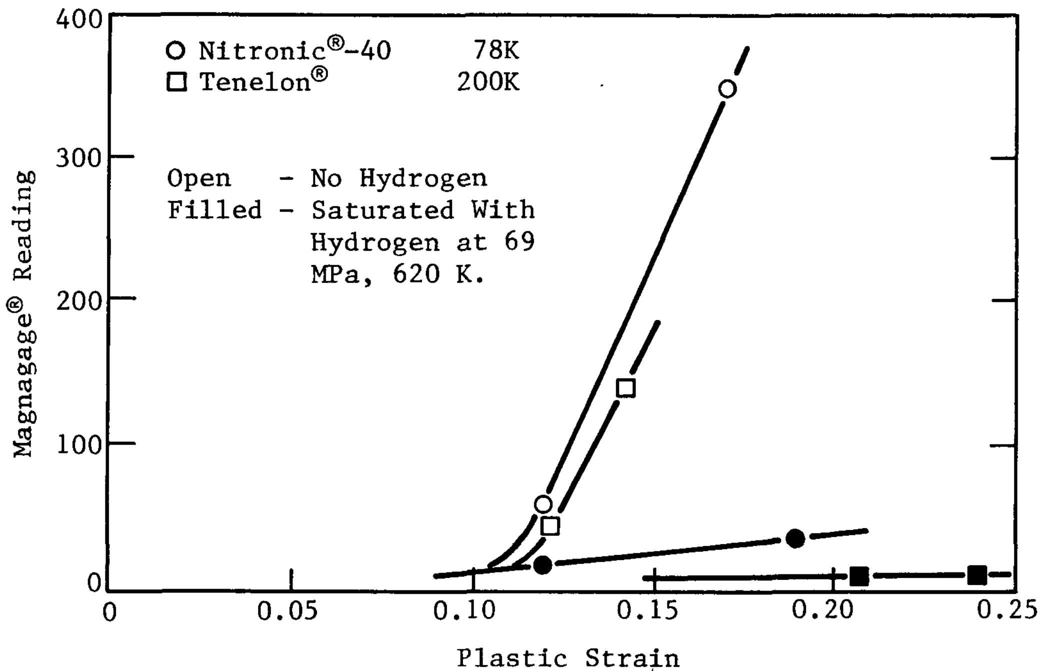

FIGURE 17. Effect of Hydrogen on Strain-Induced Martenite Formation in Tenelon® and Nitronic® 40

therefore, is also affected by stress state and strain rate. Different test methods may assess hydrogen degradation of mechanical properties differently, depending upon how stress state and strain rate influence hydrogen interactions with the alloys.

A biaxial stress state occurs during burst testing of discs. Hydrogen environment damage may be assessed by pressurizing discs of the same material with helium or hydrogen gas and measuring the burst pressure.[28] A ratio of burst pressures of one indicates no hydrogen damage, whereas ratios greater than one indicate hydrogen damage with severity of damage increasing as the ratio increases. Steels such as A-286, Type 310, and Type 316 are relatively immune to hydrogen damage in this test; CG-27 behaves poorly; and Type 304 or 304L are variable, depending upon the treatment prior to testing. The ranking of the alloys in the disc burst test is generally the same as for notch tensile tests in helium and hydrogen for a pressure of 69 MPa.

Notch Tensile Tests. Stress concentration and plastic constraint at the root of a notch can increase the severity of hydrogen damage under some circumstances. Notched specimens of Type 304L and Nitronic® 40 stainless steels tested in high-pressure hydrogen at room temperature illustrate the notch effect. The strength and ductility of the notched specimens are degraded more than that of the smooth specimens, Figures 18 and 19. In contrast, ductility loss in notched specimens of hydrogen-charged Type 304L stainless steel was less than in smooth specimens, Table 6. However, absolute ductility of the notched specimens is less than for smooth specimens. Hydrogen charged specimens of Nitronic® 40 were more severely damaged when notched than when smooth, as was the case for tests in a hydrogen environment.

J-Integral Analysis. C-shaped and notched specimens were fatigue cracked and then tested in hydrogen or helium at 69 MPa pressure. Susceptibility to environmental and internal hydrogen damage was evaluated by comparing J-integral values at maximum load (J_m) and dJ/da for four stainless steels machined from HERF bar stock. Ranking of the alloys was not consistent and depend on which specimen orientation was chosen for the comparison (Table 7).

Based on plastic strain to failure (reduction in area), HERF Type 304L stainless steel is more susceptible to environmental hydrogen damage than HERF Nitronic® 40 stainless steel in direct opposition to the ranking based on J_m. These measures of hydrogen damage are biased differently, however, with respect to deformation and fracture. J_m depends on flow stress and plastic strain up to the point where crack advance is assumed to begin. Plastic strain to failure, on the other hand, is affected strongly by the ability of the alloy to neck down without breaking and is effectively sampling a region of deformation not included in J_m.

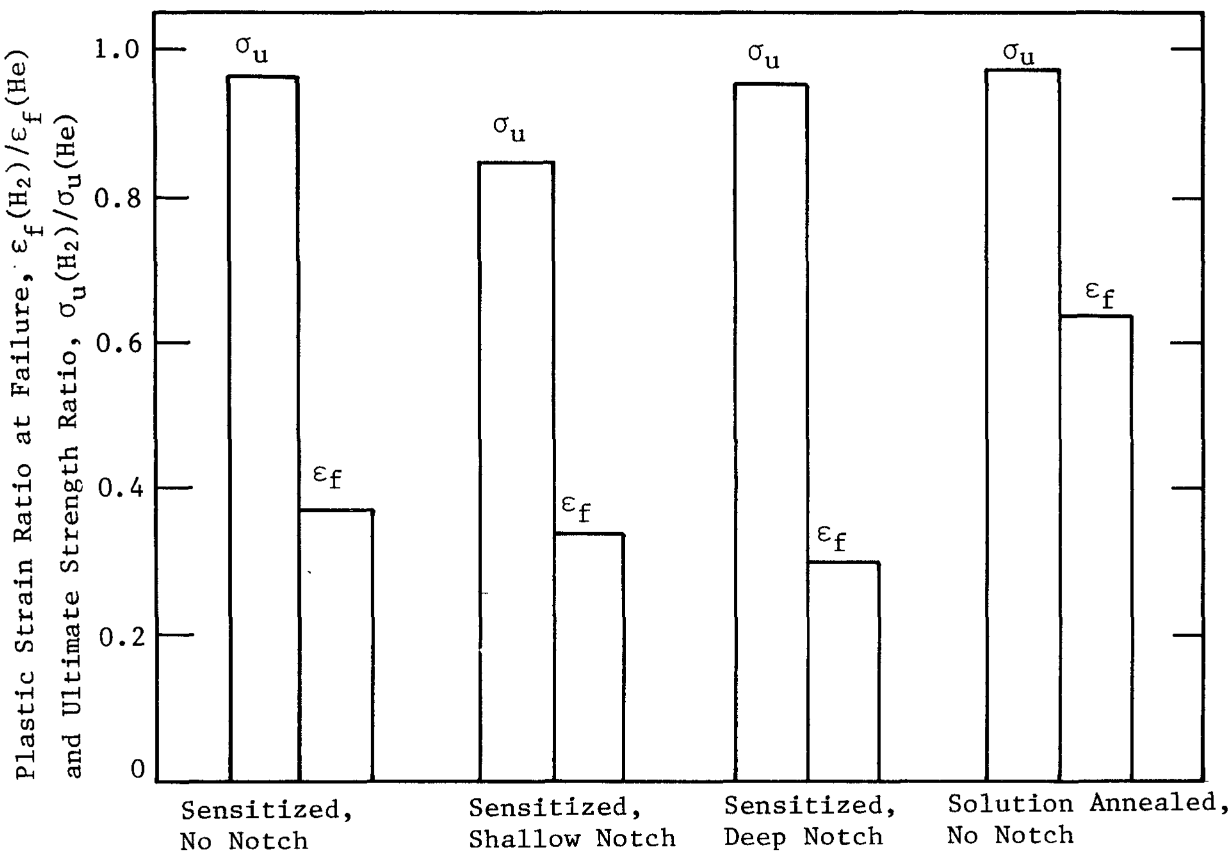

FIGURE 18. Relative Effect of Hydrogen on Properties of Sensitized Type 304L Stainless Steel

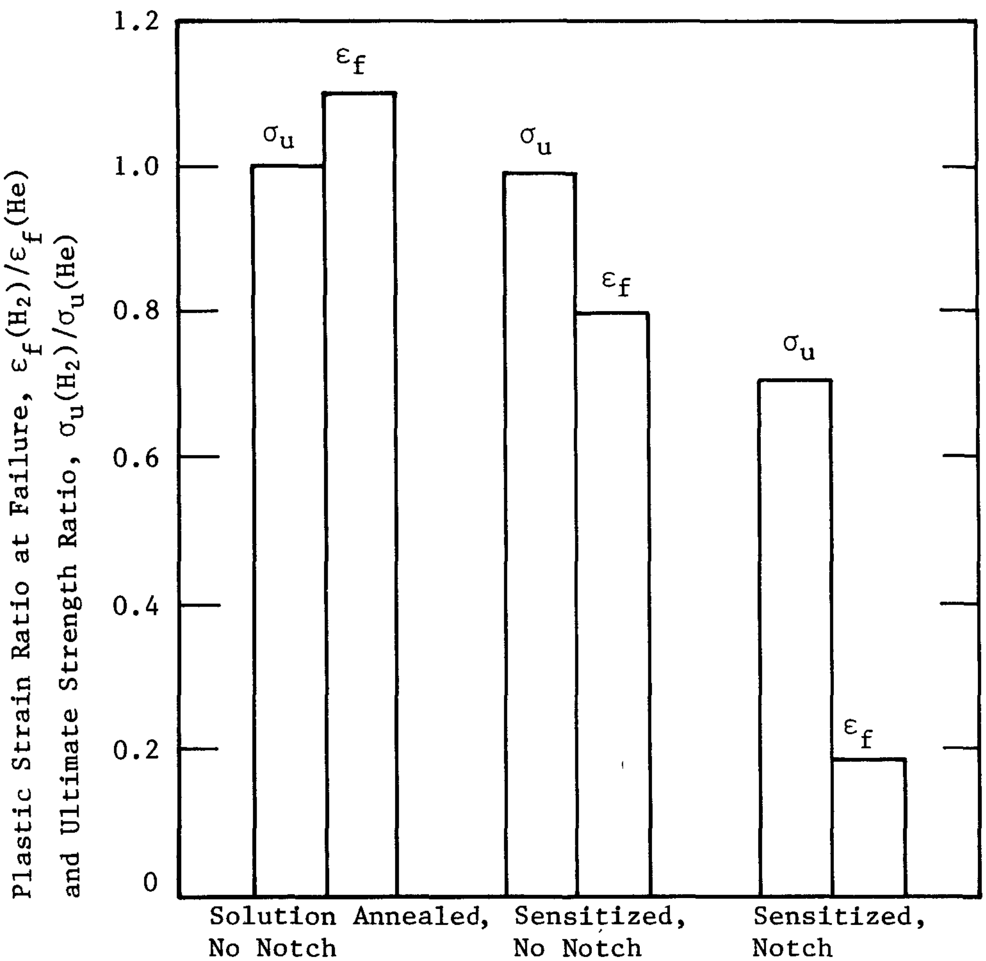

FIGURE 19. Environmental Hydrogen Damage in Nitronic® 40 Stainless Steel at Room Temperature

TABLE 6

Effect of Hydrogen Charging on Tensile Properties of Type 304L Stainless Steel

Condition	Specimen	Nominal Tensile Strength, MPa	Plastic Strain To Failure
As received	Smooth	600	1.50
	Notch	770	0.30
Annealed*	Smooth	600	1.43
	Notch	710	0.24
Hydrogen charged**	Smooth	530	0.37
	Notch	580	0.13

* Annealed 200 days at 380 K in argon.

** Exposed to hydrogen gas at 69 MPa for 200 days at 380 K.

TABLE 7

Ranking of Hydrogen Compatibility (HERF Stainless Steels)

Environmental Hydrogen		
J_m	dJ/da	Tensile* Ductility
A-286**	A-286 Nitronic® 40**	Nitronic® 40
304L Nitronic® 40	Nitronic® 50**	304L
Nitronic® 50**	304L	

Internal Hydrogen		
J_m**	dJ/da	Tensile* Ductility
Nitronic® 40 Nitronic® 50	Nitronic® 50 Nitronic® 40	Nitronic® 40
304L	304L	304L
A-286	A-286	

* Orientation dependence not measured.

** Ranking is orientation dependent.

Furthermore, compact tensile specimens such as the C-shaped specimens of this study are not susceptible to unstable plastic tearing, whereas tensile specimens can be driven to tearing instability by internal microcracks in the necked region.

There is agreement in ranking of HERF Type 304L and HERF Nitronic® 40 stainless steels between tensile ductility and tearing resistance, dJ/da. In both cases, HERF Nitronic® 40 stainless steel is less susceptible to hydrogen damage. In this comparison, both parameters are influenced by the deformation and crack growth processes that succeed the onset of crack growth at load maximum.

Static Loading. Static loading may lead to slow-crack growth in high-pressure hydrogen in some stainless steels, Figure 20.[26,29-33] The only alloys where crack growth was not seen had yield strengths below 800 MPa. The specimens were too thin to permit reaching a stress intensity high enough to cause crack growth. In all cases, the threshold stress intensities are substantially less than the fracture toughness. The scatter band for fracture toughness derives from valid J-integral tests made at 4.2 or 77 K. K_{IC} may be higher or lower at room temperature depending upon the steel.[34-35]

Crack propagation has been observed in notched specimens of Type 304 stainless steel at stresses equal to 80% of the ultimate tensile strength.[29] These tests were in dry hydrogen at one atmosphere pressure at room temperature. A notched tensile specimen of Type 304L stainless steel failed after 41 hours in air under a stress of 490 MPa, or 85 percent of the notch tensile strength. This specimen had been exposed to D/T for 200 days at 69 MPa and 380 K. An unexposed control specimen survived 200 hours at 650 MPa (85% of notch tensile strength) without failure. In another experiment with smooth specimens of Type 304L stainless steel, no crack growth was observed after cathodic charging for stresses close to the ultimate tensile strength.[30] As seen in Table 8, a pre-existing crack did not progagate in Type 304L stainless steel tensile tube until the stress reached a very high level. Also, crack growth has not been observed in Type 310 stainless steel at 80% of the ultimate strength.[29] In A-286 stainless steel, hydrogen enhanced crack growth was observed at stresses above the yield strength, but tensile properties were unaffected by exposure to 69 MPa hydrogen.[31] The threshold stress intensity for crack growth in 35 MPa hydrogen was less than 113 MPa $\sqrt{m}$ compared to greater than 154 MPa $\sqrt{m}$ in helium.

Measurements of sustained-load cracking were made on a modified A-286 stainless steel (JBK-75) in hydrogen gas at 100 and 200 MPa pressure.[32] Yield strengths varied from 690 to 930 MPa with different thermomechanical treatments. Crack advance was intergranular

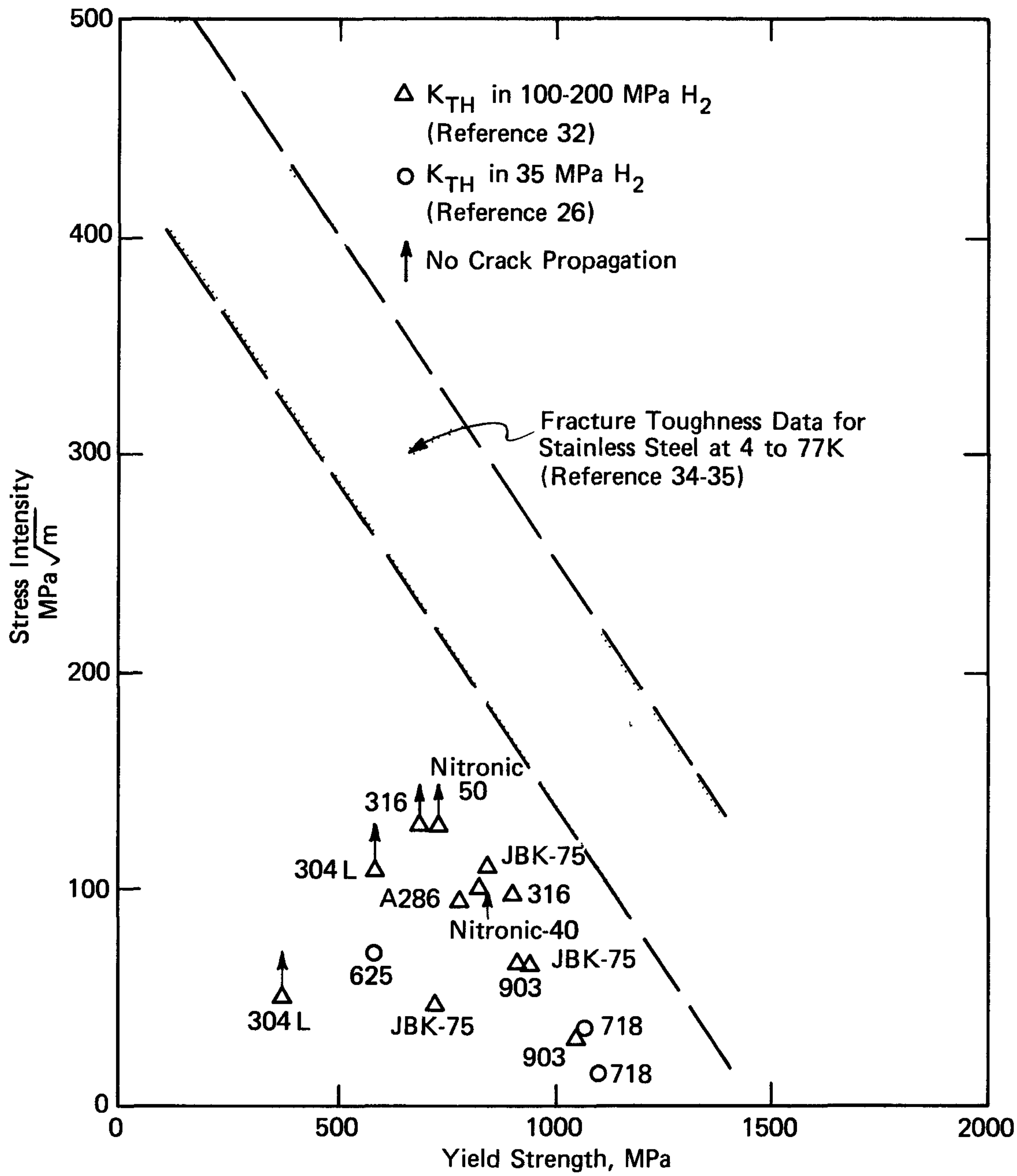

FIGURE 20. Hydrogen Effects on Crack Growth in Stainless Steels

TABLE 8

Stress Necessary for Slow-Crack Growth in Type 304L* Stainless Steel

Net Section Stress, MN/m^2	Time, Hours Incremental	Time, Hours Accumulated	Crack Growth
600	325	325	No
641	72	397	No
682	72	469	No
724	72	541	No
765	72	613	No
786	1.4 (failed)	614.4	Yes

* Crack developed during room temperature tensile test in hydrogen environment; net section stress when tensile test was stopped was 772 MN/m^2. Specimen then loaded in creep frame at indicated stresses without removal from the hydrogen environment.

at threshold stress intensities of 110 to 44 MPa $\sqrt{m}$. The presence of grain-boundary precipitates led to the lowest threshold stress intensities. Slow-crack growth was also seen in Nitronic® 40, where the threshold stress intensity was around 100 MPa $\sqrt{m}$. Sustained load crack growth was not observed in HERF Type 304L, HERF Type 316, or HERF Nitronic® 50 stainless steels at either 100 or 200 MPa hydrogen pressure.[32]

Inconel® 718 is the only alloy for which hydrogen compatibility has been systematically evaluated by several test methods.[26] Mechanical tests included notched- and smooth-bar tensile tests, low- and high-cycle fatigue, fracture mechanics, disc pressure tests, and stress rupture. Ductility of notched tensile specimens and fatigue life were more severely degraded than the other properties. Notched tensile and disc pressure tests were sensitive to hydrogen damage at pressures below about 6.9 MPa. These results and tests on other materials suggest that notched tensile and disc pressure tests are suitable for screening alloys for possible hydrogen service. However, selection of a test method for more detailed investigation depends not only on sensitivity of the method and severity of degradation but also on how well the test duplicates loading conditions and hydrogen pressures for the intended service application and possible material flaws.

Strain Rate. Hydrogen-assisted fracture in Type 304L stainless steel displays an inverse strain rate effect. This effect is common in all metals where hydrogen-assisted fracture is observed. The more usual strain rate effect, observed in low-temperature brittleness of carbon steels for example, is for higher strain rates to increase brittleness. The inverse strain-rate effect in hydrogen-assisted fracture has been cited as evidence that hydrogen diffusion to high stress regions is necessary for embrittlement.

FRACTOGRAPHY

Detailed examination of fractured specimens has been carried out in recent years by scanning electron microscopy (SEM) which is the basis for the descriptions of fracture modes in this section.

Fracture Modes

Ductile fracture of stainless steels occurs ordinarily by a process of microvoid coalescence. Decohesion at the matrix-inclusion interfaces or fracture of brittle inclusions creates microvoids. The material between the voids fails by localized flow or shear. This process originates throughout the individual grains with no preferred fracture path, leading finally to the common cup-cone or slant fracture.

Hydrogen-assisted fracture of stainless steels is not associated with a unique fracture mode. On a macroscopic scale, fractures are mixed mode, partly flat, and partly slant or a modified cup-cone fracture. The microscopic fracture modes observed in hydrogen-assisted fracture of stainless steels are microvoid coalescence, cleavage, twin-boundary parting, intergranular separation, and interphase separation. In the following section, these fracture modes are described and related where possible to alloy composition, treatment, and external conditions, such as temperature and stress state.

Microvoid Coalescence

Most hydrogen-assisted fractures of stainless steels are, to some extent, ductile, with areas of dimpled fracture evident even when gross ductility is only 10 to 20%, Figure 21. With some alloys and test conditions, a change in dimple size is evident for the HAF. Dimple diameters were measured for several Type 304L stainless steel specimens, both with and without prior exposure to hydrogen. The average dimple size in HAF was always smaller than that for fracture of hydrogen-free specimens. Loss of tensile ductility has been correlated with change in dimple size for austenitic steels. The larger the change in dimple size, the greater the ductility loss. However, the results from tensile tests of Type 304L steel at 250 and 270 K do not fall on the published curve, which was derived from room temperature tensile tests.[17]

Twin-Boundary Parting

Twin-boundary parting, in Figure 22, was the characteristic mode of HAF in Type 304L stainless steel, Tenelon®, and Nitronic® 40. The incidence of this fracture mode was strongly dependent on temperature and composition. For example, twin-boundary parting was observed in Type 304L stainless steel but not in Type 316 stainless steel. The most clearly defined examples of twin-boundary parting occurred at test temperatures of 200 to 250 K in Type 304L stainless steel, at 78 and 200 K in Tenelon® and at 200 K in Nitronic® 40. Twin-boundary parting is observed in Tenelon® at 78 K even when there is no hydrogen present.

Examination of numerous fractures has shown that twin-boundary parting is characterized by the following features:

- A single facet extends over one grain only.
- Facets usually have steps about 5 μm in height.
- Traces of deformation bands in the underlying grain are visible.

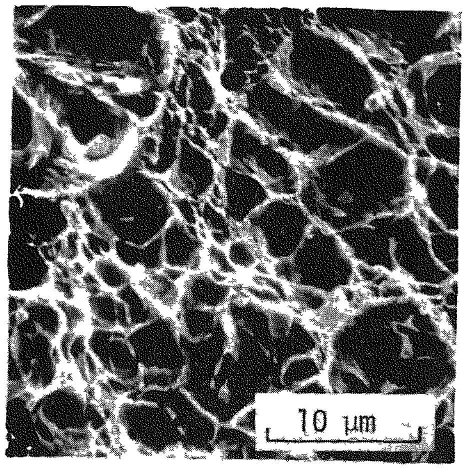

FIGURE 21. Dimpled Fracture of Type 304L Stainless Steel

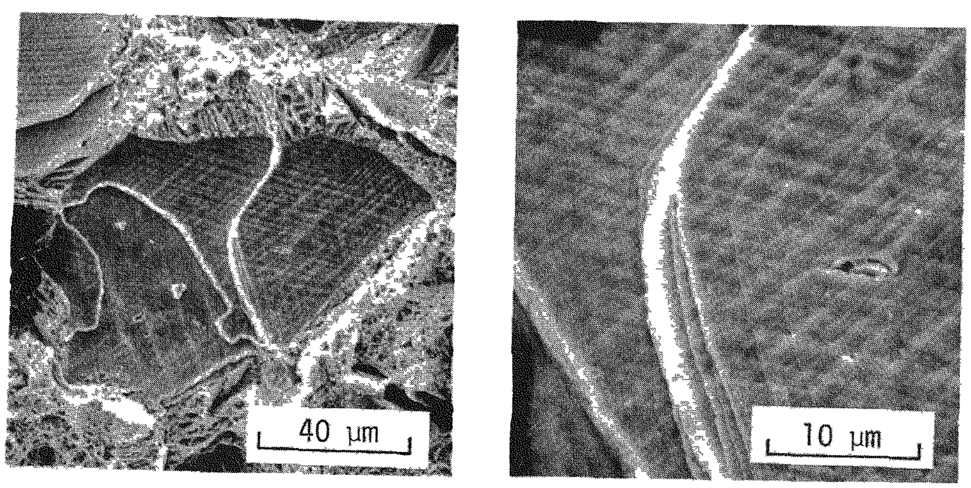

FIGURE 22. Twin-Boundary Parting in Type 304L Stainless Steel. High Energy Rate Forged. Tested at 200 K.

- Opposing halves of the fracture match and interlock.

- Facets are slightly curved because of lattice bending prior to separation along the twin boundary.

- River patterns characteristic of cleavage are never seen.

On a longitudinal section of a tensile specimen, twin-boundary parting shows as microcracks throughout the deformed portion of the specimen. Microcracks form on boundaries oriented roughly transverse to the tensile axis, Figure 23. The frequency of occurrence of microcracks correlates with the temperature of maximum hydrogen damage, Table 9, just as the number of facets on the fracture face varies with temperature, Figure 24. Multiple nucleation of microcracks is seen also, Figure 25, and suggests that twin-boundary parting proceeds by the linking of many cracks which nucleate at intersections of deformation bands with the twin-boundary. Acoustic emission confirms the notion that crack growth is by many small steps rather than one abrupt energy release.

Transgranular Cleavage

Transgranular cleavage was a form of HAF observed in ferritic and martensitic stainless steels. For example, the fracture mode of 17-4PH was predominatly transgranular cleavage as seen in Figure 26. This fracture mode can yield facets similar to those of twin-boundary parting, but the facets are readily distinguished at high magnification by the occurrence of river patterns.

Intergranular Separation

Intergranular separation was characteristic of HAF of alloys containing more than about 30 or 35% nickel but was not limited to these alloys. Commercial grades of nickel displayed the most clearly delineated intergranular separation, Figure 27. However, specific thermal treatment could evoke intergranular separation in most alloys. In the case of nickel, intergranular separation was increased by prolonged heating at 770 K.

Intergranular separation has been observed in C-shaped specimens of HERF Nitronic® 40 and A-286 stainless steel also, Figure 28. Precharging with hydrogen is needed to evoke the intergranular separation. The presence of intergranular fracture in C-shaped specimens and its absence in smooth bar tensile specimens suggests that stress state affects fracture mode in stainless steels. There is a bending moment on the C-shaped specimens which is absent in a tensile test.

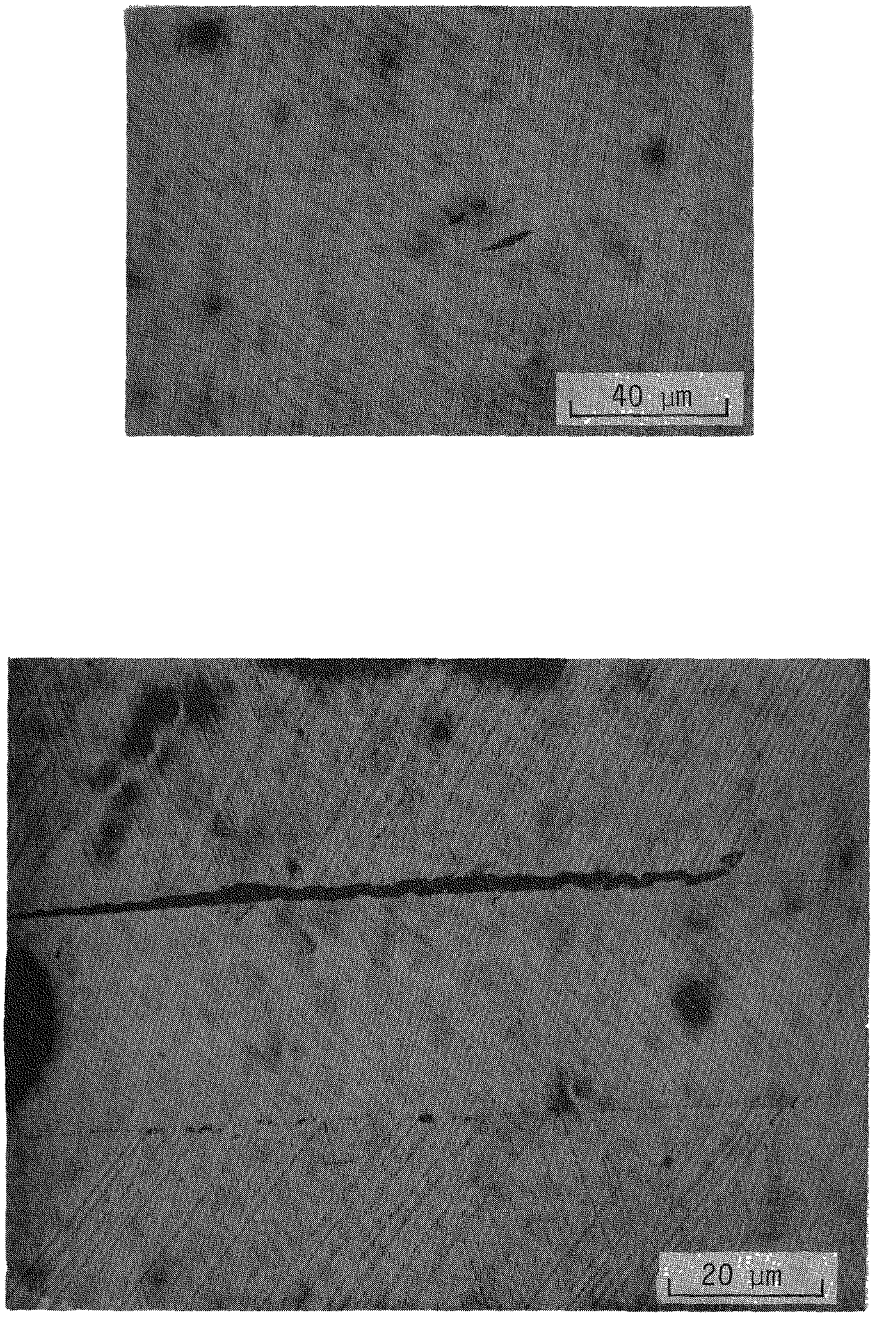

FIGURE 23. Microcracks Along Boundaries of Annealing Twins

TABLE 9

Occurrence of Microcracks in Hydrogen-Saturated Austenitic Stainless Steel

Test Temp, K	Microcrack Frequency (Number Cracks/cm^2) Type 304L	Tenelon®	Nitronic® 40
380	0	-	0
348	-	0	-
298	-	-	60
273	90	900	-
248	150	-	230
198	1800	1100	1400
78	0	(4)*	0

* Number of microcracks observed in close proximity to the fracture surface.

All specimens saturated with deuterium at 69 MPa pressure at 570-620 K.

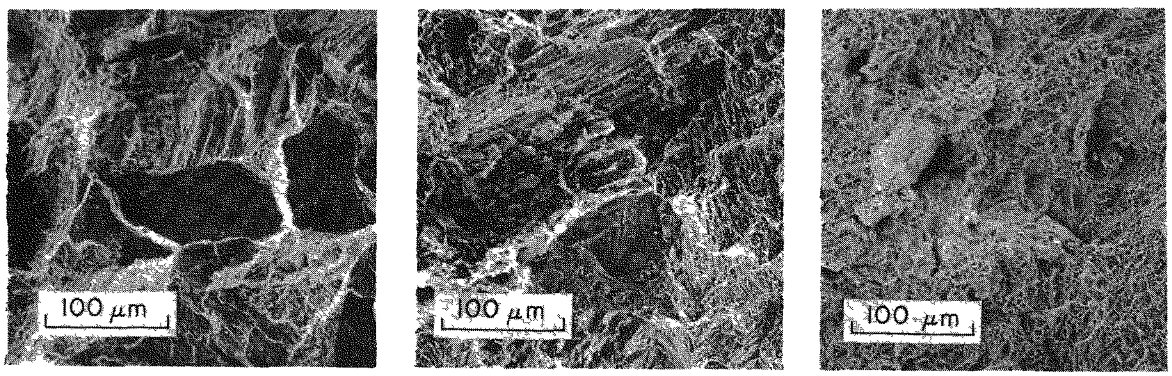

198 K 273 K 298 K

FIGURE 24. Variation of Facet Appearance with Test Temperature in Type 304L Stainless Steel

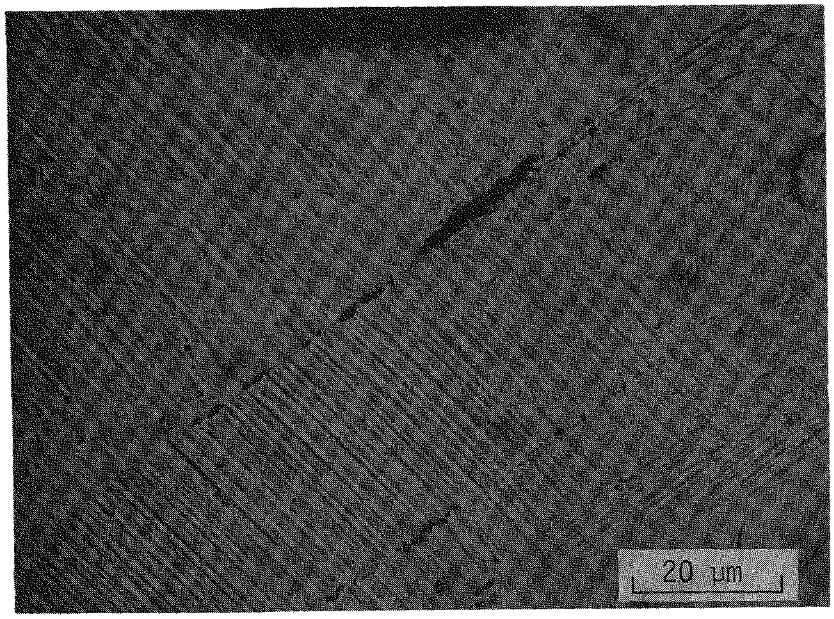

a) On Twin Boundary

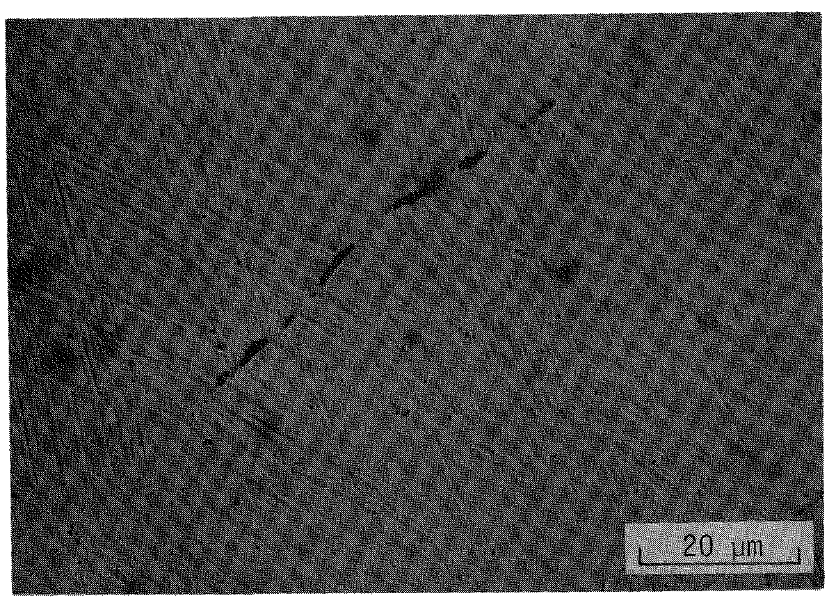

b) On Grain Boundary

FIGURE 25. Multiple Crack Nucleation Along Boundaries

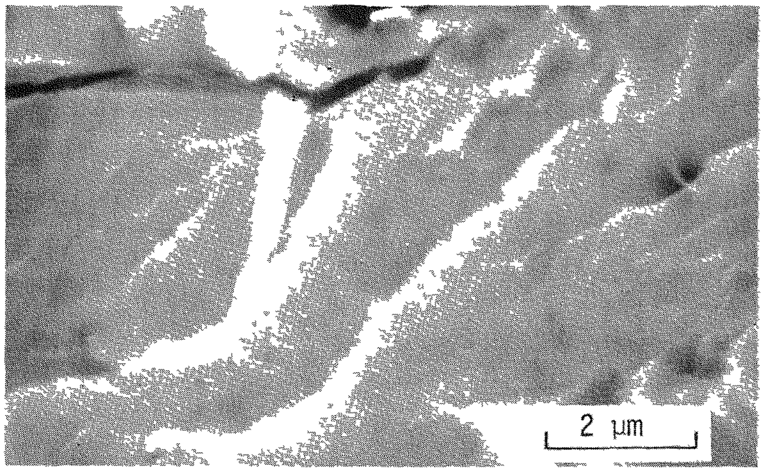

FIGURE 26. Transgranular Cleavage in 17-4 PH
Precipitation-Hardenable Stainbless Steel

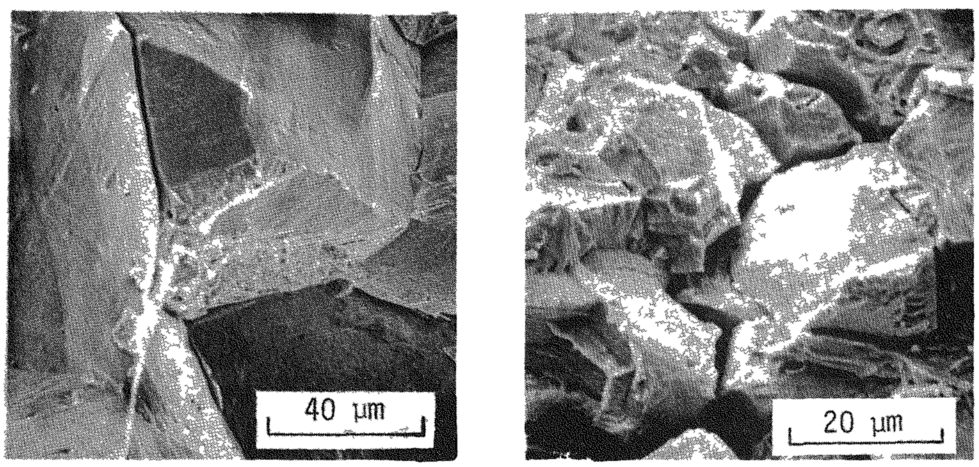

FIGURE 27. Intergranular Separation in Nickel and Inconel® 718

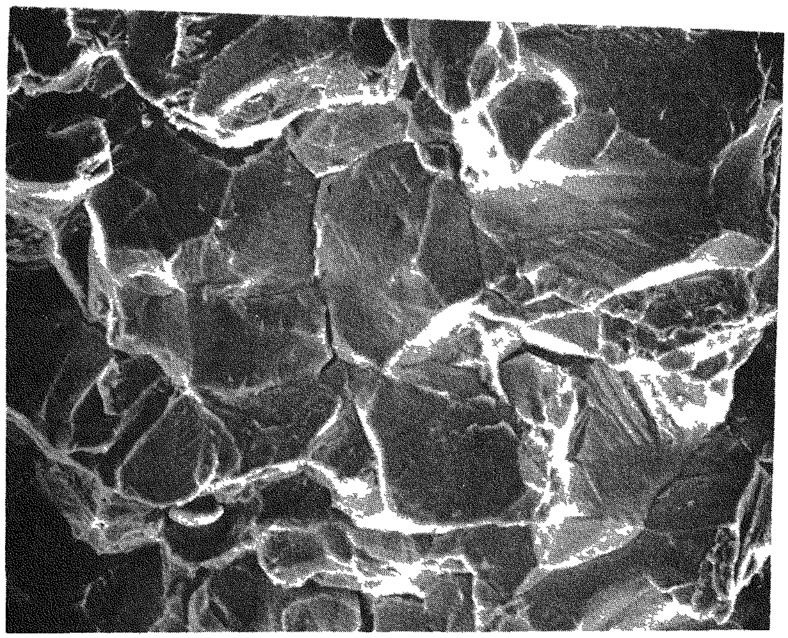

FIGURE 28. HERF Nitronic® 40, Orientation 1.
Integranular Fracture in Hydrogen.

Intergranular fracture paths were observed after tensile tests in a hydrogen environment in sensitized specimens of Type 304L, 304,[23] and Nitronic® 40 stainless steel but not Type 309S.[24] Moreover, the presence of an intergranular fracture does not appear to be contingent upon apparent continuity of the carbide phase. Continuous carbides and intergranular fracture were observed in Type 304 and Nitronic® 40 stainless steels, but no intergranular fracture occurred in Type 309S stainless steel in spite of formation of continuous grain-boundary carbides. Furthermore, extensive intergranular fracture took place during failure of Type 304 stainless steel where carbide precipitation was discontinuous. In the case of Type 304L steel, a distinct difference in fracture appearance was noted which depends upon the frequency of occurrence of grain boundary carbides. An intergranular fracture path occurred only when the carbide network was nearly continuous on at least some grain faces. Otherwise, the fracture was mixed void coalescence and partially brittle but not intergranular.

Although continuity of carbide precipitation on grain faces appears to be the dominant factor controlling the fracture path, one or more other factors must be present to explain the above observations. Phosphorus segregation to the grain boundaries and possible formation of an (Fe, Cr) Ni-P surface phase have been demonstrated as the cause of temper embrittlement of Type 304 stainless steel.[36] Intergranular fracture at 150 K was observed on notched tensile specimens annealed 2 hours at 920 K. Surface segregation of phosphorus is also found by Auger electron spectroscopy after vacuum annealing at 820 to 1020 K. These studies suggest that phosphorus may be a factor in causing intergranular fracture of sensitized austenitic steels, but experimental data are inadequate to confirm the possibility.

Interphase Separation

HAF in austenitic steels often propagates along interphase interfaces such as austenite-martensite or austenite-ferrite interfaces. Welds in austenitic steels, such as Type 304L, contain several percent of δ-ferrite which forms during solidification of the weld bead. The presence of the δ-ferrite helps prevent hot shortness or weld cracking but is a preferred path for crack propagation in the presence of hydrogen, Figure 29a.

Some stainless steels are unstable when deformed and transform to ε-martensite (a HCP lattice) or α-martensite (a BCC lattice). Again the interfaces between the austenite and either form of strain-induced martensite are likely crack paths. Fracture surfaces in these cases have a crystallographic appearance with many intersecting planar facets, Figure 29b. In Type 304L steel, this fracture path is common around room temperature in specimens that have been precharged with hydrogen prior to deformation.

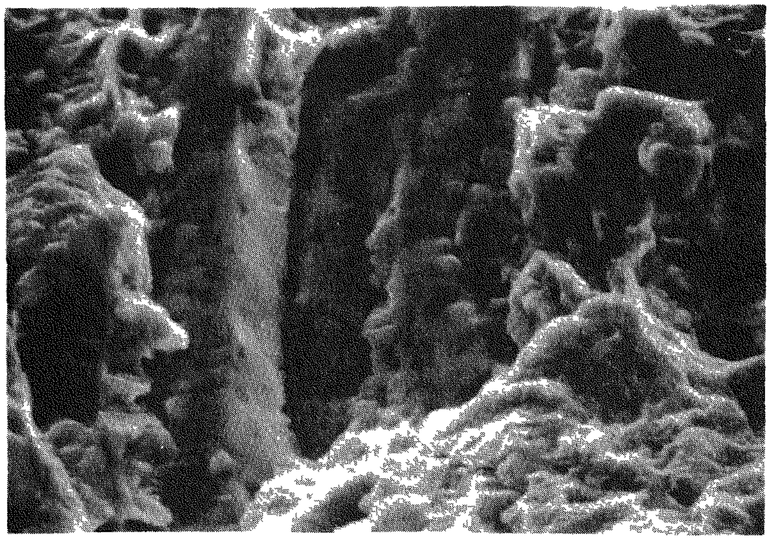

a) Austenite-Ferrite Interface in Type 304L Weld Metal

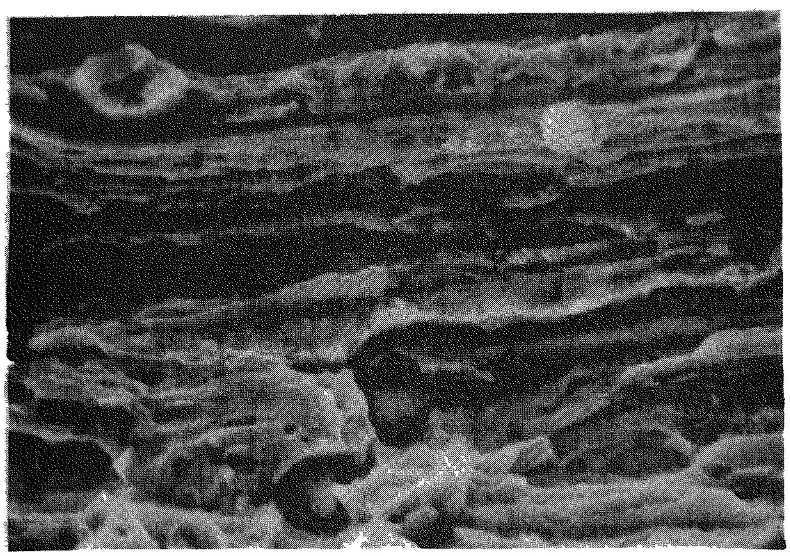

b) Austenite-Martensite Interface in Type 304L

FIGURE 29. Fracture Along Interphase Interfaces in Austenitic Steels

Fracture along austenite-martensite interfaces in Type 304L stainless steel appears more common around room temperature than at lower temperatures. Twin-boundary parting dominates the fracture at 200-250 K and microvoid coalescence is seen at 78 K. Clearly, the operative fracture path is very sensitive to test temperature.

Correlation of Fracture Mode With Composition

Fracture modes for HAF of iron-chromium-nickel alloys vary with percent of nickel in the alloy, Figure 30. Alloys such as 17-4PH with only 4% nickel fail by transgranular cleavage. As the nickel content increases, the steels become austenitic (metastable), and fracture by twin-boundary parting appears at around 10% nickel. A region of dimpled fracture occurs from 15 to 25 or 30% nickel, which is gradually supplanted by intergranular separation as the nickel content increases. However, there were only a few alloys in which only a single fracture mode was observed. In most instances, two or more fracture modes occurred, one of them being microvoid coalescence.

Alloy composition is a controlling factor in HAF in two ways: 1) the base alloy determines slip character and phase stability during straining, and 2) impurity and trace elements may be strongly segregated and induce intergranular separation either alone or in combination with hydrogen. Planar slip is associated with low-nickel austenites and leads to high-stress concentrations at slip barriers, such as inclusion, twin, and grain boundaries. Sites of high-stress concentration may act as microcrack nucleation centers, especially in the presence of hydrogen, which may lower the cohesive strength. Austenite stability under strain is also correlated with nickel content. Formation of deformation twins, ε-phase, and α-martensite occurs more readily with lower nickel concentrations. Both slip planarity and phase stability are related to stacking-fault energy. Greater resistance to hydrogen damage in austenitic steels has been correlated with higher stacking-fault energy. The transition from twin-boundary parting to dimpled fracture at around 12 to 14% nickel correlated with an increase in stacking-fault energy to over 30 or 40 mJ/m^2.

Intergranular separation in all of the stainless steels may be attributable to impurity segregation. Sulfur in high-nickel alloys and phosphorus in austentic steels are known to cause intergranular failures. These impurities are not the only causes of intergranular fracture, however. Sensitization of austenitic steels leads to carbide pecipitation and grain-boundary regions depleted in chromium and causes intergranular fracture in Type 304L stainless steels. These examples illustrate the sensitivity of HAF to relatively small changes in either base alloy composition or impurity content. Control of melting, casting, and mechanical and thermal

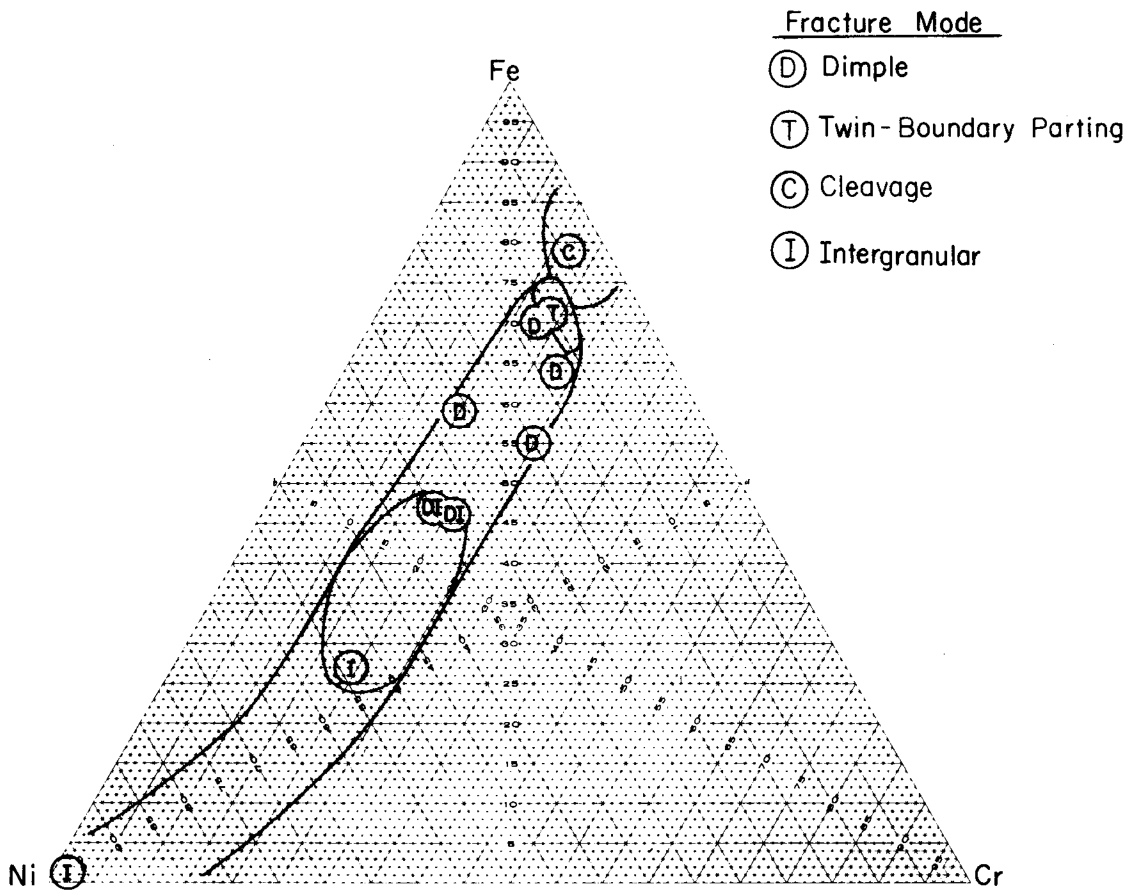

FIGURE 30. Composition Regimes for Fracture Modes Observed in HAF of Iron-Chromium-Nickel Alloys

processing becomes more important for hydrogen service than for service in air. Small changes in local composition due to variations in process control can develop conditions for HAF in an otherwise resistant alloy.

HELIUM EMBRITTLEMENT

The hydrogen isotopes are alike in their short-term chemical effect on the properties of stainless steels. Long-term effects differ, however, because tritium decays with a 12.35 year half-life to helium-3 by emission of a low energy (5.7 keV average) beta particle, whereas protium and deuterium are stable. Helium is known to embrittle many metals but normally elevated temperatures are required for an observable effect.[37] Exposure of metals to tritium causes "hydrogen damage," which occurs immediately and slowly diminishes as tritium decays, as well as helium embrittlement, which becomes significant after tritium decay has generated sufficient helium. Helium damage is additive to the damage caused by the hydrogen isotopes and has been identified in Armco® (Armco, Inc.) iron - and niobium as well as in several grades of stainless austenitic steel.

The earliest studies of the effects of helium-3 on the mechanical properties of stainless steel were reported in 1975.[37,38] Foil specimens (0.025 cm thick) were exposed to 47.5 MPa tritium at 343 K for 17 months; helium build-in was estimated at 6.2 mol He(STP)/m^3. Subsequent tests at room temperature indicated that the exposure increased the yield strength, but had little effect on the ductility of the Type 309S steel specimens, although the ductility of Type 304L steel was lowered. Microvoid coalescence was the primary fracture mode. Helium bubbles about 5 nm in size were found in both steels in grains and on grain boundaries.

Transmission electron microscopy of samples charged with tritium showed gas bubbles formed on dislocation networks (Figure 31), and grain boundaries following a 0.5 hour anneal at 973 K. Further a tensile test at 973 K showed that the helium, which had built in , during the charging, agglomerated during the test, which caused the fracture mode to change from ductile rupture to intergranular separation and reduced the strength and ductility of both Type 309S and 304L stainless steels.

Helium damage at ambient temperature was convincingly demonstrated in smooth-bar tensile specimens (2.5-cm gage length and 0.356-cm diameter) of HERF Nitronic® 40 stainless steel gas-phase charged with tritium at 64 MPa at 470 K for 1450 hours and aged

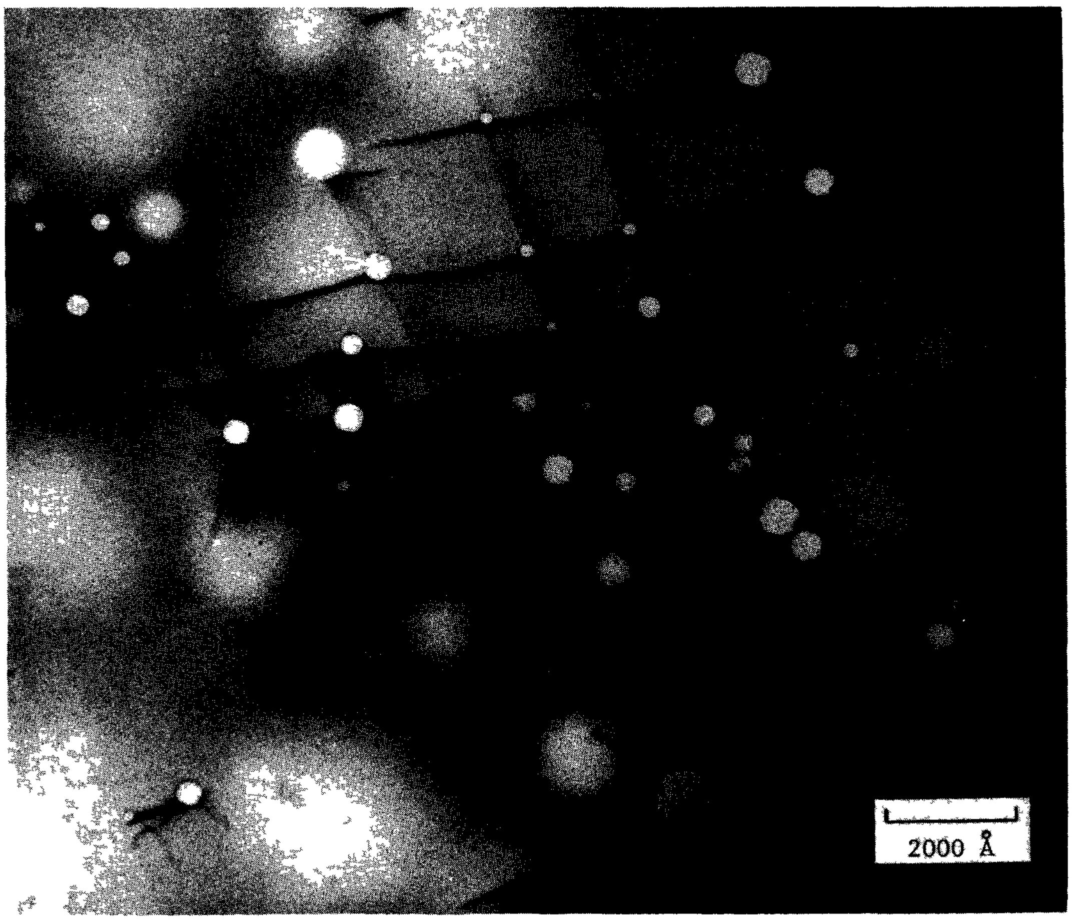

FIGURE 31. Helium Bubbles in Type 304L Stainless Steel. Tritium Charged, Aged, and Annealed at 1273 K

5.5 years at 250 K. Comparison specimens of Type 304L stainless steel were only affected a small amount by the same treatement.[39] Tritium and helium distributions in the specimens are nonuniform for these charging conditions. Some of the charged specimens were tested at 298 K immediately after charging, and others were stored from five to seven years at 250 K before testing, Tables 10 and 11. After 5.5 years' storage, helium concentrations were about 100 mol He(STP)/m^3 at the surface of the Type 304L steel specimen and about 174 mol He(STP)/m^3 in the Nitronic® 40. Average concentrations over the specimen cross section were 31 and 52 mol He(STP)/m^3.

These test results show:

1) Hydrogen and tritium reduce ductility of both Type 304L and Nitronic® 40 stainless steel (Tables 10 and 11).

2) There was only a small change in the mechanical properties and no change of fracture mode in Type 304L stainless steel with 100 mol He(STP)/m^3.

3) A drastic reduction in ductility and a change in fracture mode from microvoid coalescence to intergranular separation occurred in Nitronic® 40 stainless steel (Table 11) with 174 mol He(STP)/m^3.

There was a high density of small defects in the tritium-charged and aged Nitronic® 40 stainless steel, Figure 32. Contrast analysis of the strain fields produced by these defects indicated that they were helium bubbles approximately 5 nm in size. The size and density of bubbles (2×10^{16} bubbles/cm^3) was consistent with the estimated helium content of the specimen. Measurements of the images produced by these defects indicate a misfit strain of about 0.017. Rather than being located at grain boundaries, the bubbles were dispersed throughout the matrix. A few bubbles were found in the Type 304L stainless steel specimens, in keeping with the lower helium content. Helium is known to cause intergranular fracture by the formation of intergranular helium bubbles at high temperatures ($T/T_m = 0.5$), where helium migration to internal boundaries can occur.[37] Data for Types 304L and 309S stainless steel and Armco® (Armco, Inc.)[40] iron charged with tritium have shown helium embrittlement with only 0.2 mol He(STP)/m^3 can occur after a high-temperature anneal or testing at a high temperature.

HERF Nitronic® 50 and welds in Type 304L stainless steel have shown ductility losses associated with helium-3.[41] Calculated helium concentration profiles in these specimens were similar to those in the HERF Nitronic® 40 and HERF Type 304L stainless steels but the surface concentration of tritium was higher. All fractures in the HERF Nitronic® 50 and welds of Type 304L stainless steels were ductile.

TABLE 10

Mechanical Properties of HERF Type 304L Stainless Steel

Exposure Conditions	Strength, MPa Yield	Strength, MPa Ultimate	Total Elongation, %	Plastic Strain to Fracture
None	630	790	32	1.83
69 MPa H_2 at 480 K, 55 days	600	840	35	0.87
47 MPa T_2 at 480 K, 17 months and aged 5.5 years at 250 K	620	745	33	0.73

TABLE 11

Mechanical Properties of HERF Nitronic® 40 Stainless Steel

Exposure Conditions	Strength, MPa Yield	Strength, MPa Ultimate	Total Elogation, %	Plastic Strain to Fracture
None	800	930	29	1.20
30 MPa H_2 at 480 K, 56 days and aged 7 years at 250K	845	990	28	0.76
65 MPa T_2 at 480 K, 60 days	830	940	32	0.73
47 MPa T_2 at 344 K, 17 months and aged 5.5 years at 250 K	870	925	6	0.10

ORNL - Photo 3598-80

a) Hydrogen charged 69 MPa at 470K and aged 5.5 years

b) Tritium charged 47.5 MPa at 345K and aged 5.5 years

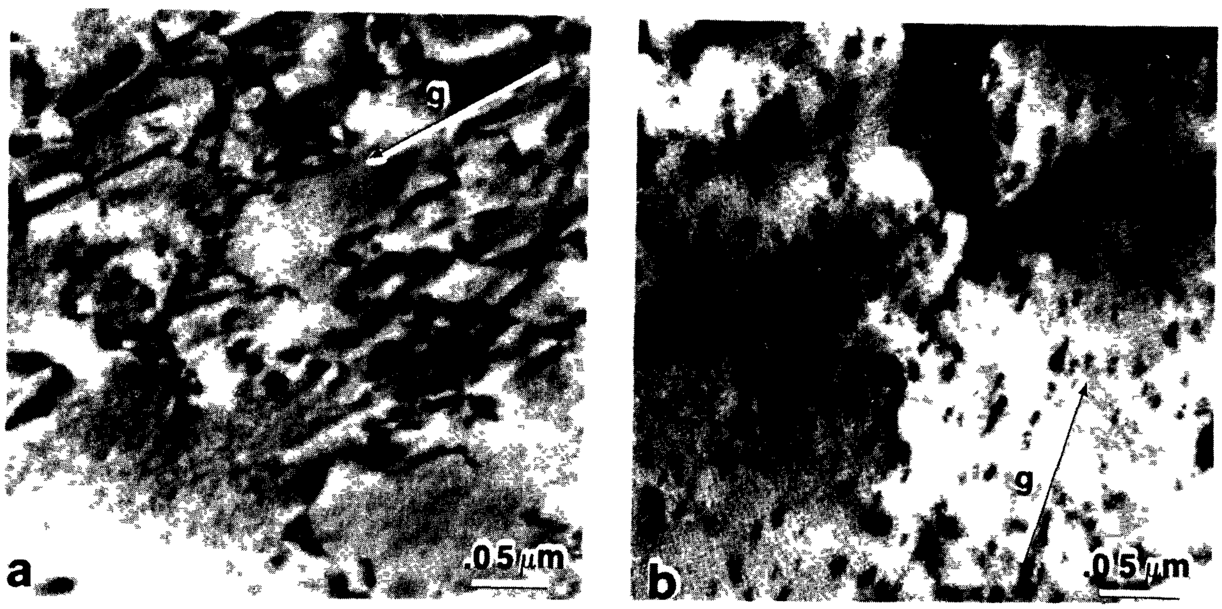

FIGURE 32. Microstructures in HERF Nitronic® 40

A new investigation of helium effects was begun and is still in progress.[46] Notched C-shape specimens 3.8 mm thick and 25 mm outer radius were machined from five stainless steels: Type 304L, Type 316, Nitronic® 40, A-286, and a modified A-286. The modified A-286 was in the annealed condition, all others were HERF. Specimens were not fatigue precracked. The specimens were exposed to tritium at 61 MPa pressure at 422 K for six months.

Calculated tritium concentrations in Type 304L stainless steel were 270 mol $T_2(STP)/m^3$ at the surface and 60 mol $T_2(STP)/m^3$ at the center based on the hydrogen solubility equation of Louthan and Derrick.[43] Tritium and helium contents average over the cross section were 167 mol $T_2(STP)/m^3$ and 10 mol $He(STP)/m^3$. Following the 15-month ageing, average tritium and helium contents were 160 mol $T_2(STP)/m^3$ and 24 mol $He(STP)/m^3$. Actual concentrations in Nitronic® 40 are probably higher since measurements of hydrogen solubility at 470 K have shown that hydrogen solubility is 70% higher than in Type 304L steel.[44]

Tensile tests were run immediately after exposure and following 15 months' storage at 273 K. Control specimens were exposed to air at 422 K for six months and stored at low temperature. Tensile tests were made in air at room temperature and the load-deflection curves were analyzed by the J-integral technique.[45] J-integral at maximum load (Jm) and deflection at maximum load are given in Table 12 for the several test conditions.

The data demonstrate that helium has degraded the mechanical properties of all five steels. Immediately after the six-month exposure, the difference in Jm between the control and charged specimens was due mostly to the tritium with only a small helium effect. After 15 months' storage at 273 K, the difference between charged and control specimens was due to the additional helium generated during storage. HERF Type 316 and HERF Type 304L stainless steels were affected the least by the helium, and HERF Nitronic® 40 and annealed A-286 (modified) were affected the most. The occurrence of a large helium effect in Nitronic® 40 was not surprising, as a comparable result was observed earlier.[40] The difference in response to the presence of helium shown by HERF A-286 and annealed A-286 (modified) appears to be associated with microstructural differences arising from prior thermal or thermo- mechanical treatments. Composition differences between the two varieties of A-286 are small and probably contributed little to the relative helium effect.

Sustained load tests were initiated after 22 months storage on all steels except modified A-286. Loads corresponded to 80 percent of the fracture load that was measured after 15 month's storage. Rapid crack growth occurred in Nitronic® 40 and A-286 stainless steels but has not yet been detected in Type 316 or Type 304L after five months under load. The latter tests are continuing.

TABLE 12

Tritium and Helium Effects on Fracture Toughness of Stainless Steel

Alloy	History*	Deflection at Max. Load, mm	Fracture Toughness Jm, kJ/m^2
304L	C	3.71	1280
HERF	T	1.55	360
	C + A	3.33	1120
	T + A	1.32	190
A-286	C	1.95**	610**
HERF	T	1.80	530
	C + A	1.70	350
	T + A	1.14	130
Nitronic® 40	C	2.67	1200
HERF	T	1.50	480
	C + A	2.62	960
	T + A	1.02	75
316	C	3.51**	1500**
HERF	T	2.39	890
	C + A	2.97	950
	T + A	2.03	630
A-286	C	2.86	840
(modified)	T	1.50	350
Annealed	C + A	2.79**	680**
	T + A	0.84**	70**

* C - Control
C + A - Control + Aged
T - Tritium Charged
T + A = Tritium Charged + Aged.

** Single Specimen. All others in duplicate.

The fracture mode tended to change from void coalescence to intergranular in all alloys except HERF Type 316. Fracture of annealed A-286 (modified) was partly intergranular after tritium charging and entirely intergranular after subsequent aging. Intergranular fracture was evident in isolated areas of the Nitronic® 40 after tritium charging and became dominant after aging. Both Type 304L and Type A-286 stainless steels failed by mixed fracture (void coalescence and intergranular) after charging and aging, whereas only void coalescence was observed in the tritium charged specimens of these alloys.

Helium and hydrogen (tritium) damage occurred simultaneously, and no attempt was made to factor the measured damage between the two causes. The magnitudes of the two effects will change with time, as the tritium decays to helium. The data accumulated so far suggest however, that helium damage is more potent than hydrogen (tritium) damage for equal atomic concentrations of the two elements. There were decreases in Jm of 50 to 90% as a consequence of the 15-month aging during which time the average helium content increased by a factor of 2 and the average tritium content decreased by 4%.

Distribution of the helium within the specimens has not been established as yet. In the Nitronic®-40, helium is presumably distributed in fine bubbles throughout the matrix as in the earlier specimens. There is no reason to believe that this same helium distribution should apply to the other alloys, particularly when their widely differing microstructures are taken into account. For example, fine carbo-nitride particles occur more commonly in Nitronic® 40 than in Type 304L or Type 316 stainless steels, and both varieties of A-286 may contain gamma prime ($Ni_3[Al, Ti]$, eta (Ni_3Ti) and TiC phases in varying quantities and distributions. All of these phases could act as traps for tritium and thus create localized high helium concentrations or bubbles which would be distributed within the alloy in the same manner as the phases. Severity of helium damage would be related then to trap characteristics such as, quantity of trapped tritium at the interface, interface coherency and whether the trap were reversible or irreversible. However, the relation between helium damage and the trap characteristics need not be the same as between hydrogen damage and trap characteristics because the strain fields of helium and hydrogen differ and hydrogen is chemically reactive.

CONCLUSIONS

Substantial progress has been made in identifying important material and processing variables which influence hydrogen compatibility of stainless steels. The results provide guidance in alloy selection and thermomechanical processing for a limited range of hydrogen pressures (to 69 MPa), operating temperatures (78-400 K), and mechanical loading conditions (constant or rising load). However, there are service conditions for which data are inadequate to allow selection of a reliable alloy or prediction of its service life.

Several unresolved issues remain that are important to utilization of stainless steel in environments where hydrogen isotopes are present:

- The relative importance of base alloy composition, precipitate structure and morphology, and mechanical processing in attaining high strength (>900 MPa yield strength) with good hydrogen compatibility (K_{TH} >80 MPa$\sqrt{m}$) is not certain.

- Selection of alloys for low hydrogen pressure (0.01 to 10 MPa) applications has not been systematically examined. Pressure limits and acceptable temperature ranges have not been correlated with service life and stress states for low pressure service, particularly at elevated temperatures (T >400 K) where hydrogen attacks occur and creep conditions are encountered.

- Segregation of alloy elements, impurities, and hydrogen can adversely affect hydrogen compatibility in an alloy otherwise acceptable for a given service. The relationships of segregation to hydrogen compatibility on the one hand and to processing variables and control on the other have not been examined in detail.

- Mechanical test techniques need to be analyzed and compared to permit selection of those methods which best relate to and predict hydrogen compatibility for given service conditions (loading, hydrogen pressure, and temperature). J-integral methods were investigated to characterize ductile fracture and hydrogen degradation of tough alloys such as austentic stainless steels. Initial results were encouraging and suggest continued development of experimental and analytical procedures.

- Mechanisms of hydrogen-assisted fracture and low temperature helium embrittlement are not known. Several hypotheses have been advanced to account for each form of degradation, but there are as yet no generally accepted explanations for these phenomena.

- Material, processing, and environmental conditions controlling helium embrittlement are not well known. Experiments have begun to examine systematically the phenomenon of low temperature helium embrittlement.

Investigation of hydrogen effects on the mechanical behavior of stainless steels is continuing at the Savannah River Laboratory. The issues identified above serve in part to guide the research activity.

ACKNOWLEDGEMENTS

This report includes work by several investigators in the Savannah River Laboratory whose contributions are acknowledged: T. L. Capaletti, M. R. Dietrich, J. A. Donovan, C. W. Krapp, M. R. Louthan, Jr., D. A. Mezzanotte, L. P. McCabe, D. E. Rawl, Jr., and P. E. Zapp. The high-purity stainless steels were supplied by N. F. Fiore, Notre Dame University. Transmission microscopy of Nitronic® 40 stainless steel, Figure 32, was performed by P. S. Sklad, Oak Ridge National Laboratory.

ALLOY DATA SHEETS

ALLOY INDEX

Nominal compositions of alloys are shown in Table A-1. Nominal tensile properties are shown in Table A-2. Measured properties under various experimental conditions are summarized in the data sheets listed below.

TABLE A-1

Nominal Alloy Composition, wt %

Alloy	Cr	Ni	Mn	Mo	Other
Fe-Cr-Ni-Alloys					
304L	19	10	-	-	
304N	19	9	-	-	0.13 N
309S	23	13	-	-	
310	25	20	-	-	0.25 C
316	17	12	-	2.5	
440C	19	-	-	0.75	0.95 to 1.20 C
Carpenter 20 Cb-3	20	34	-	2.5	3.5 Cu, 06 Nb
I800H	21	32	-	-	0.75 Cu, 0.3 Al, 0.3 Ti
I718	19	52	-	13	5 (Nb + Ta), 1 Ti, 0.5 A
Ni200	-	99+	-	-	
Ni301	-	bal	-	-	1 Si, 4.5 Al, 0.6 Ti
Fe-Cr-Ni-Mn-N Alloys					
216	20	6	8	2	0.32 N
Tenelon®	18	-	15	-	
Nitronic®-40	21	6	9	-	0.15 to 0.4 N
Nitronic®-50	22	13	5	2	0.2 to 0.4 N
18-18 Plus®	18	0.5	18	1	0.4 N, 1 Cu, 0.1 Co
X 18-3 Mn	18	3	12	-	0.3 N
18-2 Mn	18	2	13	-	
Precipitation-Hardenable Alloys					
17-4 PH	16.5	4	-	-	4 Cu, 0.3 Nb
A-286	15	26	-	1.25	2 Ti, 0.25 Al, 0.3 V
JBK-75	15	30	-	1.25	2 Ti, 0.25 Al, 0.001 B, 0.25 V
AM363	11.5	4.5	-	-	0.5 Ti
CG27	13	38	-	6	2.5 Ti, 1.6 Al, 0.6 Nb
AM350	16.5	4.3	-	2.8	0.1 N
Ni-SPAN-C Alloy 902	5	42	-	-	0.5 Al, 2.5 Ti
High-Purity Alloys					
A	18	10	-	-	N <0.01 in all
B	18	14	-	-	three alloys
C	18	19	-	-	

TABLE A-2

Nominal Tensile Properties (Annealed Material Unless Otherwise Noted)

Alloy	Strength, MPa Yield*	Tensile	Elongation, %
304L	230-270	540-560	55-60
304N	290-330	620	50-55
309S	275-310	620-650	45
310	310	650	45-50
316	207-290	550-585	45-50
440C	450-1890	760-1965	2-14
Carpenter 20 Cb-3	250	600	50
I800H	140-345	450-650	30-50
I718	1180-1250	1350-1400	16
Ni 200	103-207	380-550	40-55
Ni 301	210-1200	620-1450	15-55
216	428	745	50
Tenelon®	570	930	56
Nitronic®-40	414	690	40
Nitronic®-50	448	828	45
18-18 Plus®	520	900	60
X 18-3 Mn	580	810	45
18-2 Mn	730	1000	51
17-4 PH	940	980	5
A-286	760	1100	25
JBK-75**	800	1090	14
AM 350	420	1160	70
AM 363	890	890	7
CG 27	810	1160	29
Ni-SPAN-C Alloy 902	760-870	900-1200	6-25

* 0.2% offset.

** HERF & Age.

IRON-CHROMIUM-NICKEL ALLOYS

DATA SHEET IA-1

Type 304L Stainless Steel Bar Stock, As Received*

Test Condition		Hydrogen**	Strength, MPa		Elongation, %		Fracture
Temp, K	Environ.	Exposure	Yield	Ultimate	Uniform	Total	Strain
380	AIR	NONE	240	680	58	69	1.78
		69 MPa	260	730	60	70	1.27
273	AIR	NONE	310	1160	80	89	1.56
		69 MPa	330	870	44	44	0.45
200	AIR	NONE	360	1500	61	70	1.27
		69 MPa	390	1210	44	44	0.25
78	LN	NONE	390	2200	60	64	1.27
		69 MPa	430	2100	59	65	1.27

* Heat Analysis, Appendix D-1; Tensile B, Appendix C-2.

** Exposure conditions: 69 MPa at 470 K for 1449 days.

DATA SHEET IA-2

Type 304L Stainless Steel, As Received

Test Conditions		Hydrogen	Impact
Temp, K	Environ.	Exposure	Energy, J
298	AIR	NONE	194
		17.9 MPa*	185
78	AIR	NONE	165
		17.9 MPa*	110

* 17.9 MPa hydrogen pressure at 470 K for 1000 hours.

DATA SHEET IA-3

Effect of Test Environment on Tensile Properties of Type 304L Stainless Steel Tubes*

Exposure Conditions			Tensile Properties		
Gas	Temp, K	Time, days	σ_y, MN/m^2	σ_{ult}, MN/m^2	% Elong.
He	425	32	270	560	59
H_2	425	32	320	480	19
T_2	425	32	300	490	22
H_2	425	8	260	490	26
T_2	425	8	250	490	22

* All tensile tubes tested at room temperature with 69 MPa gas; data reported are averages of at least two samples.

DATA SHEET IA-4

Tensile Properties of Type 304L Stainless Steels Containing Hydrogen and Helium

Test Condition		Hydrogen	Strength, MPa		Elong
Temp, K	Environment	Exposure	Yield	Ultimate	%
300	Air	none	327	734	49-56
300*	Air	**	400	733	28-32
300*	Air	**	434	744	28
973†	Air	none	152	237	31
973†	Air	**	179	190	1.5

* Specimens contained tritium and Helium-3.

** 328 mol hydrogen isotopes and 6.2 mol helium per m^3 metal.

† 146 mol hydrogen isotopes and 25 mol helium per m^3 metal. Held 1/2 hour at 973 K before testing.

DATA SHEET IA-5

Type 304L Stainless Steel, High Energy Rate Forged*

Test Condition		Hydrogen	Strength, MPa		Elongation, %		Fracture
Temp, K	Environ.	Exposure**	Yield	Ultimate	Uniform	Total	Strain
380	Air	None	440	630	32	44	1.72
		69 MPa	440	650	32	43	1.63
298	Air	None	480	930	57	68	2.00
		69 MPa	510	990	55	62	0.95
250	Air	None	490	1100	52	61	1.65
		69 MPa	610	1120	41	41	0.40
200	Air	None	660	1390	46	55	1.37
		69 MPa	620	1300	43	44	0.38

* Tensile B, Appendix C-2.

** Exposed at 620 K for 3 weeks.

DATA SHEET IA-6

Type 304L Stainless Steel, High Energy Rate Forged*

Test Condition		Hydrogen	Impact
Temp, K	Environ.	Exposure	Energy, J
298	Air	None	199
298	Air	29.6 MPa H_2**	152
77	Air	None	160
77	Air	29.6 MPa H_2**	95

* Impact, Appendix C-8.

** Exposure of 56 days at 470 K.

DATA SHEET IA-7

Fracture Parameters for Type 304L Stainless Steel, High Energy Rate Forged*

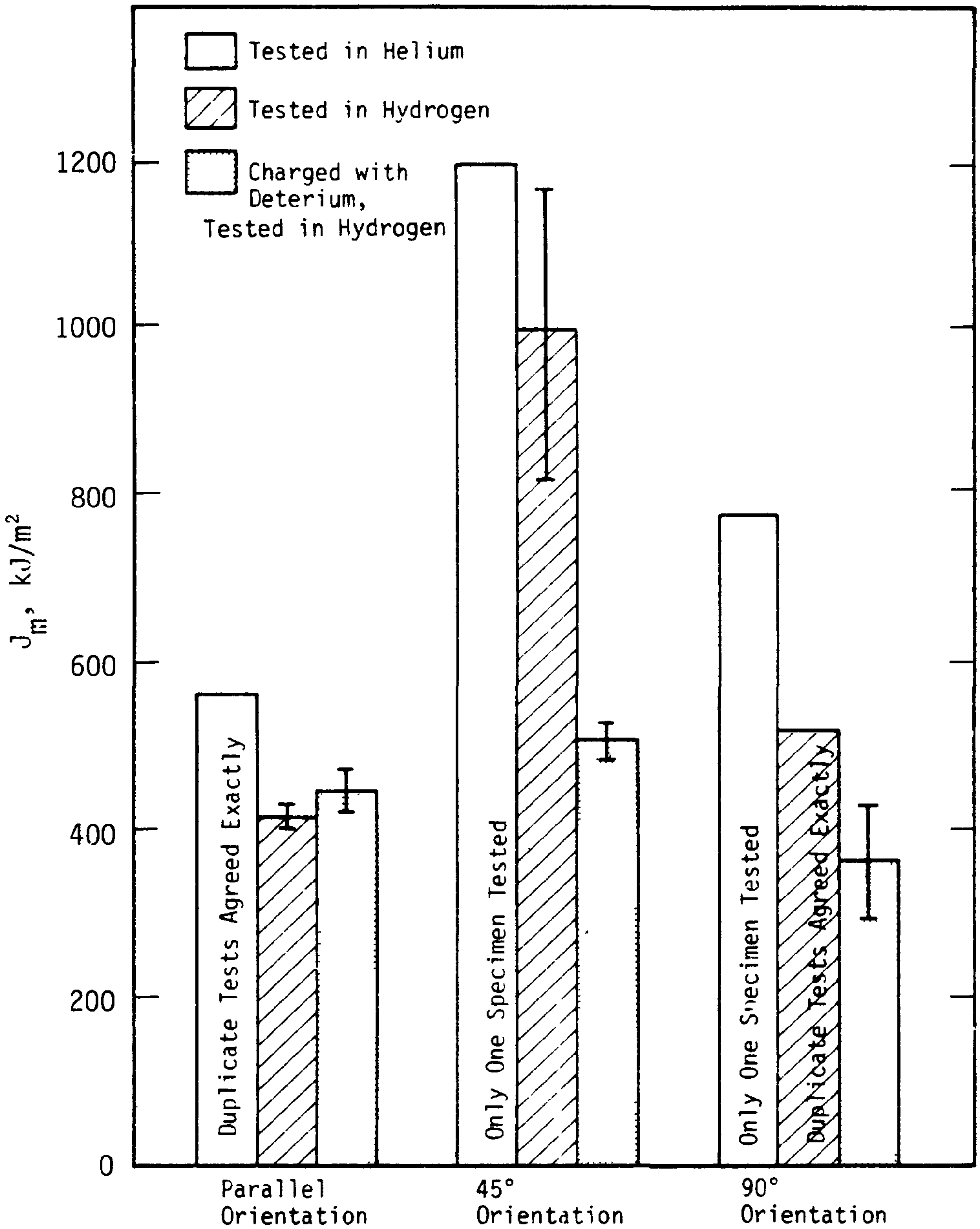

* C-shaped tensile, Appendix C-7. Test in 69 MPa He or H_2. Deuterium charge at 69 MPa at 620 K for 3 weeks.

DATA SHEET IA-8

Fracture Parameters for Type 304L Stainless Steel*

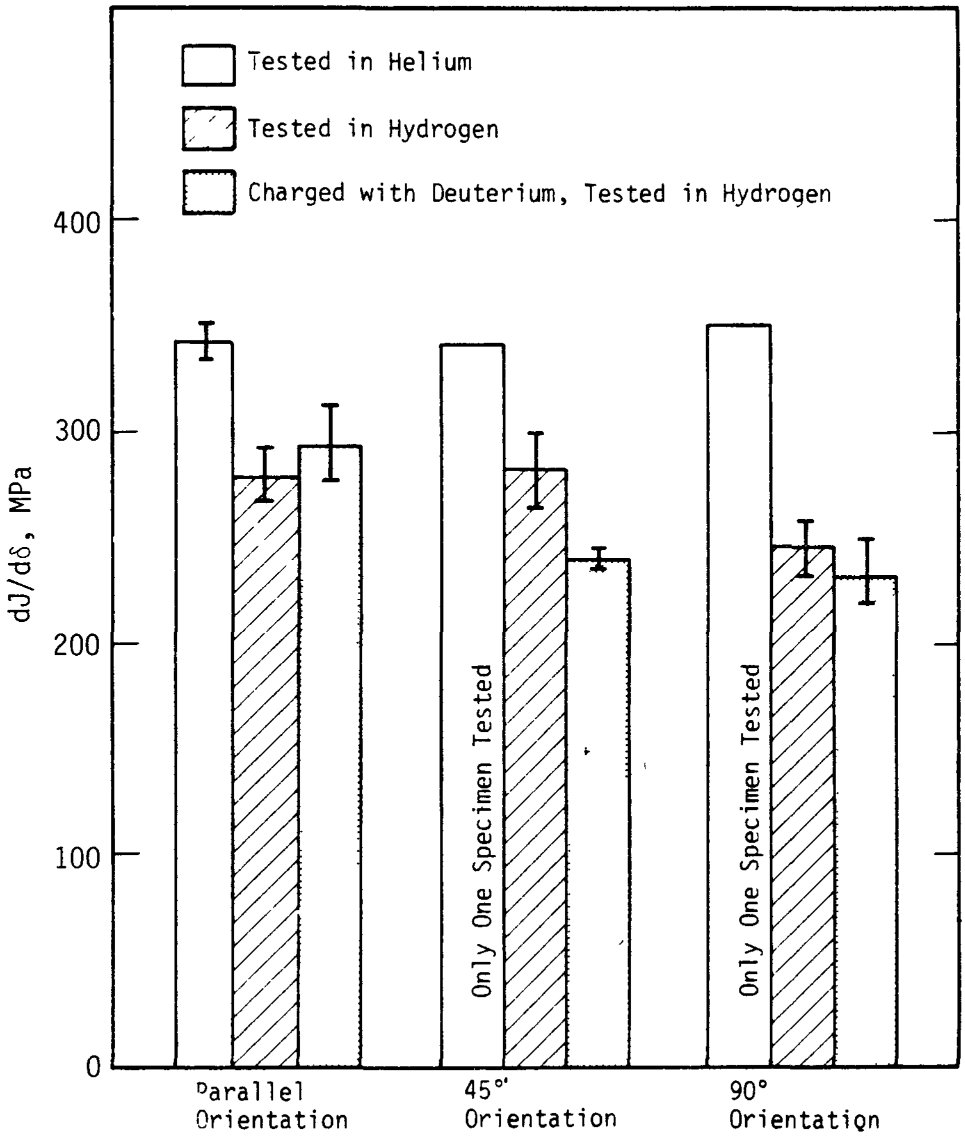

---

* C-shaped tensile, Appendix C-7. Test in 69 MPa He or H_2. Deuterium charge at 69 MPa at 620 K for 3 weeks.

DATA SHEET IA-9

Effect of Heat Treatment on Mechanical Properties of Type 304L Stainless Steel*

Heat Treatment	Test Environment	Strength, MPa		Elongation, %		Fracture Strain
		Yield	Ultimate	Uniform	Total	
As-received	69 MPa He	390	930	62	71	2.21
GS = 9.5 μm	69 MPa H_2	390	910	56	62	1.43
1170 K-24 hrs	69 MPa He	260	970	82	89	2.30
GS = 30 μm	69 MPa H_2	240	970	88	94	1.71
1270 K-24 hrs	69 MPa He	250	970	90	99	2.30
GS = 55 μm	69 MPa H_2	240	930	86	91	1.17
1470 K-24 hrs	69 MPa He	190	830	81	88	2.21
GS = 340 μm	69 MPa H_2	180	830	84	88	1.05

* Heat analysis; Appendix D-1; Tensile B, Appendix C-2.

DATA SHEET IA-10

Grain Size Dependence of Mechanical Properties - Test at 220 K*

Hydrogen Exposure	Grain Size, μm	Strength, MPa		Elongation, %		Fracture Strain
		Yield	Ultimate	Unit	Total	
None	6.4	520	1310	56	63	1.71
	42.0	340	1210	60	72	1.70
	290	250	1130	55	63	1.64
69 MPa**	6.1	630	1040	35	35	0.27
	26	400	1020	47	47	1.10
	50	370	860	37	37	0.40
	260	270	690	31	31	0.39

* Heat analysis, Appendix D-1; Tensile B, Appendix C-2.

** Average deuterium contents measured on samples from the tensile specimens were 4.7 ccD_2/cc (69 MPa).

DATA SHEET IA-11

Effect of Deformation Rate on Hydrogen Damage*

TYPE 304L Stainless Steel
T = 220 K
Grain Size: 6 m

Hydrogen Exposure**	Cross Headspeed, mm/min	Strength, MPa		Elongation, %		Fracture Strain
		Yield	Ultimate	Uniform	Total	
None	51	570	1170	50	60	1.68
	0.51	5.20	1310	56	63	1.70
69 MPa	51	675	1210	52	52	0.92
	0.51	630	1040	35	35	0.27

* Heat analysis, Appendix D-1; Tensile B, Appendix C-2.

** Exposed at 620 K for 3 weeks.

DATA SHEET IA-12

Mechanical Properties of Sensitized Type 304L Stainless Steel*
(Smooth Bar Tensile Specimens)

Treatment	Test Environment**	Strength, MPa		Fracture Strain
		Yield	Ultimate	
Solution Anneal	Air	380	630	2.00
	Helium	375	600	2.20
	Hydrogen	370	580	1.38
Sensitized	Air	300	560	1.78
	Helium	350	670	1.90
	Hydrogen†	330	660	0.70
	Hydrogen††	350	660	0.80

* Heat analysis, Appendix D-1; Tensile B, Appendix C-2.

** 69 MPa gas pressure.

† Nearly continuous carbide network on some grain boundaries.

†† Isolated carbides.

DATA SHEET IA-13

Mechanical Properties of Notch Bar Tensile Specimens of Type 304L Stainless Steel*

Treatment	Test Environment**	Strength, MPa Yield	Strength, MPa Ultimate	Fracture Strain
Solution Anneal	Air†	700	750	0.41
Sensitized	Air††	350	590	1.26
	Helium††	410	740	1.10
	Hydrogen††,¶	430	590	0.35
	Hydrogen ¶¶	480	620	0.38
	Air†	510	680	1.17
	Helium†	540	790	1.00
	Hydrogen†,¶	730	750	0.30
	Hydrogen ¶¶	-	690	0.20

* Heat analysis, Appendix D-1 and Appendix C-2.

** He and H_2 at 69 MPa. Air at 0.1 MPa.

† Deep notch.

†† Shallow notch.

¶ Nearly continuous carbide network on some grain boundaries.

¶¶ Isolated carbides.

DATA SHEET IA-14

Effect of Hydrogen Charging on Notch Bar Tensile Properties of Type 304L Stainless Steel*

Condition	Specimen	Nominal Tensile Strength, MPa	Fracture Strain
As received	Smooth	600	1.50
	Notch	770	0.30
Annealed**	Smooth	600	1.43
	Notch	710	0.24
Hydrogen charged†	Smooth	530	0.37
	Notch	580	0.13

* Tensile C, Appendix C-4.

** Annealed 200 days at 380 K in argon.

† Exposed to hydrogen gas at 69 MPa for 200 days at 380 K.

DATA SHEET IA-15

Type 304L Stainless Steel Notch Tensile Strength*

Test Environment	Notch Tensile Strength, MPa
Air	896
H_2, 0.1 MPa	786
H_2, 1.03 MPa	703
H_2, 6.89 MPa	662

* Tensile C, Appendix C-4.

DATA SHEET IA-16

Stress Necessary for Slow Crack Growth in Type 304L Stainless Steel*

Net Section Stress, MN/m^2	Time, hrs Incremental	Accumulated	Crack Growth
600	325	325	No
641	72	397	No
682	72	469	No
724	72	541	No
765	72	613	No
786	1.4 (failed)	614.4	Yes

* Crack developed during room temperature tensile test in hydrogen environment; net section stress when tensile test was stopped was 772 MN/m^2. Specimen then loaded in creep frame at indicated stresses without removal from the hydrogen environment.

Tensile E, Appendix C-5.

DATA SHEET IB-1
Type 304N Stainless Steel*

Test Condition		Hydrogen	Strength, MPa		Elongation, %		Fracture
Temp, K	Environment	Exposure	Yield†	Tensile	Uniform	Total	Strain
298	Air	none	760	880	-	33	1.24
	Air	69 MPa H_2**	740	830	-	31	1.05
	69 MPa H_2	none	640	840	-	36	0.78
	69 MPa H_2	69 MPa H_2**	550	790	-	37	0.62
	69 MPa He	none	630	850	-	43	1.35
375	Air	none	820	950	11	26	1.31
		69 MPa D_2††	820	970	11	22	1.20
298	Air	none	906	1110	16	28	1.47
		69 MPa D_2††	950	1185	16	28	0.95
245	Air	none	975	1340	27	37	1.82
		69 MPa D_2††	1063	1420	22	27	0.49
220	Air	none	1026	1450	26	35	1.67
		69 MPa D_2††	1093	1480	21	24	0.33
200	Air	none	1096	1810	47	56	1.44
		69 MPa D_2††	1160	1510	19	23	0.38

* Tensile A, Appendix C-1; Heat Analysis, Appendix D-10.

** 69 MPa H_2 at 430 K for 1000 hours.

† 0.2% offset.

†† 69 MPa D_2 at 620 K for 3 weeks.

DATA SHEET IC-1

Type 309S Stainless Steel*

Test Condition		Hydrogen	Strength, MPa		Elongation, %		Fracture
Temp, K	Environment	Exposure	Yield**	Tensile	Uniform	Total	Strain
298	Air	none	290	600	-	54	1.27
	69 MPa He	none	276	580	-	60	1.24
	69 MPa H2	none	260	586	-	63	1.35
	Air	69 MPa H_2-430K 14d	255	615	-	43	0.92
	Air	28 MPa H_2-470K 100 hr	330	615	-	57	1.17

* Tensile A, Appendix C-1.

** 0.2% offset.

DATA SHEET IC-2

Tensile Properties of Type 309S Stainless Steels Containing Hydrogen and Helium

Test Condition		Hydrogen	Strength, MPa		Elongation,
Temp, K	Environment	Exposure	Yield	Ultimate	%
300	Air	none	243	612	56
300*	Air	**	301	618	48-57
300*	Air	†	382	658	45-53
973††	Air	none	131	296	27
973††	Air	†	227	196	<1

* Specimens contained tritium and Helium-3.

** 328 mol hydrogen isotopes and 6.2 mol helium per m^3 metal.

† 146 mol hydrogen isotopes and 2.5 mol helium per m^3 metal.

†† Held 1/2 hour at 973 K before testing.

DATA SHEET ID-1

Type 310 Stainless Steel Bar Stock, As Received*

Test Condition		Hydrogen	Strength, MPa		Elongation, %		Fracture
Temp, K	Environment	Exposure**	Yield	Ultimate	Uniform	Total	Strain
380	Air	none	440	670	25	36	1.35
		69 MPa	440	700	27	40	1.71
273	Air	none	510	860	44	53	1.71
		69 MPa	510	900	46	53	1.47
200	Air	none	560	1200	60	66	1.20
		69 MPa	590	1280	62	73	1.24
78	LN	none	570	1720	74	78	1.05
		69 MPa	570	1790	71	76	1.35

* Tensile B, Appendix C-2.

** Exposed at 470 K for 1449 days.

DATA SHEET ID-2

Type 310 Stainless Steel*

Test Condition		Hydrogen	Strength, MPa		Elongation, %		Fracture
Temp, K	Environment	Exposure	Yield**	Tensile	Uniform	Total	Strain
298	Air	none	210	540	-	61	1.56
	Air	69 MPa H_2†	200	500	-	63	1.42
	69 MPa H_2	none	186	490	-	67	1.72
	69 MPa H_2	69 MPa H_2†	180	440	-	66	1.56
	69 MPa He	none	180	480	-	70	1.61

* Tensile A, Appendix C-1.

** 0.2% offset.

† 69 MPa H_2 at 430 K for 1000 hours.

DATA SHEET IE-1

Type 316 Stainless Steel; Bar Stock, As Received*

Test Condition		Hydrogen	Strength, MPa		Elongation, %		Fracture
Temp, K	Environment	Exposure**	Yield	Ultimate	Uniform	Total	Strain
380	Air	none	810	830	7	20	1.61
		69 MPa	880	930	11	22	1.19
273	Air	none	890	1040	21	33	1.47
		69 MPa	990	1160	20	32	1.13
250	Air	none	900	1150	27	40	1.51
		69 MPa	1030	1280	24	35	1.07
200	Air	none	960	1210	24	43	1.56
		69 MPa	1100	1410	26	37	1.06

* Tensile B, Appendix C-2.

** Exposed at 620 K for 3 weeks.

DATA SHEET IF-1

Carpenter 20 Cb-3® Stainless Steel As-Received*

Test Condition		Hydrogen	Strength, MPa		Elongation, %		Fracture
Temp, K	Environment	Exposure**	Yield†	Ultimate	Uniform	Total	Strain
298	Air	none	236	600	-	48	1.14
	69 MPa H_2	none	230	590	-	48	1.14
	69 MPa H_2	69 MPa D_2	262	610	-	48	1.14
200	Air	none	320	1100	60	66	1.01
	Air	69 MPa D_2	348	1177	55	62	1.08

* Tensile B, Appendix C-2; heat analysis, Appendix D-11.

** Exposed at 620 K for 3 weeks.

† 0.2% offset.

DATA SHEET IG-1

Incoloy® Alloy 800H, Hot Rolled Plate, Solution Annealed*

Test Condition		Hydrogen	Strength, MPa		Elongation, %		Fracture
Temp, K	Environment	Exposure**	Yield	Ultimate	Uniform	Total	Strain
380	Air	none	270	750	47	52	0.92
		69 MPa	290	770	48	53	0.82
298	Air	none	310	820	48	55	0.97
		69 MPa	330	840	48	53	0.78
250	Air	none	340	870	48	56	1.20
		69 MPa	360	900	49	55	0.92
200	Air	none	360	930	49	56	1.11
		69 MPa	380	990	54	63	0.94
78	LN	none	530	1520	80	84	0.78
		69 MPa	540	1490	74	76	0.69

* Tensile B, Appendix C-2; heat analysis, Appendix D-3.

** Exposed at 620 K for 3 weeks.

DATA SHEET IH-1

Nickel 200 / **Type 316 Stainless Steel; Bar Stock, As Received***

Test Condition		Hydrogen	Strength, MPa		Elongation, %		Fracture
Temp, K	Environment	Exposure	Yield	Ultimate	Uniform	Total	Strain
298	Air**	none	[illegible]	[illegible]	-	[illegible]	[illegible]
	69 MPa He**	none	120	490	-	55	2.41
	69 MPa H_2**	none	[illegible]	[illegible]	-	[illegible]	[illegible]
	Air†	none	135	480	-	50	2.21
	69 MPa He†	none	122	450	-	48	2.04
	69 MPa H_2†	none	156	460	-	45	0.69

Test Condition		Hydrogen	Strength, MPa		Elongation, %		Fracture
Temp, K	Environment	Exposure**	Yield	Ultimate	Uniform	Total	Strain
300	Air	none	[illegible]	[illegible]	7	[illegible]	[illegible]
		69 MPa	880	930	11	22	1.19
273	Air	none	[illegible]	[illegible]	21	[illegible]	[illegible]
		69 MPa	990	1160	20	32	1.13
250	Air	none	900	1150	27	40	1.51
		69 MPa	1030	1280	24	35	1.07
200	Air	none	960	1210	24	43	1.56
		69 MPa	1100	1410	26	37	1.06

* Tensile A, Appendix C-1.

** Annealed 1090 K 15 minutes and furnace cooled.

† As in **, plus annealed 773 K for 64 hours and air cooled.

* Tensile B, Appendix C-1.

** Exposed at 620 K for 3 weeks.

DATA SHEET IH-2

Nickel 200, Notch-Bar Tensile Properties*

Test Condition		Hydrogen	Strength, MPa		Elongation, %		Fracture
Temp, K	Environment	Exposure	Yield	Ultimate	Uniform	Total	Strain
298	Air**	none	-	660	-	-	0.35
	69MPa He**	none	-	810	-	-	0.37
	69 MPa H_2**	none	-	560	-	-	0.11
	Air†	none	-	635	-	-	0.44
	69 MPa He†	none	-	710	-	-	0.34
	69 MPa H_2†	none	-	580	-	-	0.20

* Tensile A, Appendix C-1 with notch.

** Annealed 1090 K 15 minutes and furnace cooled.

† As in **, plus annealed 773 K for 64 hours and air cooled.

DATA SHEET IJ-1

Nickel 301*

Test Condition		Hydrogen	Strength, MPa		Elongation, %		Fracture
Temp, K	Environment	Exposure	Yield	Ultimate	Uniform	Total	Strain
298	Air**	none	451	778	-	39	1.89
	69 MPa He**	none	486	791	-	34	1.35
	69 MPa H_2**	none	532	618	-	12	0.22
298	Air†	none	1008	1380	-	23	0.49
	69 MPa He†	none	1009	1350	-	22	0.42
	69 MPa H_2†	none	-	850	-	4	0

* Tensile A, Appendix C-1.

** Annealed 1170 K for 5 min and quenched.

† Annealed as in **, plus annealed 860 K for 16 hours, 810 K for 5 hours and 755 K for 5 hours and furnace cooled.

DATA SHEET IJ-2

Nickel 301, Notch Bar Tensile Properties*

Test Condition		Hydrogen	Strength, MPa		Elongation, %		Fracture
Temp, K	Environment	Exposure	Yield	Ultimate	Uniform	Total	Strain
298	Air**	none	-	985	-	-	0.30
	69 MPa He**	none	-	995	-	-	0.30
	69 MPa H2**	none	-	690	-	-	0.01
	Air†	none	-	1630	-	-	0.19
	69 MPa He†	none	-	1600	-	-	0.10
	69 MPa H2†	none	-	840	-	-	0.04

* Tensile A, Appendix C-1 plus notch.

** Annealed 1170 K for 5 min and quenched.

† Annealed as in **, plus annealed 860 K for 16 hours, 810 K for 5 hours and 755 K for 5 hours and furnace cooled.

DATA SHEET IK-1

Type 440C Stainless Steel*

Test Condition		Hydrogen	Strength, MPa		Elongation, %		Fracture
Temp, K	Environment	Exposure**	Yield	Ultimate	Uniform	Total	Strain
298	Air	none	377	620	-	7.1	0.010
		69 MPa D_2	377	575	-	4.6	0.006
200	Air	none	406	670	-	7.7	0.013
		69 MPa D_2	450	570	-	4.2	0.009

* Tensile B, Appendix C-2.

** Exposure at 620 K for 3 weeks.

IRON-CHROMIUM-NICKEL-MANGANESE ALLOYS

DATA SHEET IIA-1

Tenelon® Plate, As Received*

Test Condition		Hydrogen	Strength, MPa		Elongation, %		Fracture
Temp, K	Environment	Exposure**	Yield	Ultimate	Uniform	Total	Strain
350	Air	none	675	1270	48	59	1.43
		69 MPa	700	1300	53	60	0.94
273	Air	none	830	1480	50	58	1.14
		69 MPa	920	1540	48	50	0.51
200	Air	none	1050	1960	59	66	0.69
		69 MPa	1020	1620	40	40	0.36
78	LN	none	1740	1780	19	19	0.08
		none†	1730	2040	22	22	0.07
		none††	1670	2120	25	25	0.13
		none¶	1450	1730	21	21	0.14
		69 MPa	1720	1780	20	20	0.06

* Tensile B, Appendix C-2; heat analysis, Appendix D-4

** Exposed at 620 K for 3 weeks.

† Electropolished.

†† Annealed 1170 K for 24 hours.

¶ Annealed 1270 K for 24 hours.

DATA SHEET IIA-2

Tenelon®*

Test Condition		Hydrogen	Strength, MPa		Elongation, %		Fracture
Temp, K	Environment	Exposure	Yield**	Tensile	Uniform	Total	Strain
298	Air	none	570	930	-	56	1.05
	69 MPa He	none	500	875	-	65	1.14
	69 MPa H_2	none	500	900	-	55	0.63
	Air	69 MPa H_2†	550	840	-	41	0.45
	69 MPa H_2	69 MPa H_2†	470	760	-	24	0.26

* Tensile A, Appendix C-1.

** 0.2% offset.

† 69 MPa H_2 for 1000 hours at 423 K.

DATA SHEET IIA-3

Fracture Toughness of Tenelon®*

Test Temp, K	Specimen Condition	Fracture Toughness, MPa $\sqrt{m}$
78	As received	68.6
	Anneal 1170 K	36.5
	Anneal 1270 K	71.4
200	As received	127.8
	Anneal 1170 K	99.6
	Anneal 1270 K	120.5

* Heat analysis, Appendix D-4; single edge notched, Appendix C-6.

DATA SHEET IIB-1

Nitronic® 40 Stainless Steel Bar Stock, As Received*

Test Condition		Hydrogen	Strength, MPa		Elongation, %		Fracture
Temp, K	Environment	Exposure**	Yield	Ultimate	Uniform	Total	Strain
380	Air	none	680	940	30	39	1.66
		69 MPa	690	1020	36	46	1.02
298	Air	none	770	1170	41	51	1.61
		69 MPa	800	1270	46	56	0.92
250	Air	none	860	1360	46	57	1.51
		69 MPa	-	1380	41	46	0.45
200	Air	none	970	1550	48	58	1.56
		69 MPa	1060	1650	44	48	0.65
78	LN	none	1580	2140	45	49	0.64
		69 MPa	1600	2060	36	36	0.38

* Tensile B, Appendix C-2; heat analysis, Appendix D-5.

** Exposed at 620 K for 3 weeks.

DATA SHEET IIB-2

Mechanical Properties of Nitronic® 40 Alloy: Heat Treatment and Notch Effects*

Test Temp, K**	Treatment	Specimen	Strength, MPa Yield	Strength, MPa Ultimate	Elongation, % Uniform	Elongation, % Total	Fracture Strain
300	Solution Anneal	Smooth bar	700	1170	41	51	1.59
		Notch bar	800	1160	24	27	0.74
	Sensitize	Notch bar	750	1070	18	18	0.53
200	Solution	Smooth bar	880	1550	48	58	1.57
		Notch bar	1130	1500	19	19	0.72
	Sensitize	Smooth bar	720	1490	51	60	1.03
		Notch bar	1120	1250	10	10	0.17

* Heat analysis, Appendix D-5; Tensile B, Appendix C-2.

** Air environment.

DATA SHEET IIB-3

Mechanical Properties of Sensitized Nitronic® 40 Stainless Steel Tested in a High-Pressure Hydrogen Environment at Room Temperature*

Specimen Condition	Test Atmosphere	Strength, MPa Yield	Ultimate	Elongation, % Uniform	Total	Fracture Strain
Solution Annealed	69 MPa He	650	1050	42	52	1.11
	69 MPa H_2	670	1060	41	50	1.22
920 K-2 hr	69 MPa He	640	1100	43	50	1.51
	69 MPa H_2	640	1080	42	49	1.50
920 K-24 hr	69 MPa He	625	1110	46	53	1.38
	69 MPa H_2	620	1100	46	52	1.10
920 K-24 hr	69 MPa He**	760	1060	16	16	0.32
	60 MPa H_2**	700	760	9	9	0.06

* Heat analysis, Appendix D-5; Tensile B, Appendix C-2.

** Notch bar specimen.

DATA SHEET IIB-4

Mechanical Properties of Sensitized Nitronic® 40 Stainless Steel Saturated with Hydrogen*

Temp, K	Treatment**	Hydrogen Exposure	Strength, MPa Yield	Ultimate	Elongation, % Uniform	Total	Fracture Strain
200	Solution Anneal	none	970	1550	48	58	1.57
	Solution Anneal	69 MPa H_2†	1060	1650	44	48	0.66
	920 K-24 hr	none	790	1490	51	60	1.03
	920 K-24 hr	69 MPa H_2	920	1470	37	37	0.33
	920 K-24 hr	69 MPa H_2††	900	1350	35	40	0.45

* Heat analysis, Appendix D-5; Tensile B, Appendix C-2.

** Smooth bar tensile specimens.

† Exposed at 620 K for 3 weeks.

†† Crosshead speed, 5 mm/sec; all others, 0.5 mm/sec.

DATA SHEET IIB-5

Nitronic® 40*

Test Condition		Hydrogen	Strength, MPa		Elongation, %		Fracture
Temp, K	Environment	Exposure	Yield**	Tensile	Uniform	Total	Strain
298	Air	none	400	670	-	58	1.51
	69 MPa He	none	350	700	-	59	1.47
	69 MPa H_2	none	360	700	-	61	1.43

* Tensile A, Appendix C-1.

** 0.2% offset.

DATA SHEET IIB-6

Nitronic® 40; Cold Worked 30%*

Test Condition		Hydrogen	Strength, MPa		Elongation, %		Fracture
Temp, K	Environment	Exposure	Yield**	Tensile	Uniform	Total	Strain
298	Air	none	1240	1290	-	26	0.87
		30 MPa H_2	1075	1150	-	32	0.43
	69 MPa He	none	1010	1050	-	26	0.99
	69 MPa H_2	none	980	1100	-	26	1.02
	69 MPa H_2	30 MPa H_2	1060	1130	-	36	0.44

* Tensile A, Appendix C-1.

** 0.2% offset.

DATA SHEET IIB-7

Nitronic® 40 Stainless Steel, High Energy Rate Forged*

Test Condition		Hydrogen	Strength, MPa		Elongation, %		Fracture
Temp, K	Environment	Exposure	Yield	Ultimate	Uniform	Total	Strain
380	Air	none	540	1040	47	59	1.81
		69 MPa**	570	1070	50	68	1.26
		none	780	970	21	31	1.17
		69 MPa†	690	930	26	33	0.67
298	Air	none	780	1140	32	44	1.24
		69 MPa†	890	1220	30	42	0.96
273	Air	none	640	1300	57	69	1.81
		69 MPa**	690	1430	67	78	1.06
220	Air	none	900	1320	33	45	1.31
		69 MPa†	960	1420	37	47	0.80
200	Air	none	930	1700	51	59	1.26
		69 MPa**	1050	1830	49	54	0.90
		none	1020	1610	42	54	1.26
		69 MPa†	990	1740	53	60	0.66
78	LN	none	1450	2840	46	56	0.83
		69 MPa**	1400	2600	46	46	0.53

* Tensile B, Appendix C-2.
** 69 MPa at 470 K for 1449 days.
† 69 MPa at 620 K for 21 days.

DATA SHEET IIB-8

Nitronic® 40 Stainless Steel, High Energy Rate Forged*

Test Condition		Hydrogen	Strength, MPa		Elongation, %		Fracture
Temp, K	Environment	Exposure	Yield**	Tensile	Uniform	Total	Strain
298	Air	none	610	790	-	34	1.35
		28 MPa H_2	660	820	-	31	0.89
	69 MPa He	none	570	780	-	34	1.39
	69 MPa H_2	none	570	790	-	30	1.31
		28 MPa H_2	630	830	-	31	0.78

* Tensile A, Appendix C-1.
** 0.2% offset.

DATA SHEET IIB-9

Nitronic® 40 Stainless Steel, High Energy Rate Forged*

Test Condition		Hydrogen	Impact
Temp, K	Environment	Exposure	Energy, J
298	Air	none	110
		29.6 MPa H_2**	91
77	LN	none	37
		29.6 MPa H_2**	35

* Impact, Appendix C-8.

** 470 K - 56 days.

DATA SHEET IIB-10

Nitronic® 40 Stainless Steel, High Energy Rate Forged*

Test Condition		Hydrogen	Fracture Toughness, MPa $\sqrt{m}$	
Temp, K	Environment	Exposure	Long	Trans
298	69 MPa He	none	79	74
	69 MPa H_2	none	81	68
	69 MPa H_2	0.6 MPa H_2	76	62

* C-shaped tensile, Appendix C-7.

DATA SHEET IIB-11

Fracture Parameters for Nitronic® 40 Stainless Steel*

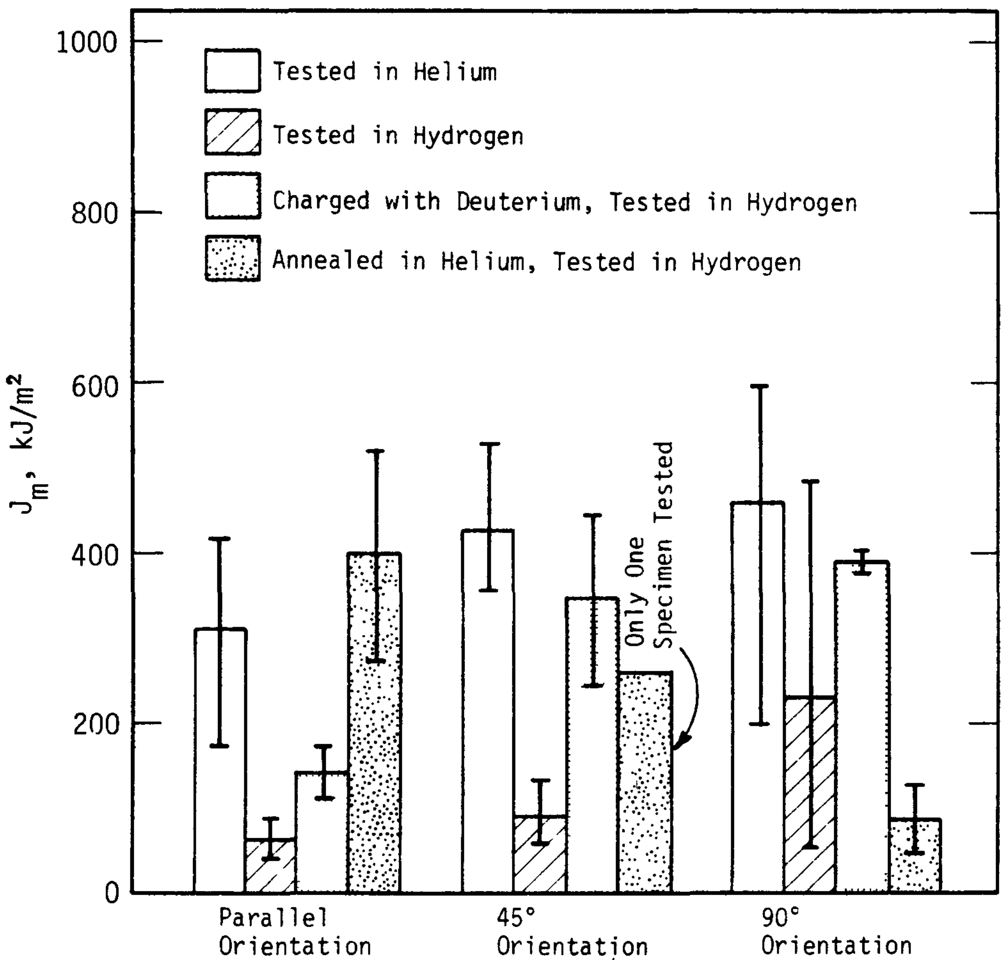

* C-shaped tensile, Appendix C-7. Test in 69 MPa He or H_2. Deuterium exposed at 69 MPa at 620 K for 3 weeks.

DATA SHEET IIB-12

Fracture Parameters for Nitronic® 40 Stainless Steel*

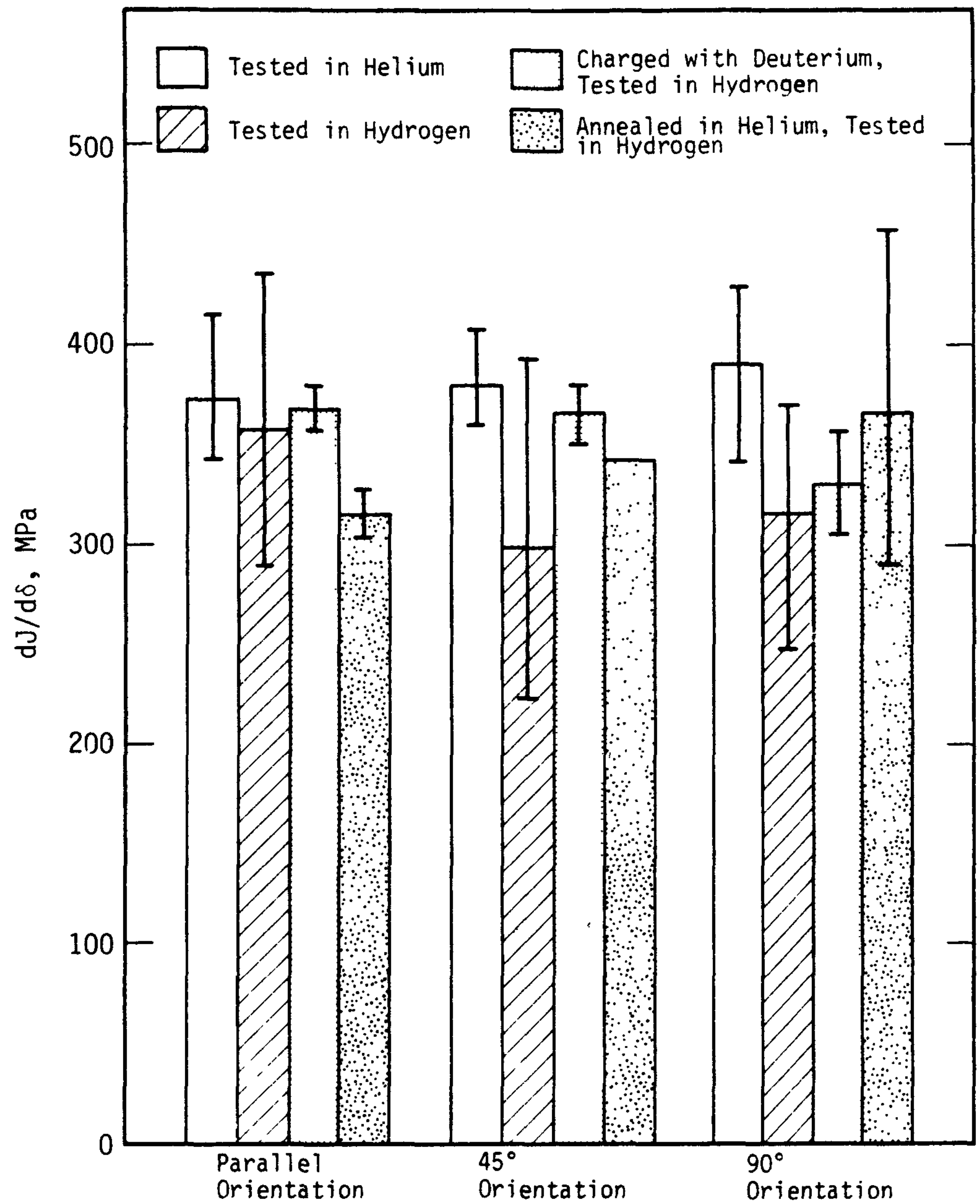

* C-shaped tensile, Appendix C-7. Test in 69 MPa He or H_2. Deuterium charged at 69 MPa at 620 K for 3 weeks.

DATA SHEET IIC-1

Nitronic® 50 Stainless Steel Bar Stock, As Received*

Test Condition		Hydrogen	Strength, MPa		Elongation, %		Fracture
Temp, K	Environment	Exposure**	Yield	Ultimate	Uniform	Total	Strain
380	Air	none	700	990	26	34	1.23
		69 MPa	720	1060	29	37	1.16
298	Air	none	800	1190	32	41	1.17
		69 MPa	820	1240	33	44	1.05
248	Air	none	870	1310	34	43	1.23
		69 MPa	900	1390	35	43	1.00
200	Air	none	1030	1550	35	44	1.08
		69 MPa	1020	1620	37	44	0.97
78	LN	none	1590	2310	38	44	0.91
		69 MPa	1590	2350	38	44	0.90

* Tensile B, Appendix C-2.

** Exposed at 620 K for 3 weeks.

DATA SHEET IIC-2

Nitronic® 50 Stainless Steel Bar Stock, As Received.*

Test Condition		Hydrogen	Strength, MPa			Fracture
Temp, K	Environment	Exposure	Yield**	Tensile	Elongation, %	Strain
298	Air	none	440	710	43	1.27
	69 MPa He	none	400	680	47	1.35
	69 MPa H_2	none	400	680	45	1.31

* Tensile A, Appendix C-1; heat analysis, Appendix D-6.

** 0.2% offset.

DATA SHEET IIC-3

Nitronic® 50 Stainless Steel, High-Energy-Rate-Forged*

Test Condition		Hydrogen	Deflection J_m	Jm	dJ/da
Temp, K	Environment	Exposure	mm	kJ/m^2	MPa
298	69 MPa He†	none	-	32	176
	69 MPa H_2	none	-	23	137
	69 MPa H_2	D_2	-	33	211
	69 MPa He††	none	-	936	360
	69 MPa H_2††	none	-	107	209
	69 MPa H_2††	D_2	-	181	264

* C-Shaped tensile, Appendix C-7.

** Exposed at 620 K for 3 weeks.

† Crack parallel to forging pattern

†† Crack perpendicular to forging patterns.

DATA SHEET IID-1

18-18 Plus® Stainless Steel*

Test Condition		Hydrogen	Strength, MPa		Elongation, %		Fracture
Temp, K	Environment	Exposure	Yield**	Tensile	Uniform	Total	Strain
298	69 MPa He	none	520	910	-	63	1.51
	69 MPa H_2	none	506	880	-	42	0.42

* Tensile A, Appendix C-1; heat analysis, Appendix D-9.

** 0.2% offset.

DATA SHEET IIE-1

X18-3 Mn Stainless Steel*

Test Condition		Hydrogen	Strength, MPa		Elongation, %		Fracture
Temp, K	Environment	Exposure	Yield**	Tensile	Uniform	Total	Strain
298	Air	none	580	810	-	45	1.24
	69 MPa He	none	530	790	-	50	1.35
	69 MPa H_2	none	520	790	-	46	1.31

* Tensile A, Appendix C-1; heat analysis, Appendix D-8.

** 0.2% offset.

DATA SHEET IIF-1

18-2 Mn Stainless Steel*

Test Condition		Hydrogen	Strength, MPa		Elongation, %		Fracture
Temp, K	Environment	Exposure	Yield**	Tensile	Uniform	Total	Strain
298	Air	none	730	1007	-	51	0.87
	69 MPa H_2	none	660	924	-	33	0.31

* Tensile A, Appendix C-1.

** 0.2% offset.

DATA SHEET IIG-1

Type 216 Stainless Steel*

Test Condition		Hydrogen	Strength, MPa		Elongation, %		Fracture
Temp, K	Environment	Exposure	Yield**	Tensile	Uniform	Total	Strain
298	Air	none	640	810	-	40	1.10
298	Air	69 MPa H_2†	630	790	-	36	1.05
298	69 MPa H_2	none	590	780	-	44	1.17
298	69 MPa H_2	69 MPa H_2†	560	760	-	45	1.02
298	69 MPa He	none	590	790	-	45	1.20

* Tensile A, Appendix C-1; heat analysis, Appendix D-7.

** 0.2% offset.

† 69 MPa H_2 at 430 K for 1000 hours.

PRECIPITATION HARDENABLE ALLOYS

DATA SHEET IIIA-1

A-286 Stainless Steel*

Test Condition		Hydrogen	Strength, MPa		Elongation, %		Fracture
Temp, K	Environment	Exposure	Yield	Tensile	Uniform	Total	Strain
298	Air	none	765	1098	–	25	0.77
		2.1 MPa Argon	776	1089	–	24	0.79
		69 MPa D/T**	750	1041	–	13	0.34
		none¶	–	1500	–	4	0.15
		2.1 MPa Argon¶	–	1380	–	3.6	0.11
		69 MPa D/T**,¶	–	1310	–	3	0.06
		none	1010†	1350††	23	28	0.50
		69 MPa D_2¶¶	1070†	1380††	23	24	0.24
220	Air	none	1100†	1520††	28	34	0.49
		69 MPa D_2¶¶	1130†	1530††	27	27	0.25

* Tensile A, Appendix C-1.

** 69 MPa D/T at 370 K for 200 days.

† True stress at 5% strain.

†† True stress at maximum load.

¶ Notched-bar tensile specimens, all others smooth-bar specimens.

¶¶ 69 MPa D_2 at 620 K for 3 weeks.

DATA SHEET IIIA-2

A-286 Stainless Steel High Energy, Rate Forged*

Test Condition		Hydrogen	Fracture
Temp, K	Environment	Exposure	Toughness, MPa $\sqrt{m}$
298	69 MPa He	none	76**
	69 MPa H_2		89**
	69 MPa He	none	71***
	69 MPa H_2		90***
	69 MPa He	none	81†
	69 MPa H_2		82†
	69 MPa He	none	93††
	69 MPa H_2		89††
	69 MPa He	1.6 MPa D_2	88††
	69 MPa H_2	1.6 MPa D_2	97††
	69 MPa He	none	52¶
	69 MPa H_2	none	56¶
	69 MPa H_2	1.5 MPa D_2	59¶
	69 MPa He	none	93¶¶
	69 MPa H_2	none	90¶¶
	69 MPa H_2	1.5 MPa D_2	97¶¶

* Single edge notched, Appendix C-6.

** Aged 4 hours at 990 K (Heat 1).

*** Aged 8 hours at 990 K (Heat 1).

† Aged 16 hours at 990 K (Heat 1).

†† Aged 8 hours at 990 K (Heat 2).

¶ HERF only not aged. R_C-11.

¶¶ Aged 8 hours at 990 K. R_C-11.

DATA SHEET IIIA-3

A-286 Stainless Steel Notch Impact Test*

Test Condition		Hydrogen	Impact
Temp, K	Environment	Exposure	Energy, J
298	Air	Base Metal	
		As Received	6.10
		Argon**	5.08
		D/T†	4.74
298	Air	Weld Metal	
		As Received	4.18
		Argon**	3.40
		D/T†	4.51

---

* Impact Appendix C-8.

** 0.21 MPa at 370 K for 200 days.

† 69 MPa D/T at 370 K for 200 days.

DATA SHEET IIIA-4

Fracture Parameters for A-286 Stainless Steel*

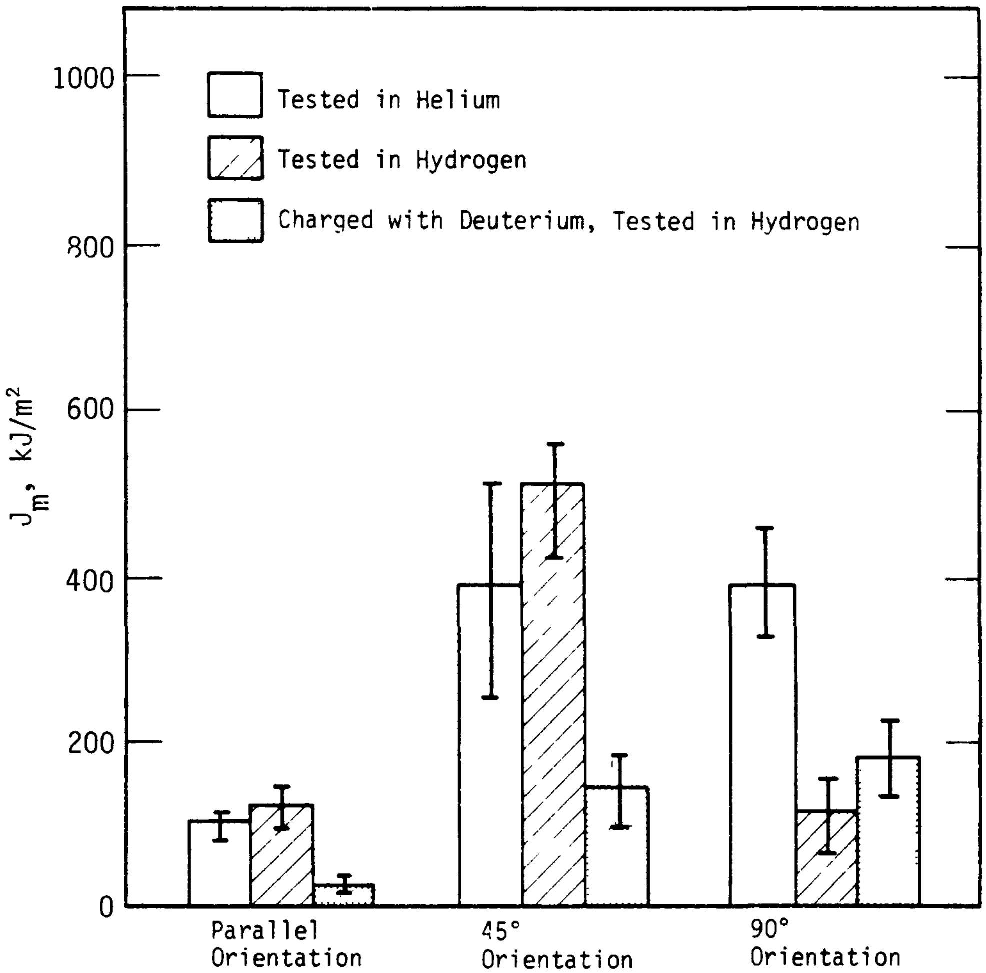

* C-shaped tensile, Appendix C-7. Tested in 69 MPa H_2 or He. Deuterium charged at 69 MPa at 620 K for 3 weeks.

DATA SHEET IIIA-5

Fracture Parameters for A-286 Stainless Steel*

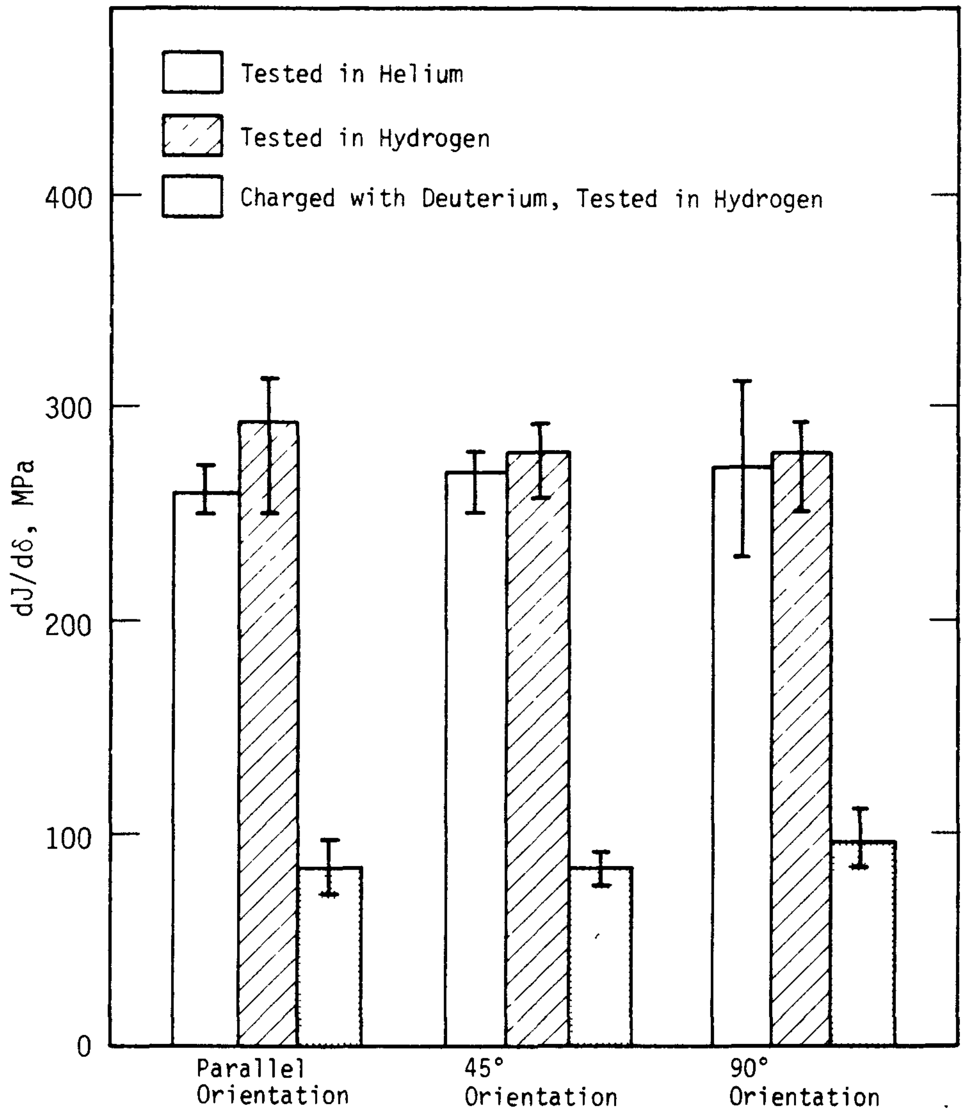

* C-shaped Tensile, Appendix C-7. Tested in 69 MPa He or H_2. Deuterium charged at 69 MPa at 620 K for 3 weeks.

DATA SHEET IIIB-1

JBK-75 HERF and Age*

Test Condition		Hydrogen	Strength, MPa		Elongation, %		Fracture
Temp, K	Environment	Exposure	Yield**	Tensile	Uniform	Total	Strain
298	69 MPa He	none	800	1090	10	14	0.63
	69 MPa H_2	none	890	1160	10	13	0.40

* Tensile, Appendix C-3.

** 0.2% offset.

DATA SHEET IIIB-2

JBK-75 HERF and Age*

Test Condition		Hydrogen	Stress Intensity,	Fracture Energy,
Temp, K	Environment	Exposure	MPa $\sqrt{m}$	MJ/m^2
298	69 MPa He	none	80	0.350
	69 MPa H_2	none	80	0.333
	69 MPa H_2	0.7 MPa D_2 at 625 K	81	0.294

* C-shaped tensile, Appendix C-7.

DATA SHEET IIIC-1

17-4 Stainless Steel, Tensile Tubes*

Test Condition		Hydrogen	Strength, MPa		Elongation, %		Fracture
Temp, K	Environment	Exposure	Yield**	Tensile	Uniform	Total	Strain
298	Air	none	940	980	-	4.7	-
	69 MPa He	69 MPa He	1076	1145	-	6.4	-
	35 MPa D/T	35 MPa D/T†	1000	1000	-	0.7	-
	69 MPa D/T	69 MPa D/T††	1062	1096	-	1.2	-

* Tensile E, Appendix C-5.

** 0.2% offset.

† 8 hours at 315 K.

†† 2 hours at 370 K.

DATA SHEET IIIC-2

Fracture Toughness 17-4 PH Stainless Steel*

Fracture Toughness, MPa$\sqrt{m}$

Material	Test Environment		
Condition	69 MPa He	3.5 MPa H_2	69 MPa H_2
Underaged	104	31	20
Peak Aged	97	29	13
Overaged	-	57	34
Solution Annealed	97	71	31

Heat Treatments

Material Condition	Aging Temp, K	Hardness R_C
Underaged	709	38
Peak Aged	783	42
Overaged	866	35
Solution Annealed	-	28

* C-shaped tensile, Appendix C-7.
All specimens were solution annealed 2 hours at
1339 K and aged 1 hour at indicated temperatures.

DATA SHEET IIID-1

AM-350 Stainless Steel*

Test Condition		Hydrogen	Strength, MPa		Elongation, %		Fracture
Temp, K	Environment	Exposure	Yield**	Tensile	Uniform	Total	Strain
298	Air	none	420	1160	-	70	-
		69 MPa†	455	580	-	3/4	-
	69 MPa He	none	420	1240	-	55	-
	6.9 MPa D_2	none	345	430	-	4	-
	69 MPa D_2	none	430	520	-	2.6	-
	0.69 MPa D_2	none	410	455	-	3	-

* Condition H - annealed at 1310 to 1350 K air cool or water quench.

** 0.2% offset.

† 26 days at 570 K.

DATA SHEET IIIE-1

AM-363 Stainless Steel

Test Condition		Hydrogen	Strength, MPa		Elongation, %		Fracture
Temp, K	Environment	Exposure	Yield*	Tensile	Uniform	Total	Strain
298	Air	none	890	890	-	7	-
	Air	0.21 MPa H_2**	900	900	-	8.6	-
	Air	none	1340†	1480	-	3	-
	Air	0.21 MPa H_2**	1400†	1500	-	3	-

* 0.21 MPa D_2 at 630 K for 5 days.

** 0.2% offset.

† Notched - 45° notch. Notch diameter = 0.5X outer diameter.

DATA SHEET IIIF-1

CG-27 Stainless Steel*

Test Condition		Hydrogen	Strength, MPa		Elongation, %		Fracture
Temp, K	Environment	Exposure	Yield**	Tensile	Uniform	Total	Strain
298	69 MPa He	none	806	1165	-	29	0.30
	69 MPa H_2	none	855	1117	-	10	0.13
298	69 MPa H_2	69 MPa H_2 at 425 K-72 hrs	855	1020	-	4	0.03
298	69 MPa He†	none	1070	1385	-	12	0.13
	69 MPa H_2†	none	1034	1138	-	1	0.03

* Tensile A, Appendix C-1.

** 0.2% offset.

† HERF specimens.

DATA SHEET IIIG-1

Ni-SPAN-C* (Alloy 902)

Test Condition		Hydrogen	Strength, MPa		Elongation, %		Fracture
Temp, K	Environment	Exposure	Yield**	Tensile	Uniform	Total	Strain
298	Air	none	676	1186	-	10	-
	69 MPa He	none	750	1160	-	16	-
	6.9 MPa H_2	none	-	1170	-	14	-
	69 MPa H_2	none	650	1130	-	15	-

* Sheet specimens 0.25 mm and 19 mm gauge length.

** 0.2% offset.

HIGH PURITY ALLOYS

DATA SHEET IVA-1

Mechanical Properties (Alloy A)*

Test Condition		Hydrogen	Strength, MPa		Elongation, %		Fracture
Temp, K	Environment	Exposure**	Yield	Ultimate	Uniform	Total	Strain
370	Air	none	230	610	45	52	1.57
		69 MPa	270	660	50	59	1.65
298	Air	none	350	1270	62	73	1.66
		69 MPa	290	1030	60	60	0.50
235	Air	69 MPa	390	1110	38	38	0.27
200	Air	none	540	1320	36	46	1.42
		69 MPa	420	1190	33	33	0.31
78	LN	none	-	-	-	-	1.44
		69 MPa	-	1060	42	48	1.13

* Tensile B, Appendix C-2.

** Exposed at 620 K for 3 weeks.

DATA SHEET IVB-1

Mechanical Properties (Alloy B)*

Test Condition		Hydrogen	Strength, MPa		Elongation, %		Fracture
Temp, K	Environment	Exposure**	Yield	Ultimate	Uniform	Total	Strain
370	Air	none	240	630	45	56	1.58
		69 MPa	260	660	46	56	1.40
298	Air	none	340	1020	61	69	1.56
		69 MPa	290	870	65	72	1.50
235	Air	69 MPa	320	1170	72	79	0.44
200	Air	none	340	1170	64	74	1.57
		69 MPa	380	1250	66	71	0.89
78	LN	none	260	870	63	67	1.37
		69 MPa	270	900	66	72	1.41

* Tensile B, Appendix C-2.

** Exposed at 620 K for 3 weeks.

DATA SHEET IVC-1

Mechanical Properties (Alloy C)*

Test Condition		Hydrogen	Strength, MPa		Elongation, %		Fracture
Temp, K	Environment	Exposure**	Yield	Ultimate	Uniform	Total	Strain
370	Air	none	250	630	44	52	1.62
		69 MPa	260	660	45	53	1.45
298	Air	none	330	910	49	58	1.65
		69 MPa	290	770	52	62	1.55
200	Air	none	300	1100	78	87	1.52
		69 MPa	330	1170	78	86	1.50
78	LN	none	250	850	82	89	1.53
		69 MPa	280	890	80	86	1.43

* Tensile B, Appendix C-2.

** Exposed at 620 K for 3 weeks.

REFERENCES

1. I. M. Bernstein and A. W. Thompson. Hydrogen in Metals, ed., American Society for Metals, Metals Park, Ohio (1974).

2. A. W. Thompson and I. M. Bernstein. Effect of Hydrogen on Behavior of Materials, ed., Metallurgical Society of AIME, New York, NY (1976).

3. A. W. Thompson and I. M. Bernstein. Effect of Hydrogen on Behavior of Materials, ed., Metallurgical Society of AIME, Warrendale, PA (1981).

4. M. R. Louthan, Jr. and R. P. McNitt. Environmental Degradation of Engineering Materials, ed., Virginia Polytechnic Institute, Blacksburg, VA (1977).

5. M. R. Louthan, Jr., R. P. McNitt, and R. D. Sisson, Jr. Environmental Degradation of Engineering Materials - II, ed., Virginia Polytechnic Institute, Blacksburg, VA (1981).

6. MM J. P. Fidelle et. M. Papin. L' Hydrogen Dans Les Metaux, Colloque - Valduc (27-28, September 1967).

7. "L'Hydrogen Dans Les Metaux-2." Congress International, Paris (29 Mai-2 Juin, 1972).

8. "Hydrogen in Metals." Proceedings of the 2nd International Congress, Paris, 6-10 June 1977. Pergamon Press, New York, (1977).

9. "Hydrogen in Metals," Proceedings of the 3rd International Congress, Paris, 7-2 June 1982.

10. "Hydrogen Embrittlement Testing." ASTM Special Technical Publication 543, American Society for Testing and Materials, Philadelphia, PA (1974).

11. Advanced Techniques for Characterizing Hydrogen in Metals, TMS-AIME, Warrendale, PA (1982).

12. C. D. Beachem, ed. **Hydrogen Damage,** American Society for Metals, Metals Park, OH (1979).

13. J. P. Hirth and H. H. Johnson. "Hydrogen Problems in Energy Related Technology." Corrosion 32, 3 (1976).

14. J. J. Au and H. K. Birnbaum. "Hydrogen Effects on the Deformation of Iron Whiskers." Scripta Met 12, 457 (1978).

15. G. C. Smith. "Effect of Hydrogen on Nickel and Nickel-Base Alloys." Hydrogen in Metals. p. 485, American Society for Metals, Metals Park, Ohio (1974).

16. J. K. Tien, A. W. Thompson, I. M. Bernstein, and Rebecca J. Richards. "Hydrogen Transport by Dislocations." Met. Trans. 7A, 821 (1976).

17. A. W. Thompson, "The Mechanism of Hydrogen Participation in Ductile Fracture." Effect of Hydrogen on Behavior of Materials. p. 467, Metallurgical Society of AIME, Warrendale, PA (1976).

18. J. F. Breedis and L. Kaufmann. "Formation of HCP and BCC Phases in Austenitic Iron Alloys." Met. Trans. 2, 2359 (1971).

19. D. V. Neff, T. E. Mitchell, and A. R. Troiano. "The Influence of Temperature, Transformation, and Strain-Rate on the Ductility Properties of Austenitic Stainless Steels." Trans. ASM 62, 858 (1969).

20. B. C. Odegard, J. A. Brooks, and A. J. West. "The Effect of Hydrogen on the Mechanical Behavior of Nitrogen Strengthened Stainless Steel." p. 116 in Effect of Hydrogen on Behavior of Materials. Metallurical Society of AIME, Warrendale, PA (1976).

21. R. E. Stoltz and J. B. Vander Sande. "The Effect of Nitrogen on Stacking Fault Energy of Fe-Cr-Ni-Mn Steels." Met. Trans. 11A, 1033 (1980).

22. H. Mecking. "Deformation of Polycrystals." p. 1573 in Strength of Metals and Alloys, Vol. 3, Pergamon Press, New York (1980).

23. C. L. Briant. "Hydrogen Assisted Cracking of Sensitized 304 Stainless Steel." Met. Sci. 9A, 731 (1978).

24. A. W. Thompson. "The Behavior of Sensitized 309S Stainless Steel in Hydrogen." Mat. Sci. and Eng. 14, 253 (1974).

25. J. D. Hobson and J. Hewitt. "The Effect of Hydrogen on the Tensile Properties of Steel." Journal Iron and Steel Institute 172, 131 (1953).

26. H. R. Gray. "Testing for Hydrogen Environment Embrittlement: Experimental Variables." p. 133 in Hydrogen Embrittlement Testing. ASTM STP 543, American Society for Testing and Materials, Philadelphia, PA (1974).

27. M. B. Whiteman and A. R. Troiano. "Hydrogen Embrittlement of Austenitic Stainless Steels." Corrosion 21, 53 (1965).

28. J. P. Fidelle, et al. "Disk Pressure Testing of Hydrogen Environment Embrittlement." p. 221 in Hydrogen Embrittlement Testing. ASTM STP 543, American Society for Testing and Materials, Philadelphia, PA (1974).

29. D. Eliezer, D. G. Chakrapani, C. J. Alstetter, and E. N. Pugh. "The Influence of Austenite Stability on the Hydrogen Embrittlement and Stress Corrosion Cracking of Stainless Steel." Met. Trans. 10A, 935 (1979).

30. D. Eliezer. Hydrogen Assisted Cracking in Type 304L and 316L Stainless Steel. Third International Conference on Effect of Hydrogen on Behavior of Materials, August 1980.

31. R. J. Walter and W. T. Chandler, p. 104 discussion to paper by A. W. Thompson. "Ductility Losses in Stainless Steel." Hydrogen in Metals. American Society for Metals, Metals Park, Ohio (1974).

32. M. W. Perra. "Sustained-Load Cracking of Austenitic Steels in Gaseous Hydrogen." Environmental Degradation of Engineering Materials. ed., M. R. Louthan, Jr., R. P. McNitt, and R. D. Sisson, Jr., VPI, Blacksburg, VA 321-333 (1981).

33. A. W. Loginow and E. H. Phelps "Steels for Seamless Hydrogen Pressure Vessels" Corrosion 31 404 (1975).

34. R. L. Tobler and R. P. Reed. "Tensile and Fracture Behavior of a Nitrogen Strengthened Chromium-Nickel-Manganese Stainless Steel at Cryogenic Temperatures", p. 537 in Special Technical Publication, ASTM STP 668. American Society for Testing and Materials, Philadelphia, PA (1979).

35. R. L. Tobler, D. T. Read, and R. P. Reed. "Strength/Toughness Relationship for Interstitially Strengthened AISI 304 Stainless Steel at 4 K Temperature," p. 250 in Special Technical Publication ASTM STP 743, American Society for Testing and Materials, Philadelphia, PA (1982).

36. W. Losch and I. Andreoni. "Grain Boundary Surface Phases Observed in Temper Embrittled High-Alloy Steels." Scripta Met. 12, 277 (1978).

37. A. W. Thompson. "Mechanical Behavior of Face-Centered Cubic Metals Containing Helium." Mater. Sci. and Eng. 21, 41-48 (1975).

38. M. R. Louthan, Jr., G. R. Caskey, D. E. Rawl, Jr., and C. W. Krapp. "Tritium Effects in Austenitic Steels." p. 117 in Proceedings of International Conference on Radiation Effects and Tritium Technology for Fusion Reactors IV. CONF-752026-13 (1976).

39. D. E. Rawl, Jr., G. R. Caskey, Jr., and J. A. Donovan. "Low Temperature Helium Embrittlement of Tritium Charged Stainless Steel." 109th Annual AIME Meeting, Las Vegas, Nevada, February 24-28, 1980.

40. J. A. Donovan. "Effects of Helium on Mechanical Properties of Armco Iron." Fall TMS-AIME Meeting, Niagara Falls, New York, September 20-23, 1976.

41. A. J. West and D. E. Rawl, Jr. "Hydrogen in Stainless Steel: Isotopic Effects on Mechanical Properties." Proceedings of Conference in Tritium Technology in Fusion, Fusion and Isotopic Applications. Conference 800427 (1980).

42. M. R. Louthan and R. G. Derrick, "Hydrogen Transport in Austenitic Stainless Steel." Corros. Sci. 15 565 (1975).

43. G. R. Caskey, Jr., and R. D. Sisson, Jr. "Hydrogen Solubility in Austenitic Stainless Steel." Scripta Met 15, 1187 (1981).

44. M. R. Dietrich, G. R. Caskey, Jr., and J. A. Donovan. J-Controlled Crack Growth as an Indicator of Hydrogen-Stainless Steel Compatibility, Hydrogen Effects in Metals, ed. I. M. Bernstein and A. W. Thompson, Metallurgical Society of AIME, Warrendale, PA, p. 637 (1981).

45. G. R. Caskey, Jr., D. A. Mezzanotte, Jr., and D. E. Rawl, Jr. "Helium Embrittlement Stainless Steels at Ambient Temperature." Scripta Met 16, 969 (1982).

46. T. L. Capeletti and M. R. Louthan, Jr. "The Tensile Ductility of Austenitic Steels in Air and Hydrogen." Journal of Engineering Materials and Technology, 99, 153-158 (1977).

47. T. L. Capeletti. "Effect of Hydrogen Exposure or the Fracture Toughness of 17-4 pH Stainless Steel." Int. Conference on Mechanical Behavior of Materials, Boston, August 16-20 (1976). Conference 760819-12.

48. G. R. Caskey, Jr. "The Role of Twinning and Transformation in Hydrogen Embrittlement of Austenitic Stainless Steels" in Environmental Degradation of Engineering Materials, ed. by M. R. Louthan and R. P. McNitt, Virginia Polytechnic Institute, Blacksburg, VA, pp. 437-449 (1977).

49. G. R. Caskey, Jr. "Fractography of Hydrogen Embrittled Stainless Steel." Scripta Met 11, 1077-1083 (1977).

50. G. R. Caskey, Jr. "A Mechanism for Hydrogen-Induced Brittle Fracture of Austenitic Stainless Steel." DP-MS-77-86, E. I. du Pont de Nemours & Co., Savannah River Laboratory, Aiken, SC, 107th Annual AIME Meeting, Denver, CO, February 26 - March 2, 1978.

51. G. R. Caskey, Jr. "Fracture of Fe-Cr-Mn Austenitic Steel." DP-MS-78-68, E. I. du Pont de Nemours & Co., Savannah River Laboratory, Aiken, SC, 108th Annual AIME Meeting, New Orleans, LA, February 18-20, 1979.

52. G. R. Caskey, Jr. and J. A. Donovan. "Effect of Heat Treatment on Fracture of Type 304L Stainless Steel in a Hydrogen Environment." DP-MS-79-18, E. I. du Pont de Nemours & Co., Savannah River Laboratory, Aiken, SC, 1979, TMS-AIME Fall Meeting, Milwaukee, WI, September 16-20, 1979.

53. G. R. Caskey, Jr. "Notch and Hydrogen Effects on Sensitized 21-6-9 Stainless Steel." DP-MS-79-22, E. I. du Pont de Nemours & Co., Savannah River Laboratory, Aiken, SC, 1979 TMS-AIME Fall Meeting, Milwaukee, WI, September 16-20, 1979.

54. G. R. Caskey, Jr. "Hydrogen Effects on Flow Localization and Fracture in Type 304L Stainless Steel." DP-MS-79-57, E. I. du Pont de Nemours & Co., Savannah River Laboratory, Aiken, SC, Gordon Research Conference, Andover, NH, July 9-13, 1979.

55. G. R. Caskey, Jr. "Acoustic Emission from Hydrogen Saturated Type 304L Stainless Steel." Scripta Met 13 583-587 (1979).

56. G. R. Caskey, Jr. "Hydrogen Assisted Fracture of Sensitized Type 304L Austenitic Stainless Steel." DP-MS-79-62, E. I. du Pont de Nemours & Co., Savannah River Laboratory, Aiken, SC, 109th Annual AIME Meeting, Las Vegas, NV, February 24-28, 1980.

57. G. R. Caskey, Jr. "Fractography of Hydrogen-Embrittled Iron Chromium-Nickel Alloys." Microstructural Science 9, 413-419 (1981).

58. G. R. Caskey, Jr. "Hydrogen Induced Brittle Fracture of Type 304L Austenitic Stainless Steel." American Society for Testing and Materials, STP 733, 86-97 (1981).

59. G. R. Caskey, Jr. "Effect of Hydrogen on Work Hardening of Type 304L Austenitic Stainless Steel." Scripta Met 15, 1183-1186 (1981).

60. G. R. Caskey, Jr. "Hydrogen Damage in Stainless Steel." Environmental Degradation of Engineering Materials. Edited by M. R. Louthan, Jr., R. P. McNitt, and R. D. Sisson, Virginia Polytechnic Institute, Blacksburg, VA, pp. 283-302 (1981).

61. G. R. Caskey, Jr. "Hydrogen Effects in High Purity Stainless Steels." Third International Congress on Hydrogen and Materials, Paris, France, June 7-11, 1982.

62. J. A. Donovan. "Accelerated Evolution of Hydrogen from Metals During Plastic Deformation." Met. Trans. 7A, 1677-1683 (1977).

63. M. L. Holzworth and M. R. Louthan, Jr. "Hydrogen Induced Phase Transformations on Type 304L Stainless Steels." Corrosion 24, 110-124 (1968).

64. M. L. Holzworth. "Hydrogen Embrittlement of Type 304L Stainless Steel." Corrosion 25, 107-115 (1969).

65. M. R. Louthan, Jr., G. R. Caskey, Jr., J. A. Donovan, and D. E. Rawl, Jr. "Hydrogen Embrittlement of Metals." Mater. Sci. and Eng. 10 357 (1972).

66. M. R. Louthan, Jr., J. A. Donovan, and D. E. Rawl, Jr. "Effect of High Dislocation Density on Stress Corrosion Cracking and Hydrogen Embrittlement of Type 304L Stainless Steel." Corrosion 29, 108-111 (1973).

67. M. R. Louthan, Jr., J. A. Donovan, and G. R. Caskey, Jr. "Tritium Absorption in Type 304L Stainless Steel." Nuclear Technology 26, 192-200 (1975).

68. M. R. Louthan, Jr., D. E. Rawl, Jr., J. A. Donovan, and W. G. Holmes. "Hydrogen Embrittlement of Austenitic Stainless Steels." Trans. Am. Nuc. Soc. 21, 158 (1975).

69. M. R. Louthan, Jr. and G. R. Caskey, Jr. "Hydrogen Transport and Embrittlement in Structural Metals." 1st World Hydrogen Energy Conference (1976).

70. M. R. Louthan, Jr. and R. P. McNitt. "The Role of Test Technique in Evaluating Hydrogen Embrittlement Mechanism." Effect of Hydrogen in Behavior of Materials, ed. A. W. Thompson and I. M. Bernstein, Metallurgical Society of AIME, Warrendale, PA, p. 496 (1976).

71. M. R. Louthan, Jr. "Effect of Hydrogen on the Mechanical Properties of Low Carbon and Austenitic Steels." Hydrogen in Metals, ed. T. M. Bernstein and A. W. Thompson, American Society for Metals, Metals Park, Ohio, pp. 53-77 (1974).

APPENDIX A. DEFINITIONS

ELONGATION

Percentage increase of a gauge length, usually one inch, during plastic strain in tension. In the data presented here, crosshead motion was taken as the measure of change in length.

Total elongation is length increase at fracture.

Uniform elongation is length increase to the point where drop in load is detected which signals beginning of observable strain localization or necking.

HEAT TREATMENTS

Aging is a process of heating a previously solution-treated alloy to an intermediate temperature to cause precipitation of a finely dispersed phase which hardens the alloy.

Sensitization is a heat treatment that causes precipitation of carbides of the form $M_{23}C_6$ along grain boundaries and simultaneously reduces the chromium content of the grain boundary regions.

Solution annealing is a process of heating to elevated temperature to dissolve all precipitates and produce a homogeneous solid solution and quenching to retain the solid solution.

MECHANICAL PROCESSING

Ingots of stainless steel are formed into plate or bar by mechanical processes of rolling and forging.

Cross-rolled plate refers to turning plate 90° between passes through the rolling mills to minimize preferred orientation that arises during the rolling process.

High energy rate forged (HERF) alloys are hot forged at a very rapid rate and immediately quenched in water to retain deformation introduced during forging.

PLASTIC STRAIN

Irreversible or permanent strain of the test specimen measured by subtracting elastic or recoverable strain from total strain. This was usually done graphically on the load-deformation record obtained during a tensile test.

Plastic strain to failure ($_p$) is calculated from the measured change in cross sectional area from the original (A_0) to the final area (A_f) at the fracture.

$$\varepsilon_p = \ln A_0/A_f$$

Reduction in area (RA) is a measure of plasticity calculated from the original (A_0) and final (A_f) cross sectional areas.

$$RA = 100 \frac{A_0 - A_f}{A_0}$$

STRESS

Stress or force per unit area may be defined with respect to an initial area (engineering stress) or the instantaneous area (true stress). Both definitions have been utilized in data presented here and are distinguished in each table.

Yield strength is the stress corresponding to a plastic strain of 5% unless otherwise noted.

Ultimate strength is the true stress corresponding at maximum load.

Tensile strength is the engineering stress at maximum load.

STRESS INTENSITY

The stress intensity factor (K) relates the stress field (σ_{ij}) around a crack tip to the crack dimensions (a) and specimen dimensions (width = w), where the function f(a,W) depends on specimen shape, crack location and loading mode.

The stress intensity corresponding to the critical value for crack extension is the Fracture Toughness (K_c). Fracture toughness is a measure of the ability of a material to resist crack propagation.

Under sustained load, cracks will propagate in hydrogen at stress intensities greater than a threshold or K_{TH}.

Temperature Conversions

Albert Sauveur type of table. Look up reading in middle column; if in degrees Centigrade, read Fahrenheit equivalent in right-hand column; if in degrees Fahrenheit, read Centigrade equivalent in left-hand column. Values as printed in "Bethlehem Alloy Steels".

−459.4 to 0

C		F
−273	−459.4	
−268	−450	
−262	−440	
−257	−430	
−251	−420	
−246	−410	
−240	−400	
−234	−390	
−229	−380	
−223	−370	
−218	−360	
212	−350	
−207	−340	
−201	330	
−196	−320	
−190	−310	
−184	−300	
179	−290	
−173	−280	
−169	273	−459.4
−168	−270	−454
−162	−260	−436
−157	−250	−418
−151	−240	−400
−146	−230	−382
−140	−220	−364
−134	−210	−346
−129	−200	−328
−123	−190	−310
−118	−180	−292
−112	−170	−274
−107	−160	−256
−101	−150	−238
−96	−140	−220
−90	−130	−202
−84	−120	−184
−79	−110	−166
−73	−100	−148
−68	−90	−130
−62	−80	−112
−57	−70	−94
−51	−60	−76
−46	−50	−58
−40	−40	−40
−34	−30	−22
−29	−20	−4
−23	−10	14
−17.8	0	32

0 to 100

C		F	C		F
−17.8	0	32	10.0	50	122.0
−17.2	1	33.8	10.6	51	123.8
−16.7	2	35.6	11.1	52	125.6
−16.1	3	37.4	11.7	53	127.4
−15.6	4	39.2	12.2	54	129.2
−15.0	5	41.0	12.8	55	131.0
−14.4	6	42.8	13.3	56	132.8
−13.9	7	44.6	13.9	57	134.6
−13.3	8	46.4	14.4	58	136.4
−12.8	9	48.2	15.0	59	138.2
−12.2	10	50.0	15.6	60	140.0
−11.7	11	51.8	16.1	61	141.8
−11.1	12	53.6	16.7	62	143.6
−10.6	13	55.4	17.2	63	145.4
−10.0	14	57.2	17.8	64	147.2
−9.4	15	59.0	18.3	65	149.0
−8.9	16	60.8	18.9	66	150.8
−8.3	17	62.6	19.4	67	152.6
−7.8	18	64.4	20.0	68	154.4
7.2	19	66.2	20.6	69	156.2
−6.7	20	68.0	21.1	70	158.0
−6.1	21	69.8	21.7	71	159.8
−5.6	22	71.6	22.2	72	161.6
−5.0	23	73.4	22.8	73	163.4
−4.4	24	75.2	23.3	74	165.2
−3.9	25	77.0	23.9	75	167.0
−3.3	26	78.8	24.4	76	168.8
−2.8	27	80.6	25.0	77	170.6
−2.2	28	82.4	25.6	78	172.4
−1.7	29	84.2	26.1	79	174.2
−1.1	30	86.0	26.7	80	176.0
−0.6	31	87.8	27.2	81	177.8
0.0	32	89 6	27.8	82	179.6
0.6	33	91.4	28.3	83	181.4
1.1	34	93.2	28.9	84	183.2
1.7	35	95.0	29.4	85	185.0
2.2	36	96.8	30.0	86	186.8
2.8	37	98.6	30.6	87	188.6
3.3	38	100.4	31.1	88	190.4
3.9	39	102.2	31.7	89	192.2
4.4	40	104.0	32.2	90	194.0
5.0	41	105.8	32.8	91	195.8
5.6	42	107 6	33.3	92	197.6
6.1	43	109.4	33.9	93	199.4
6.7	44	111.2	34.4	94	201.2
7.2	45	113.0	35.0	95	203.0
7.8	46	114.8	35.6	96	204.8
8.3	47	116.6	36.1	97	206.6
8.9	48	118.4	36.7	98	208.4
9.4	49	120.2	37.2	99	210.2
			37.8	100	212.0

100 to 1000

C		F	C		F
38	100	212	260	500	932
43	110	230	266	510	950
49	120	248	271	520	968
54	130	266	277	530	986
60	140	284	282	540	1004
66	150	302	288	550	1022
71	160	320	293	560	1040
77	170	338	299	570	1058
82	180	356	304	580	1076
88	190	374	310	590	1094
93	200	392	316	600	1112
99	210	410	321	610	1130
100	212	413.6	327	620	1148
104	220	428	332	630	1166
110	230	446	338	640	1184
116	240	464	343	650	1202
121	250	482	349	660	1220
127	260	500	354	670	1238
132	270	518	360	680	1256
138	280	536	366	690	1274
143	290	554	371	700	1292
149	300	572	377	710	1310
154	310	590	382	720	1328
160	320	608	388	730	1346
166	330	626	393	740	1364
171	340	644	399	750	1382
177	350	662	404	760	1400
182	360	680	410	770	1418
188	370	698	416	780	1436
193	380	716	421	790	1454
199	390	734	427	800	1472
204	400	752	432	810	1490
210	410	770	438	820	1508
216	420	788	443	830	1526
221	430	806	449	840	1544
227	440	824	454	850	1562
232	450	842	460	860	1580
238	460	860	466	870	1598
243	470	878	471	880	1616
249	480	896	477	890	1634
254	490	914	482	900	1652
			488	910	1670
			493	920	1688
			499	930	1706
			504	940	1724
			510	950	1742
			516	960	1760
			521	970	1778
			527	980	1796
			532	990	1814
			538	1000	1832

1000 to 2000

C		F	C		F
538	1000	1832	816	1500	2732
543	1010	1850	821	1510	2750
549	1020	1868	827	1520	2768
554	1030	1886	832	1530	2786
560	1040	1904	838	1540	2804
566	1050	1922	843	1550	2822
571	1060	1940	849	1560	2840
577	1070	1958	854	1570	2858
582	1080	1976	860	1580	2876
588	1090	1994	866	1590	2894
593	1100	2012	871	1600	2912
599	1110	2030	877	1610	2930
604	1120	2048	882	1620	2948
610	1130	2066	888	1630	2966
616	1140	2084	893	1640	2984
621	1150	2102	899	1650	3002
627	1160	2120	904	1660	3020
632	1170	2138	910	1670	3038
638	1180	2156	916	1680	3056
643	1190	2174	921	1690	3074
649	1200	2192	927	1700	3092
654	1210	2210	932	1710	3110
660	1220	2228	938	1720	3128
666	1230	2246	943	1730	3146
671	1240	2264	949	1740	3164
677	1250	2282	954	1750	3182
682	1260	2300	960	1760	3200
688	1270	2318	966	1770	3218
693	1280	2336	971	1780	3236
699	1290	2354	977	1790	3254
704	1300	2372	982	1800	3272
710	1310	2390	988	1810	3290
716	1320	2408	993	1820	3308
721	1330	2426	999	1830	3326
727	1340	2444	1004	1840	3344
732	1350	2462	1010	1850	3362
738	1360	2480	1016	1860	3380
743	1370	2498	1021	1870	3398
749	1380	2516	1027	1880	3416
754	1390	2534	1032	1890	3434
760	1400	2552	1038	1900	3452
766	1410	2570	1043	1910	3470
771	1420	2588	1049	1920	3488
777	1430	2606	1054	1930	3506
782	1440	2624	1060	1940	3524
788	1450	2642	1066	1950	3542
793	1460	2660	1071	1960	3560
799	1470	2678	1077	1970	3578
804	1480	2696	1082	1980	3596
810	1490	2714	1088	1990	3614
			1093	2000	3632

2000 to 3000

C		F	C		F
1093	2000	3632	1371	2500	4532
1099	2010	3650	1377	2510	4550
1104	2020	3668	1382	2520	4568
1110	2030	3686	1388	2530	4586
1116	2040	3704	1393	2540	4604
1121	2050	3722	1399	2550	4622
1127	2060	3740	1404	2560	4640
1132	2070	3758	1410	2570	4658
1138	2080	3776	1416	2580	4676
1143	2090	3794	1421	2590	4694
1149	2100	3812	1427	2600	4712
1154	2110	3830	1432	2610	4730
1160	2120	3848	1438	2620	4748
1166	2130	3866	1443	2630	4766
1171	2140	3884	1449	2640	4784
1177	2150	3902	1454	2650	4802
1182	2160	3920	1460	2660	4820
1188	2170	3938	1466	2670	4838
1193	2180	3956	1471	2680	4856
1199	2190	3974	1477	2690	4874
1204	2200	3992	1482	2700	4892
1210	2210	4010	1488	2710	4910
1216	2220	4028	1493	2720	4928
1221	2230	4046	1499	2730	4946
1227	2240	4064	1504	2740	4964
1232	2250	4082	1510	2750	4982
1238	2260	4100	1516	2760	5000
1243	2270	4118	1521	2770	5018
1249	2280	4136	1527	2780	5036
1254	2290	4154	1532	2790	5054
1260	2300	4172	1538	2800	5072
1266	2310	4190	1543	2810	5090
1271	2320	4208	1549	2820	5108
1277	2330	4226	1554	2830	5126
1282	2340	4244	1560	2840	5144
1288	2350	4262	1566	2850	5162
1293	2360	4280	1571	2860	5180
1299	2370	4298	1577	2870	5198
1304	2380	4316	1582	2880	5216
1310	2390	4334	1588	2890	5234
1316	2400	4352	1593	2900	5252
1321	2410	4370	1599	2910	5270
1327	2420	4388	1604	2920	5288
1332	2430	4406	1610	2930	5306
1338	2440	4424	1616	2940	5324
1343	2450	4442	1621	2950	5342
1349	2460	4460	1627	2960	5360
1354	2470	4478	1632	2970	5378
1360	2480	4496	1638	2980	5396
1366	2490	4514	1643	2990	5414
			1649	3000	5432

English / Metric (SI) Stress Conversion Factors

Look up stress to be converted in the **boldface** column If in ksi (10^3 psi), read MPa in right hand column If in MPa read ksi in lefthand column Conversion factors 1 MPa 1 MN/m² (meganewton per square metre) or 1 N mm² (newton per square millimetre) 1 MPa 0 1450377 ksi and 1 ksi 6 894759 MPa

0 to 100

ksi		MPa	ksi		MPa
—	**0**	—	7 25	**50**	344 7
0 15	**1**	6 89	7 40	**51**	351 6
0 29	**2**	13 79	7 54	**52**	358 5
0 44	**3**	20 68	7 69	**53**	365 4
0 58	**4**	27 57	7 83	**54**	372 3
0 73	**5**	34 47	7 98	**55**	379 2
0 87	**6**	41 37	8 12	**56**	386 1
1 02	**7**	48 26	8 27	**57**	393 0
1 16	**8**	55 16	8 41	**58**	399 9
1 31	**9**	62 05	8 56	**59**	406 8
1 45	**10**	68 95	8 70	**60**	413 7
1 60	**11**	75 84	8 85	**61**	420 6
1 74	**12**	82 74	8 99	**62**	427 5
1 89	**13**	89 63	9 14	**63**	434 4
2 03	**14**	96 53	9 28	**64**	441 3
2 18	**15**	103 4	9 43	**65**	448 2
2 32	**16**	110 3	9 57	**66**	455 1
2 47	**17**	117 2	9 72	**67**	462 0
2 61	**18**	124 1	9 86	**68**	468 8
2 76	**19**	131 0	10 01	**69**	475 7
2 90	**20**	137 9	10 15	**70**	482 6
3 05	**21**	144 8	10 30	**71**	489 5
3 19	**22**	151 7	10 44	**72**	496 4
3 34	**23**	158 6	10 59	**73**	503 3
3 48	**24**	165 5	10 73	**74**	510 2
3 63	**25**	172 4	10 88	**75**	517 1
3 77	**26**	179 3	11 02	**76**	524 0
3 92	**27**	186 2	11 17	**77**	530 9
4 06	**28**	193 1	11 31	**78**	537 8
4 21	**29**	199 9	11 46	**79**	544 7
4 35	**30**	206 8	11 60	**80**	551 6
4 50	**31**	213 7	11 75	**81**	558 5
4 64	**32**	220 6	11 89	**82**	565 4
4 79	**33**	227 5	12 04	**83**	572 3
4 93	**34**	234 4	12 18	**84**	579 2
5 08	**35**	241 3	12 33	**85**	586 1
5 22	**36**	248 2	12 47	**86**	593 0
5 37	**37**	255 1	12 62	**87**	599 8
5 51	**38**	262 0	12 76	**88**	606 7
5 66	**39**	268 9	12 91	**89**	613 6
5 80	**40**	275 8	13 05	**90**	620 5
5 95	**41**	282 7	13 20	**91**	627 4
6 09	**42**	289 6	13 34	**92**	634 3
6 24	**43**	296 5	13 49	**93**	641 2
6 38	**44**	303 4	13 63	**94**	648 1
6 53	**45**	310 3	13 78	**95**	655 0
6 67	**46**	317 2	13 92	**96**	661 9
6 82	**47**	324 1	14 07	**97**	668 8
6 96	**48**	331 0	14 21	**98**	675 7
7 11	**49**	337 8	14 36	**99**	682 6
7 25	**50**	344 71	14 50	**100**	689 5

100 to 200

ksi		MPa	ksi		MPa
14 50	**100**	689 5	21 76	**150**	1 034
14 65	**101**	696 4	21 90	**151**	1 041
14 79	**102**	703 3	22 05	**152**	1 048
14 94	**103**	710 2	22 19	**153**	1 054
15 08	**104**	717 1	22 34	**154**	1 062
15 23	**105**	724 0	22 48	**155**	1 069
15 37	**106**	730 8	22 63	**156**	1 076
15 52	**107**	737 7	22 77	**157**	1 082
15 66	**108**	744 6	22 92	**158**	1 089
15 81	**109**	751 5	23 06	**159**	1 096
15 95	**110**	758 4	23 21	**160**	1 103
16 10	**111**	765 3	23 35	**161**	1 110
16 24	**112**	772 2	23 50	**162**	1 117
16 39	**113**	779 1	23 64	**163**	1 124
16 53	**114**	786 0	23 79	**164**	1 131
16 68	**115**	792 9	23 93	**165**	1 138
16 82	**116**	799 8	24 08	**166**	1 145
16 97	**117**	806 7	24 22	**167**	1 151
17 11	**118**	813 6	24 37	**168**	1 158
17 26	**119**	820 5	24 51	**169**	1 165
17 40	**120**	827 4	24 66	**170**	1 172
17 55	**121**	834 3	24 80	**171**	1 179
17 69	**122**	841 2	24 95	**172**	1 186
17 84	**123**	848 1	25 09	**173**	1 193
17 98	**124**	855 0	25 24	**174**	1 200
18 13	**125**	861 8	25 38	**175**	1 207
18 27	**126**	868 7	25 53	**176**	1 213
18 42	**127**	875 6	25 67	**177**	1 220
18 56	**128**	882 5	25 82	**178**	1 227
18 71	**129**	889 4	25 96	**179**	1 234
18 85	**130**	896 3	26 11	**180**	1 241
19 00	**131**	903 2	26 25	**181**	1 248
19 14	**132**	910 1	26 40	**182**	1 255
19 29	**133**	917 0	26 54	**183**	1 262
19 44	**134**	923 9	26 69	**184**	1 269
19 58	**135**	930 8	26 83	**185**	1 276
19 73	**136**	937 7	26 98	**186**	1 282
19 87	**137**	944 6	27 12	**187**	1 289
20 02	**138**	951 5	27 27	**188**	1 296
20 16	**139**	958 4	27 41	**189**	1 303
20 31	**140**	965 3	27 56	**190**	1 310
20 45	**141**	972 2	27 70	**191**	1 317
20 60	**142**	979 1	27 85	**192**	1 324
20 74	**143**	986 0	27 99	**193**	1 331
20 89	**144**	992 9	28 14	**194**	1 338
21 03	**145**	999 7	28 28	**195**	1 344
21 18	**146**	1 007	28 43	**196**	1 351
21 32	**147**	1 014	28 57	**197**	1 358
21 47	**148**	1 020	28 72	**198**	1 365
21 61	**149**	1 027	28 86	**199**	1 372
21 76	**150**	1 034	29 01	**200**	1 379

ENGLISH/METRIC (SI) STRESS CONVERSION FACTORS (Continued)

To convert ksi or MPa values above 400 use the supplemental table Example Convert 1320 MPa to ksi Solution 1000 MPa 145 04 ksi (from the small table) and 320 MPa 46 41 ksi (from the large table) Then, 145 04 46 41 191 45 ksi

200 to 300

ksi		MPa	ksi		MPa
29 01	**200**	1 379	36 26	**250**	1 724
29 15	**201**	1 386	36 40	**251**	1 731
29 30	**202**	1 393	36 55	**252**	1 737
29 44	**203**	1 400	36 69	**253**	1 744
29 59	**204**	1 407	36 84	**254**	1 751
29 73	**205**	1 413	36 98	**255**	1 758
29 88	**206**	1 420	37 13	**256**	1 765
30 02	**207**	1 427	37 27	**257**	1 772
30 17	**208**	1 434	37 42	**258**	1 779
30 31	**209**	1 441	37 56	**259**	1 786
30 46	**210**	1 448	37 71	**260**	1 793
30 60	**211**	1 455	37 85	**261**	1 800
30 75	**212**	1 462	38 00	**262**	1 806
30 89	**213**	1 469	38 14	**263**	1 813
31 04	**214**	1 475	38 29	**264**	1 820
31 18	**215**	1 482	38 43	**265**	1 827
31 33	**216**	1 489	38 58	**266**	1 834
31 47	**217**	1 496	38 73	**267**	1 841
31 62	**218**	1 503	38 87	**268**	1 848
31 76	**219**	1 510	39 02	**269**	1 855
31 91	**220**	1 517	39 16	**270**	1 862
32 05	**221**	1 524	39 31	**271**	1 868
32 20	**222**	1 531	39 45	**272**	1 875
32 34	**223**	1 538	39 60	**273**	1 882
32 49	**224**	1 544	39 74	**274**	1 889
32 63	**225**	1 551	39 89	**275**	1 896
32 78	**226**	1 558	40 03	**276**	1 903
32 92	**227**	1 565	40 18	**277**	1 910
33 07	**228**	1 572	40 32	**278**	1 917
33 21	**229**	1 579	40 47	**279**	1 924
33 36	**230**	1 586	40 61	**280**	1 931
33 50	**231**	1 593	40 76	**281**	1 937
33 65	**232**	1 600	40 90	**282**	1 944
33 79	**233**	1 606	41 05	**283**	1 951
33 94	**234**	1 613	41 19	**284**	1 958
34 08	**235**	1 620	41 34	**285**	1 965
34 23	**236**	1 627	41 48	**286**	1 972
34 37	**237**	1 634	41 63	**287**	1 979
34 52	**238**	1 641	41 77	**288**	1 986
34 66	**239**	1 648	41 92	**289**	1 993
34 81	**240**	1 655	42 06	**290**	1 999
34 95	**241**	1 662	42 21	**291**	2 006
35 10	**242**	1 669	42 35	**292**	2 013
35 24	**243**	1 675	42 50	**293**	2 020
35 39	**244**	1 682	42 64	**294**	2 027
35 53	**245**	1 689	42 79	**295**	2 034
35 68	**246**	1 696	42 93	**296**	2 041
35 82	**247**	1 703	43 07	**297**	2 048
35 97	**248**	1 710	43 22	**298**	2 055
36 11	**249**	1 717	43 37	**299**	2 062
36 26	**250**	1 724	43 51	**300**	2 068

300 to 400

ksi		MPa	ksi		MPa
43 51	**300**	2 068	50 76	**350**	2 413
43 66	**301**	2 075	50 91	**351**	2 420
43 80	**302**	2 082	51 05	**352**	2 427
43 95	**303**	2 089	51 20	**353**	2 434
44 09	**304**	2 096	51 34	**354**	2 441
44 24	**305**	2 103	51 49	**355**	2 448
44 38	**306**	2 110	51 63	**356**	2 455
44 53	**307**	2 117	51 78	**357**	2 461
44 67	**308**	2 124	51 92	**358**	2 468
44 82	**309**	2 130	52 07	**359**	2 475
44 96	**310**	2 137	52 21	**360**	2 482
45 11	**311**	2 144	52 36	**361**	2 489
45 25	**312**	2 151	52 50	**362**	2 496
45 40	**313**	2 158	52 65	**363**	2 503
45 54	**314**	2 165	52 79	**364**	2 510
45 69	**315**	2 172	52 94	**365**	2 517
45 83	**316**	2 179	53 08	**366**	2 523
45 98	**317**	2 186	53 23	**367**	2 530
46 12	**318**	2 193	53 37	**368**	2 537
46 27	**319**	2 199	53 52	**369**	2 544
46 41	**320**	2 206	53 66	**370**	2 551
46 56	**321**	2 213	53 81	**371**	2 558
46 70	**322**	2 220	53 95	**372**	2 565
46 85	**323**	2 227	54 10	**373**	2 572
46 99	**324**	2 234	54 24	**374**	2 579
47 14	**325**	2 241	54 39	**375**	2 585
47 28	**326**	2 248	54 53	**376**	2 592
47 43	**327**	2 255	54 68	**377**	2 599
47 57	**328**	2 261	54 82	**378**	2 606
47 72	**329**	2 268	54 97	**379**	2 613
47 86	**330**	2 275	55 11	**380**	2 620
48 01	**331**	2 282	55 26	**381**	2 627
48 15	**332**	2 289	55 40	**382**	2 634
48 30	**333**	2 296	55 55	**383**	2,641
48 44	**334**	2 303	55 69	**384**	2 648
48 59	**335**	2 310	55 84	**385**	2 654
48 73	**336**	2 317	55 98	**386**	2 661
48 88	**337**	2 324	56 13	**387**	2 668
49 02	**338**	2 330	56 27	**388**	2 675
49 17	**339**	2 337	56 42	**389**	2 682
49 31	**340**	2 344	56 56	**390**	2 689
49 46	**341**	2 351	56 71	**391**	2 696
49 60	**342**	2 358	56 85	**392**	2 703
49 75	**343**	2 365	57 00	**393**	2 710
49 89	**344**	2 372	57 14	**394**	2 717
50 04	**345**	2 379	57 29	**395**	2 723
50 18	**346**	2 386	57 43	**396**	2 730
50 33	**347**	2 392	57 58	**397**	2 737
50 47	**348**	2 399	57 72	**398**	2 744
50 62	**349**	2 406	57 87	**399**	2 751
50 76	**350**	2 413	58 02	**400**	2 758

500 to 5000

ksi		MPa
72 52	**500**	3447
87 02	**600**	4137
101 53	**700**	4826
116 03	**800**	5516
130 53	**900**	6205
145 04	**1000**	6895
290 08	**2000**	13 790
435 11	**3000**	20 684
580 15	**4000**	27 579
725 19	**5000**	34 474

Source Anton deS Brasunas University of Missouri Rolla

English/Metric (SI) Fracture Toughness Conversion Factors

ksi√in.*	0	1	2	3	4	5	6	7	8	9
					MPa√m					
0	—	1 1	2 2	3 3	4 4	5 5	6 6	7 7	8 8	9 9
10	11 0	12 1	13 2	14 3	15 4	16 5	17 6	18 7	19 8	20 9
20	22 0	23 1	24 2	25 3	26 4	27 5	28 6	29 7	30 8	31 9
30	33 0	34 1	35 2	36 3	37 4	38 5	39 6	40 7	41 8	42 9
40	44 0	45 1	46 2	47 3	48 4	49 5	50 6	51 7	52 8	53 8
50	54 9	56 0	57 1	58 2	59 3	60 4	61 5	62 6	63 7	64 8
60	65 9	67 0	68 1	69 2	70 3	71 4	72 5	73 6	74 7	75 8
70	76 9	78 0	79 1	80 2	81 3	82 4	83 5	84 6	85 7	86 8
80	87 9	89 0	90 1	91 2	92 3	93 4	94 5	95 6	96 7	97 8
90	98 9	100	101	102	103	104	105	107	108	109
100	110	111	112	113	114	115	116	118	119	120
110	121	122	123	124	125	126	127	129	130	131
120	132	133	134	135	136	137	138	140	141	142
130	143	144	145	146	147	148	149	151	152	153
140	154	155	156	157	158	159	160	162	163	164
150	165	166	167	168	169	170	171	173	174	175
160	176	177	178	179	180	181	182	184	185	186
170	187	188	189	190	191	192	193	194	196	197
180	198	199	200	201	202	203	204	205	207	208
190	209	210	211	212	213	214	215	216	218	219
200	220	221	222	223	224	225	226	227	229	230
210	231	232	233	234	235	236	237	238	240	241
220	242	243	244	245	246	247	248	249	251	252
230	253	254	255	256	257	258	259	260	262	263
240	264	265	266	267	268	269	270	271	273	274
250	275	276	277	278	279	280	281	282	284	285
260	286	287	288	289	290	291	292	293	294	296
270	297	298	299	300	301	302	303	304	305	307
280	308	309	310	311	312	313	314	315	316	318
290	319	320	321	322	323	324	325	326	327	329
300	330	331	332	333	334	335	336	337	338	340
310	341	342	343	344	345	346	347	348	349	351
320	352	353	354	355	356	357	358	359	360	362
330	363	364	365	366	367	368	369	370	371	373
340	374	375	376	377	378	379	380	381	382	384
350	385	386	387	388	389	390	391	392	393	394
360	396	397	398	399	400	401	402	403	404	405
370	407	408	409	410	411	412	413	414	415	416
380	418	419	420	421	422	423	424	425	426	427
390	429	430	431	432	433	434	435	436	437	438
400	440									

*Precise conversions can be obtained as follows
To convert from ksi√in to MPa√m, multiply by 1 098 844
To convert from MPa-√m to ksi√in, multiply by 0 910 048
(Revised April 1980)

Reproduced from the Mid-June 1980 METAL PROGRESS DATABOOK by permission from American Society for Metals, Metals Park, Ohio 44073.

English/Metric (SI) Impact Energy Conversion Factors

Look up impact energy to be converted in boldface column. If in ft-lb, read joules (J) in lefthand column. If in joules (J), read ft-lb in righthand column Decimal energy values above 10 and all values above 130 can be calculated by addition. For example, 25.5 ft-lb = 33.9 (25.0) + 0.68 (0 5) or 34 58 J Also, 165 J = 73 8 (100.0) + 47 9 (65) or 121 7 ft-lb

Note. Values for conversions are rounded off to simplify calculations. Actual conversion factors (1 ft-lb = 1.355818 joules and 1 joule = 0.737562 ft-lb) can be used if more accuracy is desired. (Reviewed February 1980)

0.1 to 20

joule (J)		ft-lb	joule (J)		ft-lb
0.14	**0.1**	0.07	7.59	**5.6**	4.13
0.27	**0.2**	0.15	7.73	**5.7**	4.20
0.41	**0.3**	0.22	7.86	**5.8**	4.28
0.54	**0.4**	0.30	8.00	**5.9**	4.35
0.68	**0.5**	0.37	8.13	**6.0**	4.43
0.81	**0.6**	0.44	8.27	**6.1**	4.50
0.95	**0.7**	0.52	8.41	**6.2**	4.57
1.08	**0.8**	0.59	8.54	**6.3**	4.65
1.22	**0.9**	0.66	8.68	**6.4**	4.72
1.36	**1.0**	0.74	8.81	**6.5**	4.79
1.49	**1.1**	0.81	8.95	**6.6**	4.87
1.63	**1.2**	0.89	9.08	**6.7**	4.94
1.76	**1.3**	0.96	9.22	**6.8**	5.02
1.90	**1.4**	1.03	9.36	**6.9**	5.09
2.03	**1.5**	1.11	9.49	**7.0**	5.16
2.17	**1.6**	1.18	9.63	**7.1**	5.24
2.30	**1.7**	1.25	9.76	**7.2**	5.31
2.44	**1.8**	1.33	9.90	**7.3**	5.38
2.58	**1.9**	1.40	10.0	**7.4**	5.46
2.71	**2.0**	1.48	10.2	**7.5**	5.53
2.85	**2.1**	1.55	10.3	**7.6**	5.61
2.98	**2.2**	1.62	10.4	**7.7**	5.68
3.12	**2.3**	1.70	10.6	**7.8**	5.75
3.25	**2.4**	1.77	10.7	**7.9**	5.83
3.39	**2.5**	1.84	10.8	**8.0**	5.90
3.53	**2.6**	1.92	11.0	**8.1**	5.97
3.66	**2.7**	1.99	11.1	**8.2**	6.05
3.80	**2.8**	2.07	11.3	**8.3**	6.12
3.93	**2.9**	2.14	11.4	**8.4**	6.20
4.07	**3.0**	2.21	11.5	**8.5**	6.27
4.20	**3.1**	2.29	11.7	**8.6**	6.34
4.34	**3.2**	2.36	11.8	**8.7**	6.42
4.47	**3.3**	2.43	11.9	**8.8**	6.49
4.61	**3.4**	2.51	12.1	**8.9**	6.56
4.75	**3.5**	2.58	12.2	**9.0**	6.64
4.88	**3.6**	2.66	12.3	**9.1**	6.71
5.02	**3.7**	2.73	12.5	**9.2**	6.79
5.15	**3.8**	2.80	12.6	**9.3**	6.86
5.29	**3.9**	2.88	12.7	**9.4**	6.93
5.42	**4.0**	2.95	12.9	**9.5**	7.01
5.56	**4.1**	3.02	13.0	**9.6**	7.08
5.69	**4.2**	3.10	13.2	**9.7**	7.15
5.83	**4.3**	3.17	13.3	**9.8**	7.23
5.97	**4.4**	3.25	13.4	**9.9**	7.30
6.10	**4.5**	3.32	13.6	**10.0**	7.38
6.24	**4.6**	3.39	14.9	**11.0**	8.11
6.37	**4.7**	3.47	16.3	**12.0**	8.85
6.51	**4.8**	3.54	17.6	**13.0**	9.59
6.64	**4.9**	3.61	19.0	**14.0**	10.3
6.78	**5.0**	3.69	20.3	**15.0**	11.1
6.91	**5.1**	3.76	21.7	**16.0**	11.8
7.05	**5.2**	3.84	23.0	**17.0**	12.5
7.19	**5.3**	3.91	24.4	**18.0**	13.3
7.32	**5.4**	3.98	25.8	**19.0**	14.0
7.46	**5.5**	4.06	27.1	**20.0**	14.8

21 to 130

joule (J)		ft-lb	joule (J)		ft-lb
28.5	**21.0**	15.5	103.0	**76.0**	56.1
29.8	**22.0**	16.2	104.4	**77.0**	56.8
31.2	**23.0**	17.0	105.8	**78.0**	57.5
32.5	**24.0**	17.7	107.1	**79.0**	58.3
33.9	**25.0**	18.4	108.4	**80.0**	59.0
35.3	**26.0**	19.1	109.8	**81.0**	59.7
36.6	**27.0**	19.9	111.2	**82.0**	60.5
38.0	**28.0**	20.7	112.6	**83.0**	61.2
39.3	**29.0**	21.4	113.9	**84.0**	62.0
40.7	**30.0**	22.1	115.2	**85.0**	62.7
42.0	**31.0**	22.9	116.6	**86.0**	63.4
43.4	**32.0**	23.6	118.0	**87.0**	64.2
44.7	**33.0**	24.3	119.3	**88.0**	64.9
46.1	**34.0**	25.1	120.7	**89.0**	65.6
47.5	**35.0**	25.8	122.0	**90.0**	66.4
48.8	**36.0**	26.6	123.4	**91.0**	67.1
50.2	**37.0**	27.3	124.7	**92.0**	67.9
51.5	**38.0**	28.0	126.1	**93.0**	68.6
52.9	**39.0**	28.8	127.4	**94.0**	69.3
54.2	**40.0**	29.5	128.8	**95.0**	70.1
55.6	**41.0**	30.2	130.2	**96.0**	70.8
56.9	**42.0**	31.0	131.5	**97.0**	71.5
58.3	**43.0**	31.7	132.9	**98.0**	72.3
59.7	**44.0**	32.5	134.2	**99.0**	73.0
61.0	**45.0**	33.2	135.6	**100.0**	73.8
62.4	**46.0**	33.9	136.9	**101.0**	74.5
63.7	**47.0**	34.7	138.3	**102.0**	75.2
65.1	48.0	35.4	139.6	**103.0**	76.0
66.4	**49.0**	36.1	141.0	**104.0**	76.7
67.8	**50.0**	36.9	142.4	**105.0**	77.4
69.1	**51.0**	37.6	143.7	**106.0**	78.2
70.5	**52.0**	38.4	145.1	**107.0**	78.9
71.9	**53.0**	39.1	146.4	**108.0**	79.7
73.2	**54.0**	39.8	147.8	**109.0**	80.4
74.6	**55.0**	40.6	149.1	**110.0**	81.1
75.9	**56.0**	41.3	150.5	**111.0**	81.9
77.3	**57.0**	42.0	151.9	**112.0**	82.6
78.6	**58.0**	42.8	153.2	**113.0**	83.3
80.0	**59.0**	43.5	154.6	**114.0**	84.1
81.3	**60.0**	44.3	155.9	**115.0**	84.8
82.7	**61.0**	45.0	157.3	**116.0**	85.6
84.1	**62.0**	45.7	158.6	**117.0**	86.3
85.4	**63.0**	46.5	160.0	**118.0**	87.0
86.8	**64.0**	47.2	161.3	**119.0**	87.8
88.1	**65.0**	47.9	162.7	**120.0**	88.5
89.5	**66.0**	48.7	164.1	**121.0**	89.2
90.8	**67.0**	49.4	165.4	**122.0**	90.0
92.2	**68.0**	50.2	166.8	**123.0**	90.7
93.6	**69.0**	50.9	168.1	**124.0**	91.5
94.9	**70.0**	51.6	169.5	**125.0**	92.2
96.3	**71.0**	52.4	170.8	**126.0**	92.9
97.6	**72.0**	53.1	172.2	**127.0**	93.7
99.0	**73.0**	53.8	173.5	**128.0**	94.4
100.3	**74.0**	54.6	174.9	**129.0**	95.1
101.6	**75.0**	55.3	176.3	**130.0**	95.9

APPENDIX C. MECHANICAL TEST SPECIMENS

APPENDIX C-1

Smooth Bar Tensile Test Specimen A

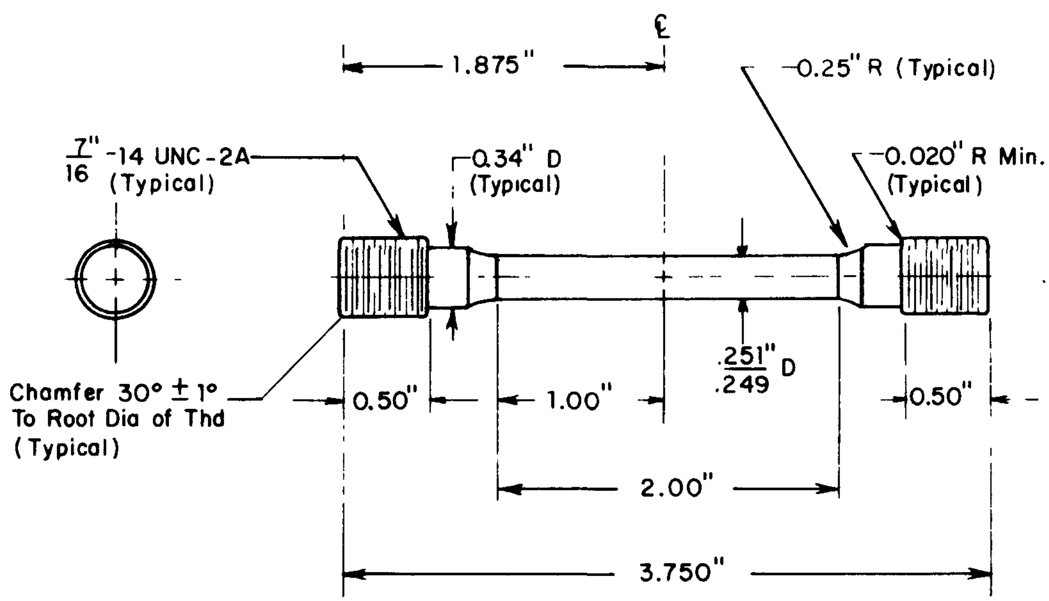

APPENDIX C-2

Smooth Bar Tensile Test Specimen B

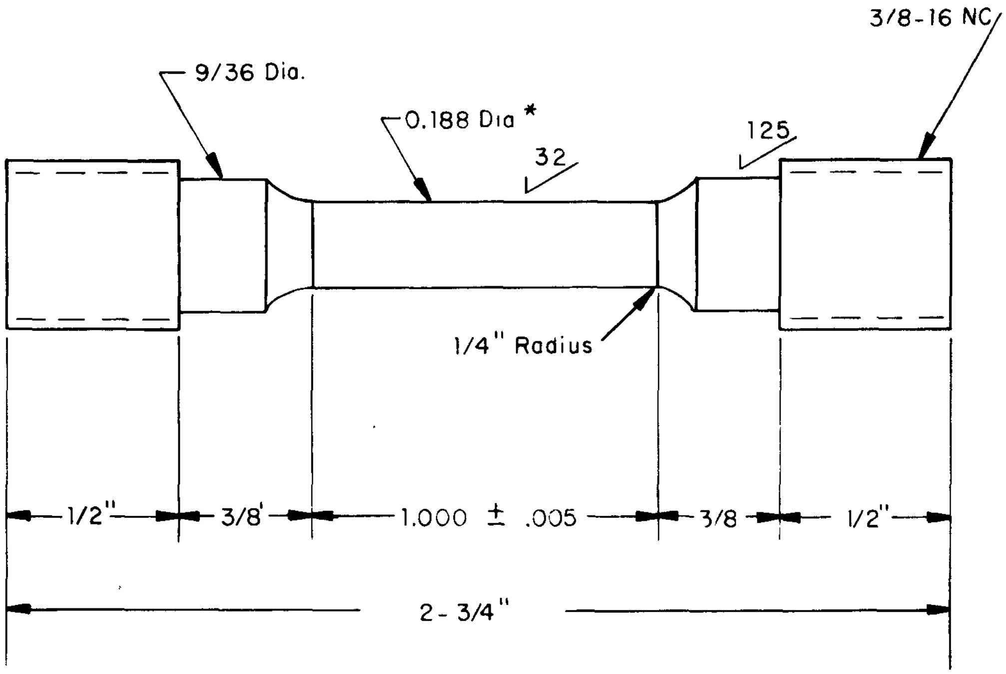

* *Increase diameter from center of gage (.188) to the ends by 0.002"*

APPENDIX C-3

Smooth Bar Tensile Test Specimen C

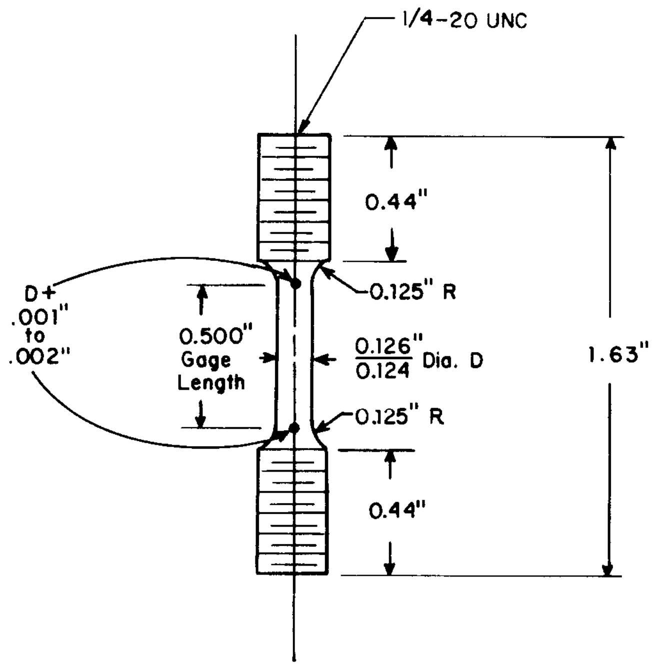

APPENDIX C-4

Circumferential Notch at Center of Specimen
for Notched Tensile Specimens

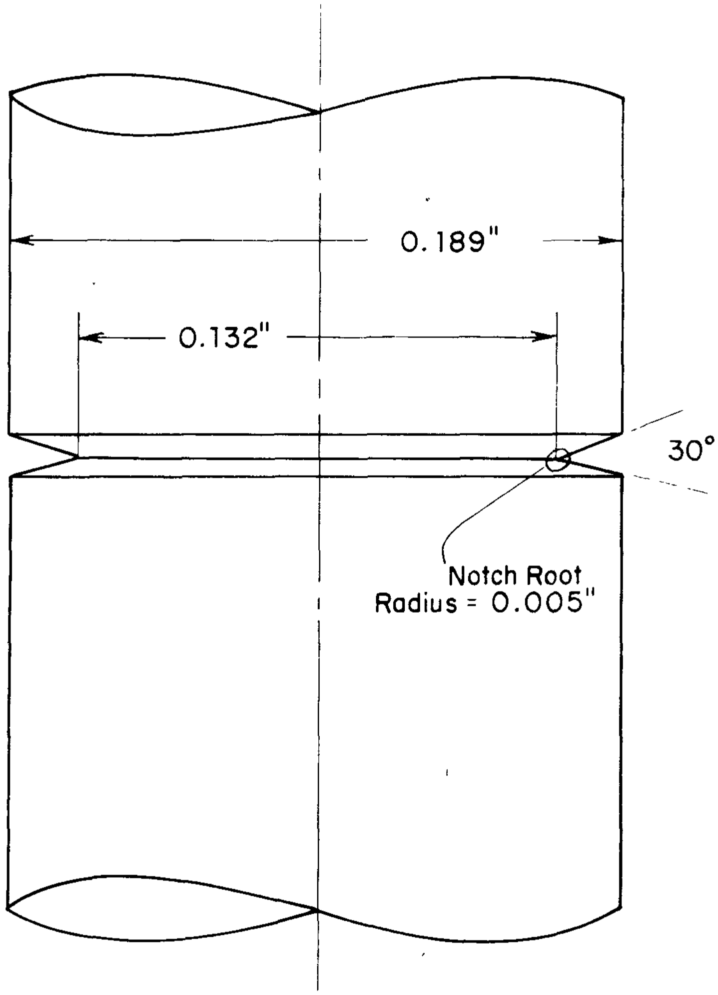

APPENDIX C-5

Tensile Tube Specimen

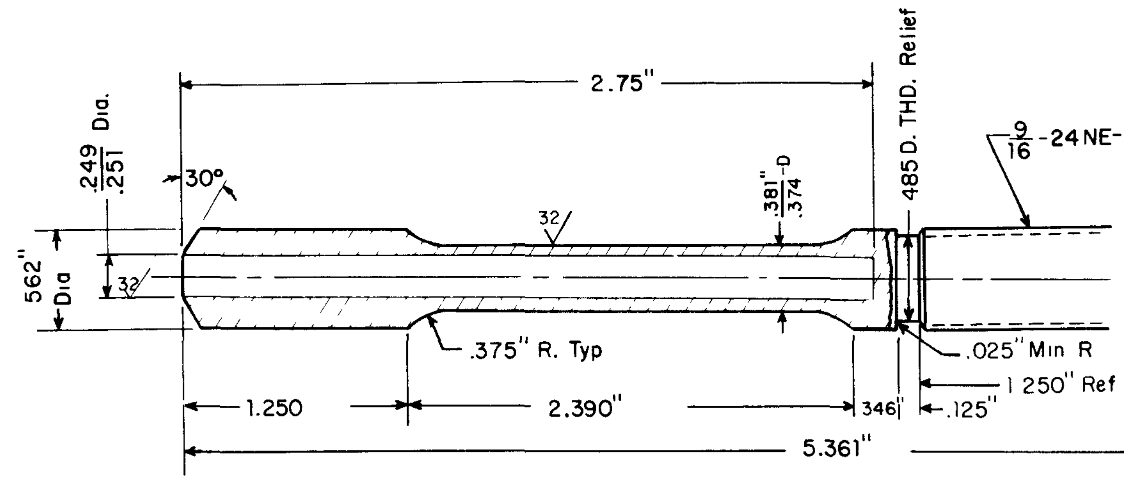

APPENDIX C-6

Single Edge Notched Tensile Specimen

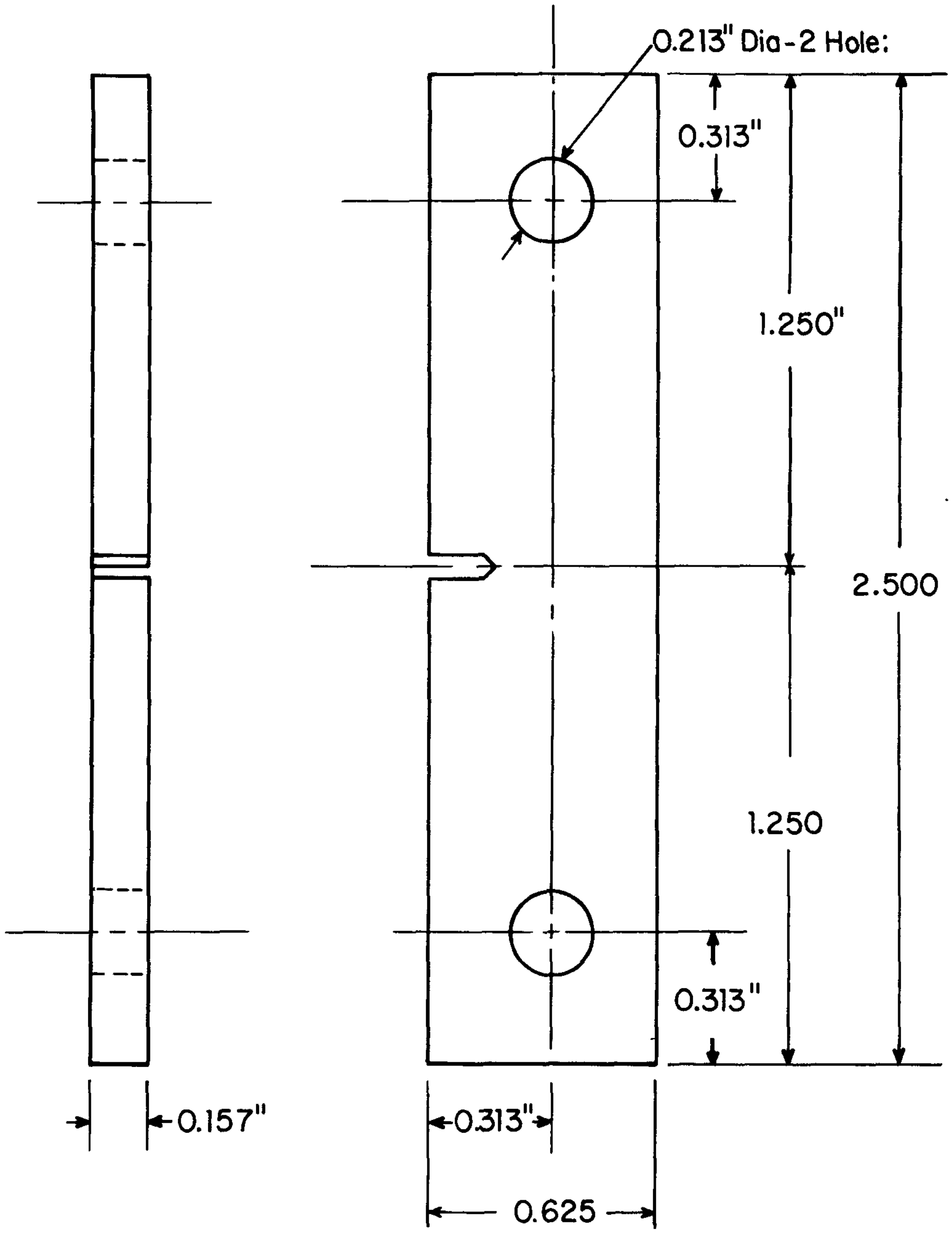

APPENDIX C-6a

Detail of Notch in Single Edge Notched Tensile Specimen

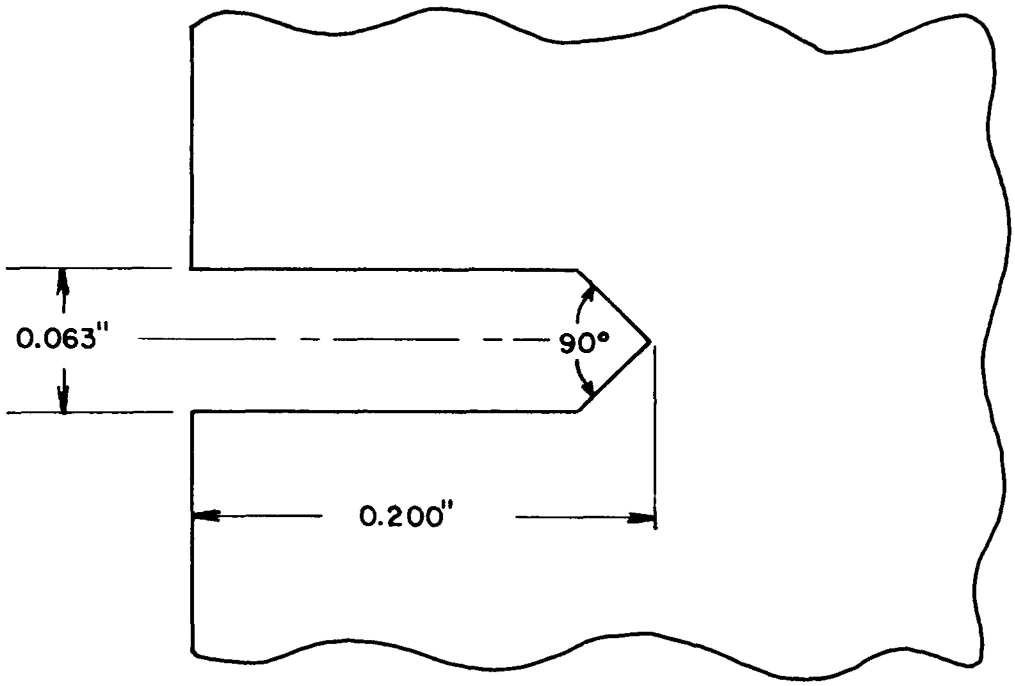

Notes: 1) All demensions ± 0.001"
2) Notch root radius = 0.005"
3) To prevent excessive hardening in notch area, machine final 0.040" of notch in five cuts (0.010" on first cut, 0.010" on 2nd cut, 0.010" on 3rd cut, 0.005" on 4th cut and 0.005" on 5th cut).

APPENDIX C-7

C-Shaped Fracture Mechanics Specimen

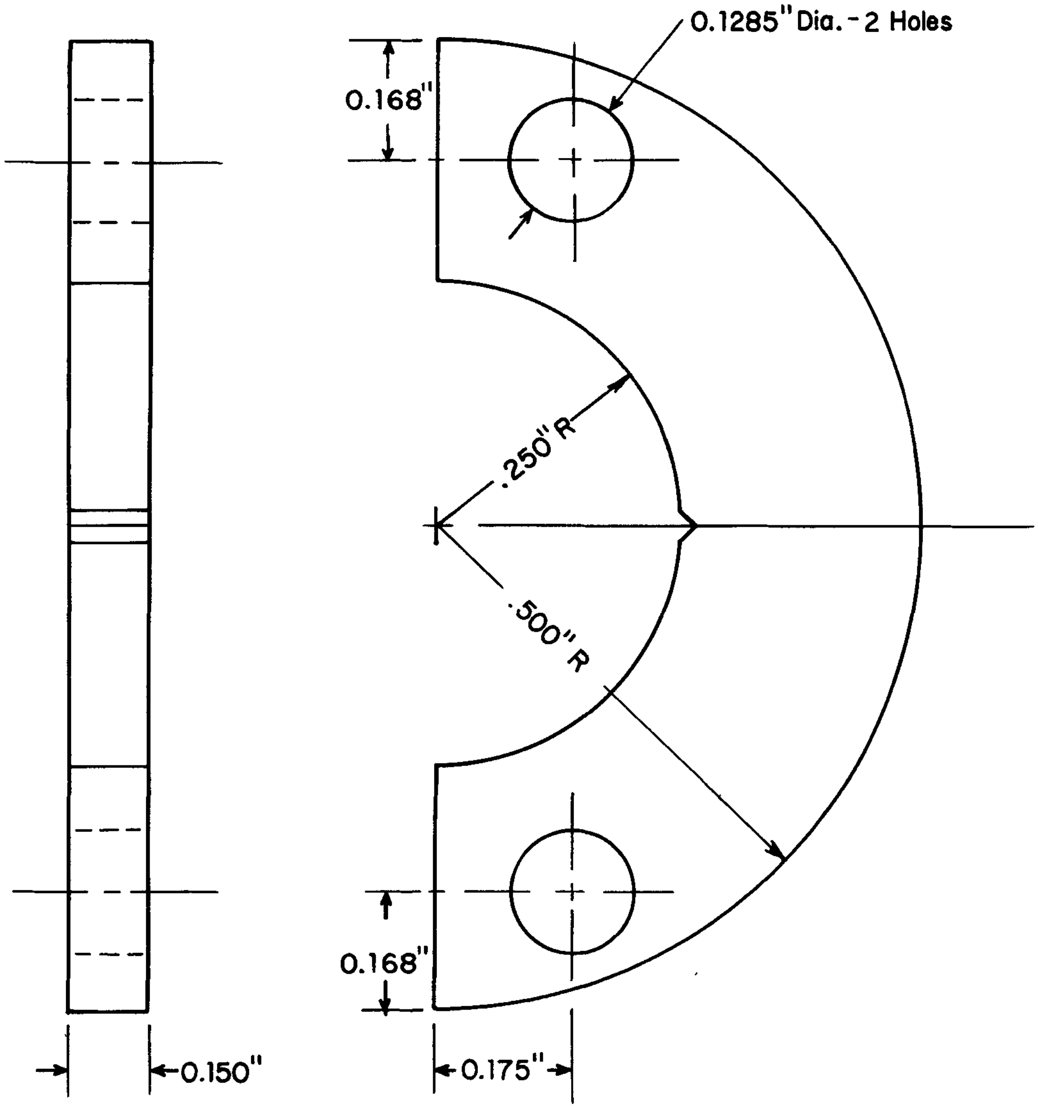

APPENDIX C-7a

Detail of Notch in C-Shaped Fracture Mechanics Specimen

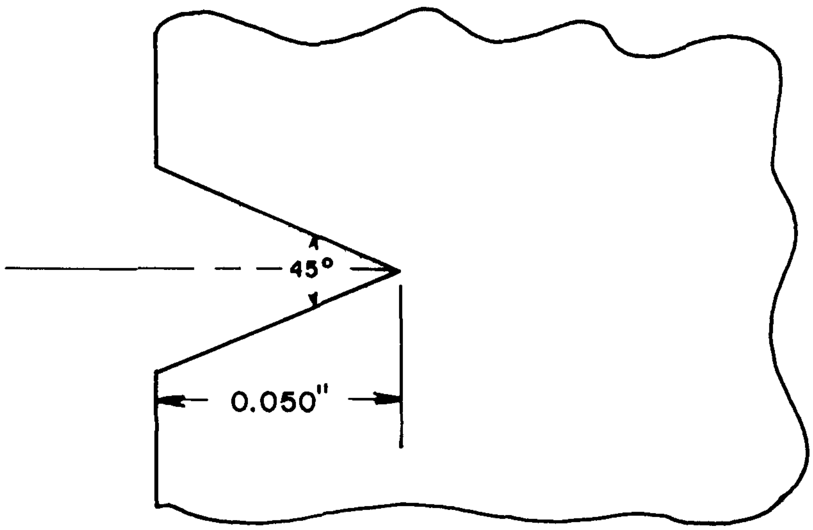

Notes: 1) All demensions ± 0.001"
2) Notch root radius = 0.005"

APPENDIX C-8

Impact Specimen: Modified Naval Research Laboratory
Dynamic Tear Specimen

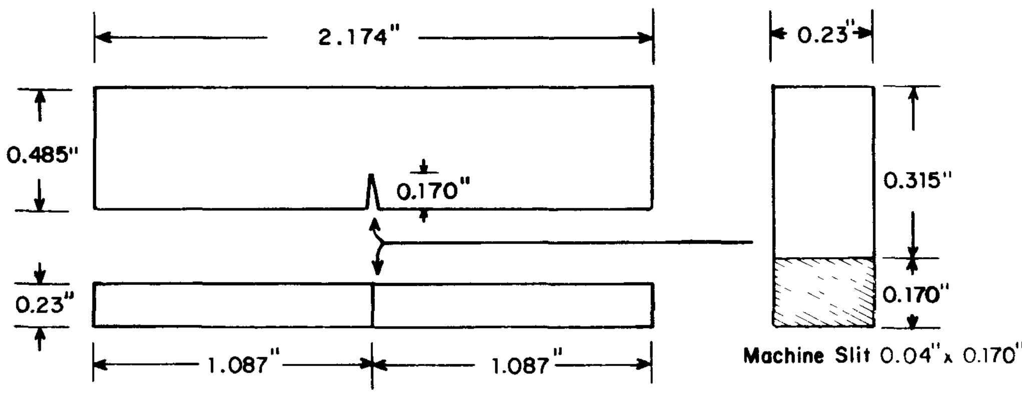

APPENDIX D. HEAT ANALYSES

These analyses are for the specific heats of steel actually tested.

DATA SHEET D-1

Heat Analysis Type 304L Stainless Steel

Element	Weight Percent
C	0.03
Mn	1.57
P	0.015
S	0.008
Si	0.43
Cr	18.35
Ni	10.29
Mo	0.17
N	-
Al	-
Ti	-
Nb	-
Cu	-

DATA SHEET D-2

Heat Analysis Type 330 Stainless Steel

Element	Weight Percent
C	0.049
Mn	1.40
P	-
S	0.005
Si	1.46
Cr	18.40
Ni	35.00
Mo	0.18
N	-
Al	-
Ti	0.45
Nb	-
Cu	0.20

DATA SHEET D-3

Heat Analysis Incoloy® 800H

Element	Weight Percent
C	0.08
Mn	0.84
P	-
S	0.002
Si	0.51
Cr	19.19
Ni	34.04
Mo	-
N	-
Al	0.36
Ti	0.41
Nb	-
Cu	0.52

DATA SHEET D-4

Heat Analysis Tenelon®

Element	Weight Percent
C	-
Mn	15.3
P	-
S	-
Si	0.53
Cr	17.4
Ni	0.22
Mo	-
N	0.4-0.6
Al	-
Ti	-
Nb	-
Cu	-

DATA SHEET D-5

Heat Analysis Nitronic® 40 Stainless Steel

Element	Weight Percent
C	0.015
Mn	9.01
P	0.018
S	0.016
Si	0.24
Cr	20.32
Ni	6.71
Mo	-
N	0.35
Al	-
Ti	-
Nb	-
Cu	-

DATA SHEET D-6

Heat Analysis Nitronic® 50 Stainless Steel

Element	Weight Percent
C	0.05
Mn	5.44
P	0.015
S	0.010
Si	0.42
Cr	21.48
Ni	12.36
Mo	2.12
N	0.25
Al	-
Ti	-
Nb	0.19
Cu	-
V	0.2

DATA SHEET D-7

Heat Analysis Type 316 Stainless Steel

Element	Weight Percent
C	0.07
Mn	8.08
P	0.015
S	0.023
Si	0.69
Cr	19.57
Ni	5.67
Mo	2.13
N	0.32
Al	-
Ti	-
Nb	-
Cu	-

DATA SHEET D-8

Heat Analysis X18-3 Mn Stainless Steel

Element	Weight Percent
C	0.067
Mn	12.4
P	0.013
S	0.013
Si	0.43
Cr	18.55
Ni	3.17
Mo	-
N	0.33
Al	-
Ti	-
Nb	-
Cu	-
B	0.0015

DATA SHEET D-9

Heat Analysis 18-18 Plus®

Element	Weight Percent
C	0.11
Mn	17.80
P	0.020
S	0.004
Si	0.56
Cr	17.78
Ni	0.46
Mo	1.09
N	0.45
Al	-
Ti	-
Nb	-
Cu	0.95
Co	0.01

DATA SHEET D-10

Heat Analysis 304N

Element	Weight Percent
C	0.06
Mn	1.66
P	0.30
S	0.025
Si	0.19
Cr	18.37
Ni	8.43
Mo	0.10
N	0.250
Al	-
Ti	-
Nb	-
Cu	0.15

DATA SHEET D-11

Heat Analysis Carpenter 20 Cb-3®

Element	Weight Percent
C	0.018
Mn	1.60
P	0.028
S	0.007
Si	0.44
Cr	20.60
Ni	34.90
Mo	4.33
N	-
Al	-
Ti	-
Nb	0.39
Cu	0.20